# BULLETIN OF THE NATIONAL INSTITUTE OF INDUSTRIAL HEALTH

No. 3

1960

# 労働衛生研究所研究報告

## 第 3 号

昭和三十五年

# EXPERIMENTAL STUDIES ON BENZENE POISONING

## 3. EFFECT OF BENZENE ON ERYTHROCYTES ENDOSOMA OF RAT

Mitsuo SATO and Hiromichi HASEGAWA

For the diagnosis of benzene poisoning, the examination of the fluctuation of blood counts and morphological changes of blood corpuscles in the peripheral blood has been mainly used. These blood changes reflect to a certain degree the severity of lesion in blood forming organs ; however, they are not always considered to be appropriate for the early diagnosis of benzene poisoning. The authors attempted to elucidate whether qualitative alteration occur within erythrocyte of animal in keeping with injection of benzene and examine their usefulness in diagnosis of benzene poisoning.

In general, for the separation and detection of components in a hemolysate of blood, several methods such as electrophoresis[1, 2, 3, 4, 5], chromatography[6, 7, 8, 9] and alkali denaturation[10] have been used. Hitherto numerous reports have accumlated on abnormal hemoglobin[11, 12] in human adult by these methods. However, the characteristic changes of hemoglobin has been disregarded for studies of industrial poisoning.

Koike et al.[13] showed in previous report that the most predominant change in early stage was appearance of numerous abnormal erythroblasts and proerythroblasts in the erythropoetic series. And these abnormalities in the erythroblastic cells remained at least to the end of the fifth week. This observation may suggest the characteristic changes of hemoglobin in benzene poisoning.

The authors, therefore, investigated the effect of benzene upon erythrocytes endosoma in rat, especially upon hemoglobin, by use of electrophresis and chromatography, and found out an interesting fact that the changes of hemoglobin appeared in early stage.

## METHOD

One ml. of benzene per Kg. (sesame-oil : benzene=1 : 1) was injected into Wister-rat and at weekly intervals blood was obtained by heart puncture with syringe containing heparin. The heparinized blood was washed three times with isotonic saline solution, ruptured with distilled water and centrifuged. The supernatant solution, i. e. erythrocytes endosoma, was used in the experiments.

Electrophoresis : The type HTD-1 of Hitachi Tiselius Electrophoresis Apparatus with schlieren optics was used for moving boundary experiments. Erythrocytes

1

endosoma solution was dialyzed at 0° against veronal buffer for 24 hours before analysis. The electrophoretic runs were carried out at a constant current of 6.4 mA, 190–200 V and the cell was cooled with ice water at 6°. The buffer solution used in this investigation was a veronal buffer adjusted to pH 8.6 with Beckman pH meter, model G, and ionic strength 0.06. The apparent mobilities were calculated from ascending boundaries according to the conventional equation. The relative percentage of area of each component was calculated graphically in the tracing of the electrophoretic patterns.

Chromatography: Cation exchanger 'Amberlite IRC-50', which had been pretreated as described by Hirs et al.[14], was used for ion-exchange chromatography. Citrate-phosphate (McIlvaine) buffer solution was selected as described by Morrison and Cook[8]. The resin was previously equilibrated with 0.035 M $[N_a^+]$ buffer of pH 6.5 and poured into chromatographic tube which had an internal diameter of 0.9 cm. The erythrocytes endosoma solution had previously been dialysed against the 0.035 M buffer, then 1.0 ml. of the sample was added into column. This solution was allowed to drain into the resin and washed three times with 0.035 M buffer of 0.3 ml. each. The endosoma was eluted with citrate-phosphate buffer (pH 6.5), increasing sodium ion concentration stepwise from 0.14 M to 0.28 M. The rate of flow was 1 ml. per 20 minutes. The effluent from the column was collected in 1 ml. fractions using an automatic fraction collector of magnetic burette type. All procedures were performed in cold room of constant-temperature at 4°. The kind and the amount of proteins in the effluent was determined with Hitachi spectrophotometer, model EPU-2, at 280 and 414 mμ. Before measurement each fraction was diluted with 3.0 ml. of distilled water.

## RESULTS

*Electrophoresis of rat erythrocytes endosoma*

Dialyzed erythrocytes endosoma was filled into electrophoresis-cell, and left in the bath for 30 min. at 6°. After thermo-equillibrium was attained, electrophoretic run was started. In the very begining of electrophoretic runs, two peaks were observed. However, the apparent mobility of those peaks were relatively large, and the relative percentage were smaller than those of following peaks which were separated slowly. And the nature of the peaks will be discussed later.

As shown in Fig. 1, a larg peak A, small B, C, D, E and F peaks were observed after runs for about one hour. After the injection with daily 1 ml. of benzene per kg. body weight, it was found that F-peak decreased to a half during first week, and disappeared entirely during second week, in spite of no change was observed in A-peak. This is an interesting phenomenon taking account of the facts that peripheral white cell and total nucleic cell counts in bone marrow once decreased, but recovered to the normal level during the third or fourth week as described in
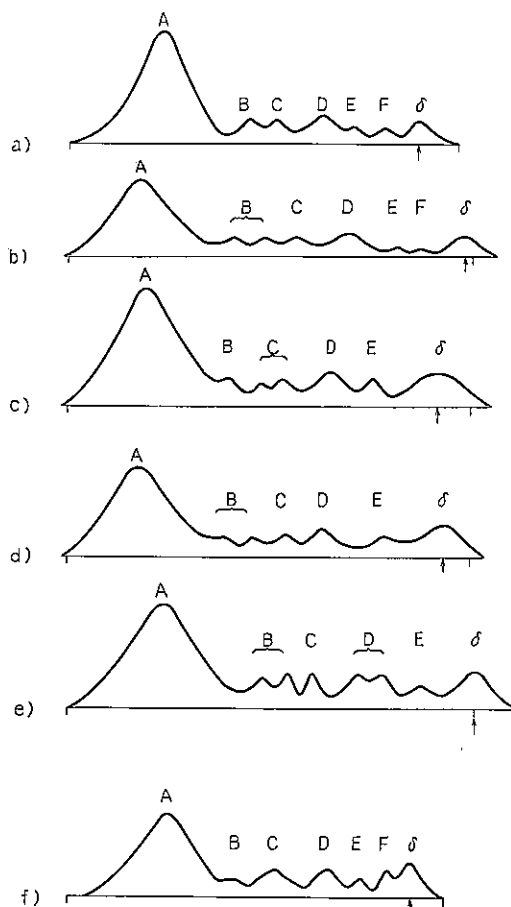
2

Fig. 1. Electrophoresis of erythrocytes endosoma of benzene-poisoned rats (1 ml./kg. body wt.) at pH 8.6 (veronal buffer, ionic strength 0.06), 0°, 6.4 mA, ca. 200 V.
Hemoglobin concentration of the solution was about $2-4\times10^{-4}$ M in all experiments.
a) represents the pattern for a normal rat (animal number 1 in the Table 1).
b) represents the pattern for an abnormal rat injected with benzene for a week (No. 7 in the Table 1).
c) represents the pattern for an abnormal rat injected with benzene for two weeks (No. 9).
d) represents the pattern for an abnormal rat injected with benzene for three weeks (No. 12).
e) represents the pattern for an abnormal rat injected with benzene for four weeks (No. 14).
f) represents the pattern of an abnormal rat left for one week without the injection of benzene after the injection of benzene had been for two weeks (No. 16).

previous report[13], notwithstanding successive injection of benzene. The diminished F-peak recovered to a normal level after one week following the interruption of benzene injection. Therefore, it may be considered that the diminish of F-peak corresponds intimately with the severity of benzene poisoning.

Other peak, B, C, D and E was not so evidently influenced with benzene as F-peak, but these peaks divided into two fractions respectively as shown in Table 1

3

Table 1. a) Apparent mobilities of electrophoretic patterns of erythrocytes endosoma of benzene-poisoned rats (1 ml/kg body wt.). All experiments were carried out at pH 8.6 (veronal buffer, ionic strength 0.06) and 6° in current condition of 6.4 mA, ca. 200 V.

| Duration of treatment (days) | Animal No. | Species of the peaks | | | | | |
|---|---|---|---|---|---|---|---|
| | | A | B | C | D | E | F |
| Normal | 1 | 100 | 66 | 56 | 38 | 26 | 12 |
| | 2 | 100 | 64 | 54 | 39 | 25 | 12 |
| | 3 | 100 | 63 | 52 | 37 | 24 | 12 |
| | 4 | 100 | 72 | 57 | 38 | 22 | 12 |
| | 5 | 100 | 63 | 50 | 38 | 21 | 13 |
| 7, Benzene | 6 | 100 | 72 | 61 | 45 | 25 | 14 |
| | 7 | 100 | 71, 63 | 52 | 37 | 24 | 13 |
| 14, Benzene | 8 | 100 | 64 | 55 | 39 | 23 | — |
| | 9 | 100 | 69 | 59, 52 | 37 | 23 | — |
| 21, Benzene | 10 | 100 | 77, 68 | 61, 56 | 41 | 25 | — |
| | 11 | 100 | 79, 74 | 58 | 45, 36 | 20 | — |
| | 12 | 100 | 73, 63 | 53 | 40 | 20 | — |
| 28, Benzene | 13 | 100 | 70 | 54, 48 | 37 | 19 | — |
| | 14 | 100 | 69, 61 | 53 | 38, 31 | 19 | — |
| | 15 | 100 | 75, 68 | 58, 47 | 42, 37 | 30, 19 | — |
| 14*, Benzene, then stand for 7 | 16 | 100 | 72 | 56 | 34 | 22 | 11 |

Table 1. b) Apparent area percentage of each peak

| Duration of treatment (days) | Animal No. | Species of the peak | | | | | |
|---|---|---|---|---|---|---|---|
| | | A | B | C | D | E | F |
| Normal | 1 | 71 | 6 | 6 | 11 | 3 | 3 |
| | 2 | 69 | 6 | 6 | 10 | 5 | 4 |
| | 3 | 69 | 6 | 5 | 12 | 4 | 4 |
| | 4 | 60 | 8 | 8 | 15 | 5 | 4 |
| | 5 | 68 | 7 | 7 | 11 | 3 | 4 |
| mean value | | 67 | 7 | 6 | 12 | 4 | 4 |
| 7, Benzene | 6 | 67 | 7 | 7 | 13 | 3 | 3 |
| | 7 | 68 | 5, 5 | 6 | 12 | 2 | 2 |
| 14, Benzene | 8 | 77 | 5 | 4 | 8 | 6 | — |
| | 9 | 69 | 5 | 4, 5 | 11 | 6 | — |
| 21, Benzene | 10 | 67 | 7, 2 | 4, 4 | 10 | 6 | — |
| | 11 | 75 | 5, 7 | 4 | 2, 5 | 2 | — |
| | 12 | 69 | 5, 4 | 4 | 10 | 7 | — |
| 28, Benzene | 13 | 71 | 7 | 3, 5 | 8 | 6 | — |
| | 14 | 67 | 6, 4 | 5 | 7, 6 | 5 | — |
| | 15 | 75 | 5, 2 | 5, 3 | 2, 3 | 3, 2 | — |
| 14*, Benzene then stand for 7 | 16 | 64 | 12 | 12 | 9 | 4 | 5 |

Note. * After injection of Benzene for fourteen days, an animal allow stand for seven days from the discontinuation of administration of benzene.

a) and b). The divided peaks which was caused by the injected of daily 1 ml. of benzene per Kg. body weight recovered to the normal pattern after three or four weeks from the discontinuation of the administration of the test materials. It is a remarkable fact that in control animals significant difference was found in apparent mobilities of each peak and in relative percentage of area as shown in Table 1 b).

*Chromatography of rat erythrocytes endosoma*

Erythrocytes endosoma added on the column was adsorbed to the resin in 1 mm width as a layer of red band. Using the citrate-phosphate buffer pH 6.5 (0.14 M) as influent, at first non-adsorbed fraction appeared having the maximum absorption spectrum at 280 m$\mu$ but non at 414 m$\mu$ as shown in Fig. 2. The amount of this
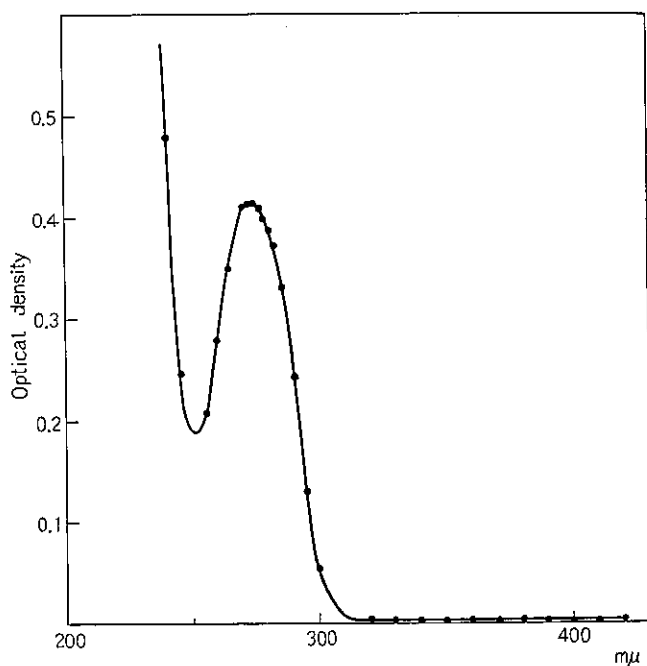


Fig. 2. Absorption curve of non-heme protein fraction, Peak-I

non-heme protein fraction, peak-I, was 41.6% of the total extinction of all effluents measured at 280 m$\mu$ (Table 2). In the course of development, two red bands which run rapidly were observed in the column. These bands could be eluted with 0.14 M buffer at the fraction number 180. These protein fractions named peak-II and -III showed a typical absorption spectrum of heme-protein, and the amounts were calculated at 10.5% for the former and 28.0% for the latter in the ratio to the total effluent by the extinction at 414 m$\mu$. After these two minor fraction of heme-protein eluted, the sodium concentration in buffer solution was changed to 0.28 M, and the main fraction named peak-IV was eluted. Fig. 3 a) shows a typical chromatogram of erythrocytes endosoma in normal rat eluted with citrate-phosphate buffer

5

Table 2.  Area percentage of each peak in chromatography of erythrocytes endosoma of benzene-poisoned rats (1 ml/kg body wt.).

| Duration of treatment (days) | Animal No. | Peak No. | | | | | | |
|---|---|---|---|---|---|---|---|---|
| | | I | II$_A$ | II | III | III$_B$ | III$_C$ | IV |
| | | % | % | % | % | % | % | % |
| Normal | 1 | 38.3 | | 7.1 | 31.0 | | | 62.5 |
| | 2 | 42.6 | | 17.6 | 20.0 | | | 62.5 |
| | 3 | 48.6 | | 10.4 | 35.0 | | | 54.6 |
| | 4 | 37.0 | | 6.8 | 25.7 | | | 67.4 |
| Normal mean | | 41.6 | | 10.5 | 28.0 | | | 61.8 |
| 14, Benzene | 8 | 14.2 | 2.3 | 10.4 | 16.7 | | | 70.4 |
| | 9 | 17.0 | 3.7 | 15.0 | 31.2 | | | 50.3 |
| 21, Benzene | 10 | 13.6 | 5.4 | 10.2 | 17.9 | 3.3 | | 63.1 |
| | 11 | 29.4 | 1.5 | 9.8 | 36.8 | 6.7 | | 45.2 |
| 28, Benzene | 13 | 25.1 | 6.3 | 21.0 | 17.5 | | | 54.6 |
| 35, Benzene | 17 | 34.8 | 6.3 | 21.8 | 18.6 | 5.7 | 3.1 | 44.5 |
| 42, Benzene | 18 | 18.3 | 3.2 | 14.8 | 21.3 | 8.1 | 3.8 | 48.4 |

Notes:  1)  The percentage in peak-1 column is the ratio of extinction for peak-1 to the total extinction of the effluent fractions measured at 280 m$\mu$.
2)  The percentage in the other columns is the ratio of extinction for each peak to the total extinction of the effluent fractions measured at 414 m$\mu$.
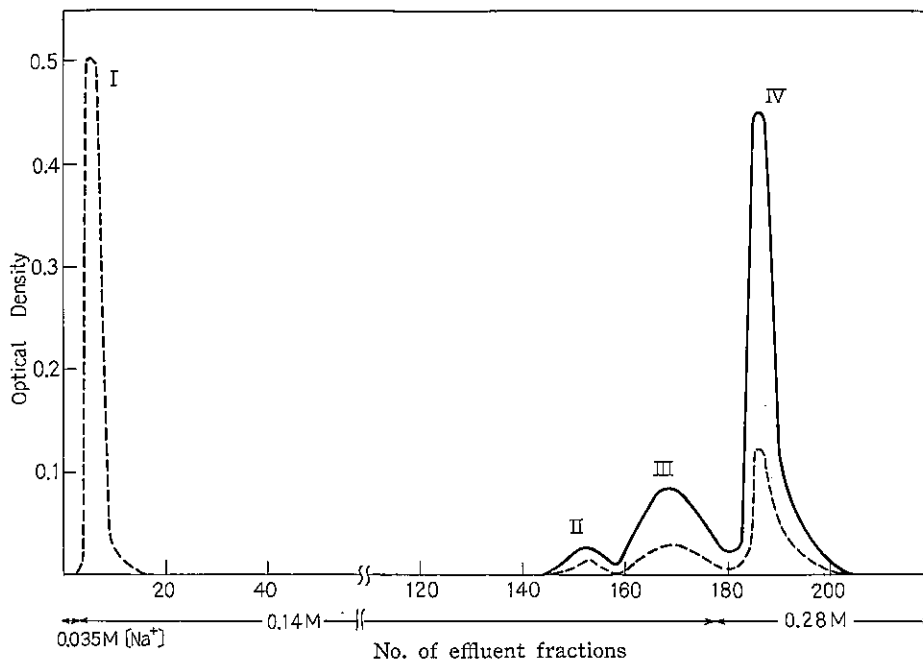


Fig. 3.  a)  Chromatography of erythrocytes endosoma in normal rat on a 0.9 cm. diameter and 10 cm. high column of IRC-50 at 4° (Animal No. 1).  Flow rate was 1 ml. per 20 min. and fraction size was 1 ml.  Elution was performed with increasing stepwise the concentration of citrate-phosphate buffer (pH 6.5) from 0.035 M to 0.28 M:
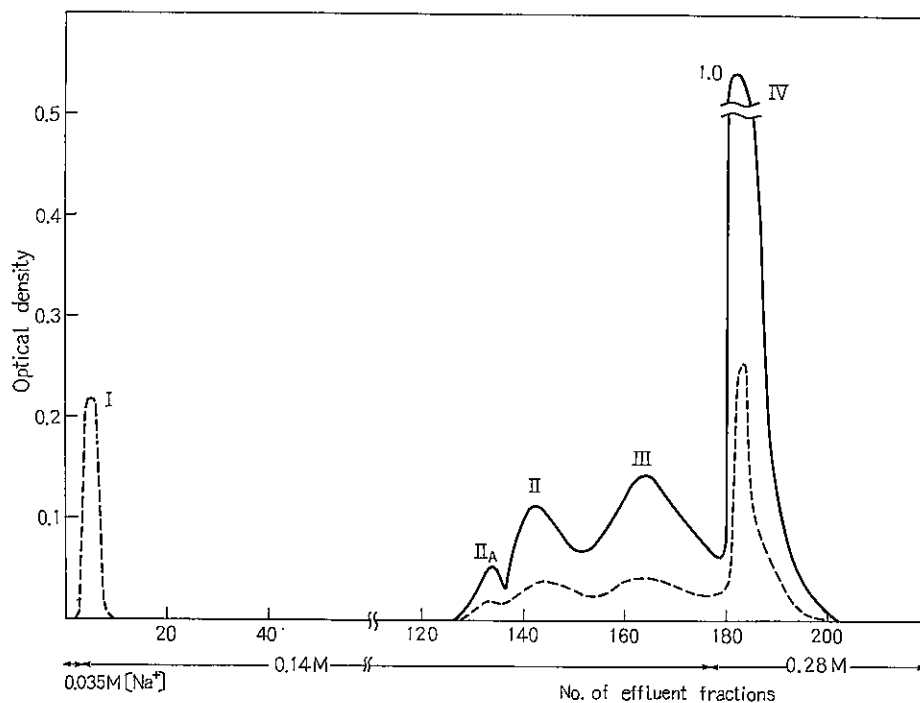- - - -, optical density at 280 m$\mu$; ———, optical density at 414 m$\mu$.

Fig. 3. b) Chromatography of erythrocytes endosoma after the administration of daily 1 ml. of benzene for two weeks (Animal No. 9)
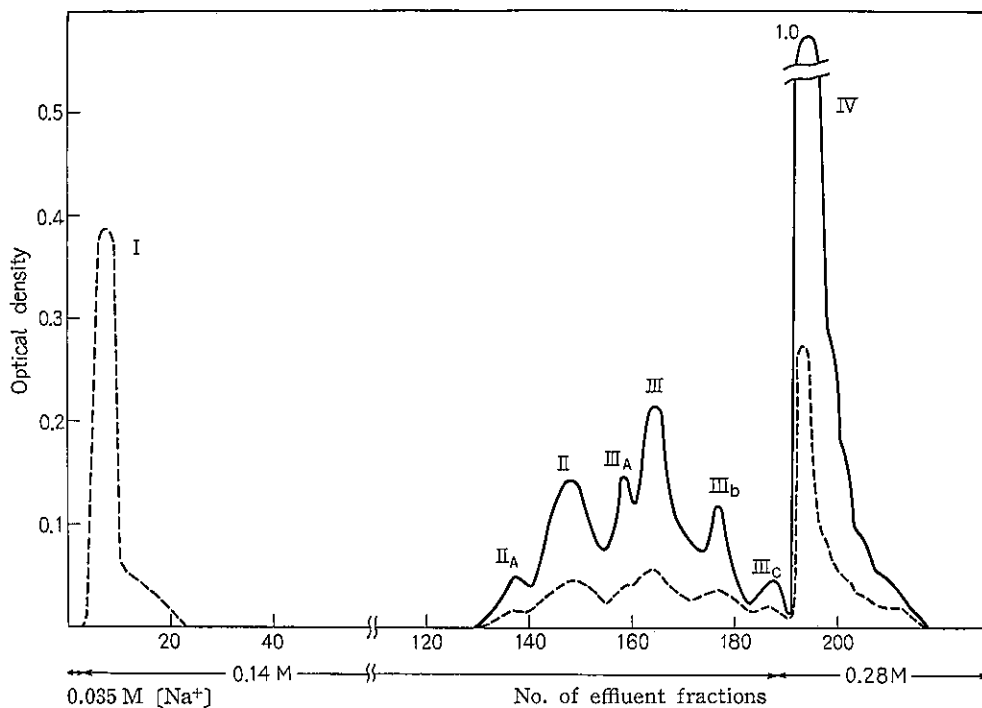


Fig. 3. c) Chromatography of erythrocytes endosoma after the administration of daily 1 ml. of benzene for 6 weeks (Animal No. 18)

7

(pH 6.5). The injection of benzene for two weeks caused a remarkable decrease of non-heme protein fraction of peak-I as shown in chromatogram of Fig. 3 b) and Table 2, simultaneously with peak-I a small peak-IIA was noted before peak-II appeared. During third weeks the peak-III fraction divided into two fractions, peak-IIIB, -IIIc and the complicated elution pattern was obtained at the end of the fifth and sixth week as shown in Fig. 3 c). Table 2 shows that no remarkable change was observed in the peak-II, III and IV except the change in peak-I which represented the non-heme protein, but new small peaks appeared in heme-protein fraction.

## DISCUSSION

The electrophoretic behavior of erythrocytes endosoma in rat was affected with the sort of buffer[4, 5]. In phosphate buffer of pH 8.0 only single peak was noted, but citrate buffer of pH 6.5 caused the appearance of two peaks. As shown in Fig. 1, good separation was obtained with veronal buffer for erythrocytes endosoma. Carboxyhemoglobin or methemoglobin showed similar behavior with oxyhemoglobin.

As described already in the term of results, small two peaks which had larger apparent mobilities than that of main peak-A were observed in the electrophoretic pattern. To compare the result of chromatography with that of electrophresis, the fraction of peak-I which has separated by chromatography was pooled, lyophilized and then tested on paper electrophoresis as well as moving boundary electrophoresis. It was ascertained that the peak-I was consisted of at least two components in paper electrophoresis (No. 51 of Toyo-Roshi Co. was used as filter paper and veronal was used as buffer solution, and colored out with B. P. B. after run), and in moving boundary electrophresis it displayed an identical behavior to the small peaks which was observed moving rapidly in electrophoresis of erythrocytes endosoma in rat. Therefore the peak-I in chromatogram corresponds to the small two peaks observed in moving boundary experiment and each peak of A, B, C, D, E and F may correspond to the peak II, III, IV. Accordingly it is probable that the pattern of divided peaks from B, C, D and F which is observed in electrophoretic experiments of erythrocytes endosoma corresponds to the new peaks IIA, IIIB and IIIc of heme-protein fraction demonstrated in chromatography of Fig. 3 b), c). It is an obvious fact that heme-protein fraction in erythrocytes endosoma is influenced sensitively by benzene. Benzene was considered to affect not only heme-protein, but also non-heme protein, because the decrease of non-heme protein fraction, peak-I, is remarkable.

## SUMMARY

1) Effect of benzene on erythrocytes endosoma in rat was investigated electrophoretically and chromatographycally.

2) In electrophoretic experiments veronal buffer (pH 8.6, ionic strength 0.06)

showed a good separation. Erythrocytes endosoma in normal rat was divided into six peaks with veronal buffer, which were named A, B, C, D, E and F according to the order of apparent mobility.

3) Except above six peaks small two peaks were observed in the early stage of electrophoretic run. Their apparent percentages were very small and apparent mobilities were larger than that of A. It was ascertained that the peaks corresponded to the peak-I observed in chromatogram.

4) By the chromatography, using IRC-50, four peaks were observed in erythrocytes endosoma of normal rat. The first peak-I was proven to belong to non-heme protein, because it has no light absorption in visible region. The other three peaks, i. e. peak II, peak III, and peak IV, have red colour and showed the characteristic property of heme-protein.

5) After two weeks with daily injection of benzene, the peak-F disappeared, and following further injection each peak began to be divided.

6) The complicated chromatogram was obtained with daily injection of benzene.

## REFERENCES

1) Pauling, L., Itano, H. A., Singer, S. J., Wells, I. C.: Science, **110**, 543 (1949).

2) Larson, D. L., Ranny, H. M.: J. Clin. Invest., **32**, 1070 (1953).

3) Morrison, D. E. Rudnicki, R. P. T. and Diggs, L. W.: Federation Proc., **13**, 267 (1945).

4) Hoch, H.: Biochem. J. (London), **46**, 199 (1950).

5) Derrien, Y. and Reynand, J.: Compt. rend. soc. biol., **147**, 660 (1953).

6) Boadman, N. K. and Partrige, S. M.: Biochem. J. (London), **59**, 543 (1955).

7) Prins, H. K. and Huisman, T. H. J.: Nature, **175**, 903 (1955).

8) Morrison, M. and Cook, J. L.: Science, **122**, 920 (1955).

9) Allen, D. W., Schroeder, W. A. and Balog, J.: J. Am. Chem. Soc., **80**, 1628 (1958).

10) Haurowitz, F.: Chemistry and Biology of Proteins, Academic Press Inc., New York, pp. 214-226 (1950).

11) Pauling, L.: The Harvey Lectuers, **41**, 216 (1955).

12) Singer, K.: Am. J. Med., **18**, 633 (1955).

13) Koike, S., Kawai, K. and Sugimoto, H.: Bull. Nat. Inst. Indust. Health., **2**, 1, (1950).

14) Hirs, C. H. W., Stein, W. H. and Moore, S.: J. Biol. Chem., **200**, 493 (1953).

## 要　　旨

### ベ ン ゼ ン 中 毒 の 実 験 的 研 究
### 3)　赤血球の内漿物に及ぼす影響

佐 藤 光 男　　長 谷 川 弘 道

ベンゼン中毒の診断項目に，末稍血液の血球数，形態の変化が主として用いられているが，こ

れらはベンゼン中毒の早期診断には適切であるとはいい難い。そこで著者等はベンゼンの注射によつて動物の赤血球内部の物質組成に質的変化が起るかどうかを電気泳動およびクロマトグラフィーの両面から追求し，ベンゼン中毒の診断に役立ちうるかどうかを検討しようと試みた。

電気泳動——赤血球を生理食塩水で数回洗い蒸留水を加えて破壊，遠心分離した上澄液内漿物を試料として用いた，泳動前に試料を pH 6.8 の veronal buffer (イオン強度 0.06) で 24 時間透析し HTD-1 型日立チゼリウス装置で 6℃ で泳動させた (6.4 mA, 200 V)，正常ラッテでは泳動順に A, B, C, D, E 及び F の 6 つの分層がみられ，みかけの易動度は夫々 100, 66, 54, 38, 24, 12 であり，面積百分率は 67, 7, 6, 12, 4, 4% であつた。ラッテに 1 ml/kg 体重の割合で毎日ベンゼンを皮下注射すると最後の F の峰はベンゼン注射 1 週間で減少を示し，2 週目以後では完全に消失する。また 2 週目以後になると C, D の区分も細分化する傾向がみられた。

クロマトグラフィー——赤血球内漿のクロマトグラフィーには弱酸性イオン交換樹脂 IRC-50 (0.9×10 cm) を用い pH 6.5 の citrate-phosphate buffer (0.035 M) で 24 時間透析したものを試料として，同じ緩衝液のナトリウムイオン濃度を 0.035 M, 0.14 M, 0.28 M と段階的に上げて 1 分画 1 ml/20 min の速度で automatic fraction collector を用い 4℃ の部屋で溶出せしめた。各溶出液について 280 mμ 及び 414 mμ の光吸収で追跡したところ正常ラッテでは最初に非ヘム蛋白区分 (41.6%) であらわれ続いて 414 mμ に大きな光吸収を示すヘム蛋白の小さな分画 (Peak-I 10.5% と Peak-II 28.0%) と大きなピーク (Peak-IV, 61.8%) が溶出された。ベンゼン注射群では 2 週目では非ヘム蛋白区分が著しく減少し Peak-II の前に新たに小さな Peak-IIA が現われ，さらにベンゼンを注射し続けると Peak-III の後にも小さなピークが現われ一層細かく分かれた複雑なクロマトグラムが得られた。

以上の結果からベンゼンを注射したラッテの赤血球内部の組成特にヘム蛋白区分に著しい影響を受けることが電気泳動及びクロマトグラフィーから得られた。

# EXPERIMENTAL STUDIES ON BENZENE POISONING

## 4. EFFECT OF BENZENE ON THE ACTIVITY
## OF LIVER XANTHINE OXIDASE

Goro KOIKE*, Hiroko KIMURA* and Shigeo KOIKE

Xanthine oxidase is an enzyme which catalyses the oxidation of xanthine to uric acid. Xanthine has been proven to arise from purine bases, the component of nucleic acids.

In 1952, Elvehjem et all[1] found that the activity of the enzyme in liver was influenced by the quantity and quality of food protein. The mechanism of the phenomenon are obscure, however, thereafter the activity of the liver xanthine oxidase in experimental animals was measured by many investigators as an indicator of nutritive value of food protein.

In benzene poisoning, the nutritive condition of the animals is affected with anorexia and other unknown factors, in spite of the fact that no marked severe damage was noted histologically in liver tissue. The decline of nutritive condition might affect the activity of the liver xanthine oxidase as well as the hematopoietic activity of the bone marrow. The present paper concerns the changes of the liver xanthine oxidase activity in benzene poisoning with reference to the nutritive condition of animals.

### METHODS

Livers were removed from the same animals as those described in Report 1 of this series. The resected liver was stored immediately in an ice bottle. After a certain period of time approximately one gram of the liver slice was extirpated and measured by a torsion balance. The slice was immersed in destilled water, and was homogenized in a Potter-Elvehjem glass homogenizer. The activity of the enzyme was measured by the modified method of Axelrod and Elvehjem.

### RESULTS

At the end of the first week of exposure, a striking decline of body weight was noted. Thereafter the weight began to gain gradually, but it could not reach the normal value at least at the end of four weeks. Fig. 1 demonstrates the change of the weight gain per day. The sharp decline of body weight recovered gradually

---

* Kagawa Nutrition College.

during exposure. The level of xanthine oxidase activity in benzene animals fell down at the end of the first week, and at the end of the second week it slightly rose up and remained at the same level throughout the experimental period.

During exposure the amount of food intake decreased due to the loss of appetite. Therefore the reduction of the activity of the enzyme might be attributed partly to the decreased amount of protein intake.

In order to elucidate the problem whether the reduction of the enzyme activity was caused by the toxic action of benzene or indirectly by the lowered nutritive condition following benzene poisoning, another group of rats were fed with reduced amount of food to obtain the similar weight to the poisoned rats and the activity of the enzyme was measured in both group.
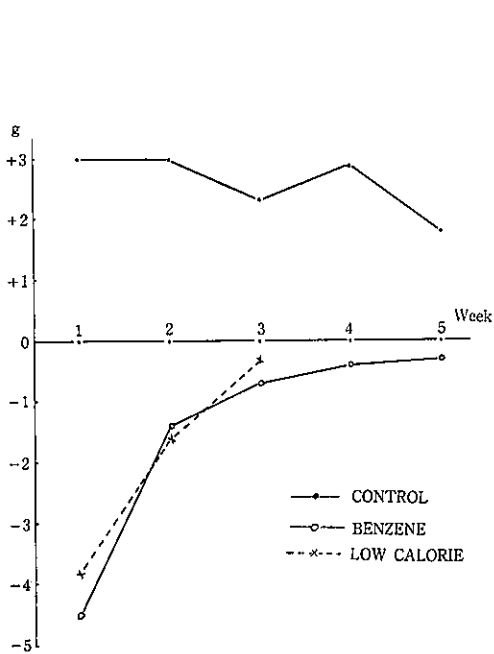
Fig. 1. Gain and loss in body weight per day
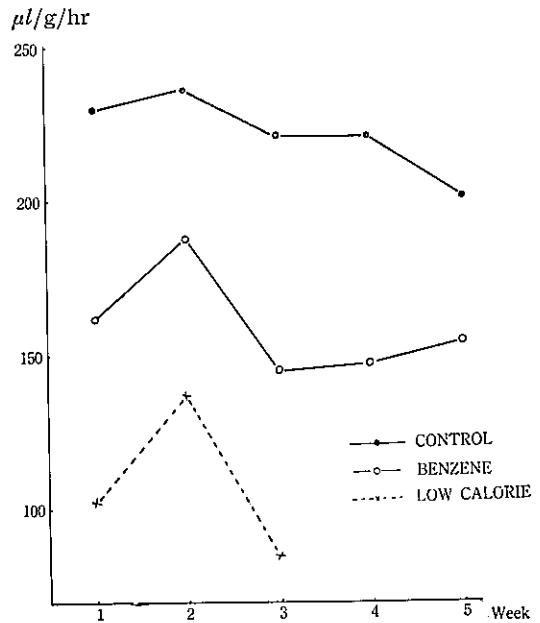
Fig. 2. Liver Xantine Oxide Activity

Table 1. Xanthine Oxidase Activity in Liver (O₂ $\mu$l/g/hr)

| Weeks after Treatment | Benzene group | | Control group | |
|---|---|---|---|---|
| | Number | X. O. A | Number | X. O. A |
| 1 | 5 | 162(116~208)$\mu$l | 4 | 230(203~254)$\mu$l |
| 2 | 7 | 189(124~267) | 5 | 237(188~271) |
| 3 | 7 | 145( 8~246) | 5 | 221(162~259) |
| 4 | 7 | 147( 91~205) | 5 | 221(173~247) |
| 5 | 7 | 155( 24~247) | 5 | 202(157~231) |

12

ACTIVITY OF LIVER XANTHINE OXIDASE

The results are shown in Fig. 1 and 2.  The reduction of xanthine oxidase in the fasted animals is greater than that of the intoxicated animals and the value of the latter lies between the control and fasted group.  From these results, it may be deduced that the activity of the enzyme would not be inhibited by benzene to the same extent as was found in the animals with restricted food.

SUMMERY

The activity of the liver xanthine oxidase was measured in rats poisoned with benzene and compared with that of fasted or control rats.

1.  Throughout the experimental period, the reduction of the activity was observed in benzene group.

2.  The activity of the enzyme in the fasted animals was proven to be lower than that of the exposured animals.

REFERENCE

1)  Elvehjem, C. A. and Litwak, G.:  J. Nutrition, **47**, 299, (1952).
2)  Axelrod, A. E. and Elvehjem, C. A.:  J. Biol. Chem. **140**, 725, (1941).

要　　旨

ベ ン ゾ ー ル 中 毒 の 実 験 的 研 究

第4報　肝キサンチン酸化酵素活性度に及ぼすベンゾールの影響について

小 池 五 郎　　木 村 広 子　　小 池 重 夫

　動物の肝臓のキサンチン酸化酵素の活性度は，食物蛋白の栄養価の決定に際して屢々測定されている。

　ベンゾール中毒に陥つた被検動物は，肝臓の組織像で顕著に障害を示さないのに，食思減退その他の原因によつて栄養状態が低下する。これが骨髄に於ける造血機能並びに肝のキサンチン酸化酵素の活性度に影響することが考えられる。この点をたしかめる為，第1報と同じ急性ベンゾール中毒にかかつた白鼠の肝についてキサンチン酸化酵素の活性度を測定した。

　体重1kg当り1ccのベンゾール注射後1週間で活性度は既に低下し，2週後に稍々上昇するが，その後5週の終りまでは1週目の値を持続する。しかし中毒群の活性度はいずれも対照に撰んだ正常群に比べて低い。この活性度の低下はベンゾールの直接の毒作用によるのか，或はベンゾール中毒に伴う食思減退の為かを調べるため，1群の白鼠の摂食量を制限して，中毒群と同じ体重を示す様にし，その肝について活性度を測定したところ，ベンゾール群よりも，却つて低下していた。即ちベンゾール中毒に伴う肝キサンチン酸化酵素の活性度の低下は，中毒による食思減退による影響を下回るものであるが，その理由については今後の研究にまたなければならない。

13

# STUDIES ON INFLUENCES OF SEVERAL FRACTIONS OF TUBERCLE BACILLI UPON THE TISSUE REACTION TO QUARTZ DUST*

Hideo YAMAMOTO, Kiyoyuki KAWAI and Hiroyuki SAKABE

In the course of several experimental studies on silico-tuberculosis, it has been noted that, the histopathologic feature of subcutaneous lesion produced by simulataneous injection of viable tubercle bacilli and of quartz dust, was characterized by a formation of conspicuous abscess, which was produced neither with the dust nor with bacilli alone[1].

Similar abscess formation was also observed in the subcutaneous tissue inoculated with viable tubercle bacilli (BCG) in combination with several kinds of dusts other than quartz[2]. Furthermore, it has been found that, used bacilli were not necessarily viable, and sufficient amount of dead tubercle bacilli were also capable to produce similar tissue reaction when administered in combination with these dusts[3-4].

The subjects of this brief report conern with a problem, which component or components of dead tubercle bacilli are responsible for the induction of such subcutaneous abscess in these experimental silico-tuberculosis.

## MATERIALS AND METHODS

Twenty healthy male guinea pigs weighing about 250 gm. were divided into five groups, and each four animals were kept in a cage and fed with pellet diet MF (Oriental Co.) and water ad libitum.

Tested fractions of tubercle bacilli were kindly supplied through courtesy of the Third Division of Bacteriology of the Institute for Infectious Diseases**, the University of Tokyo. Anderson's phosphatide $A_3$ and $A_4$, aceton soluble fat $A_5$ and purified wax were prepared from a mass of heat killed M. tuberculosis strain Aoyama B on Sauton's media, according to Anderson's original procedure[5]. Each 0.2 mg. of these fractions, with or without quartz dust, were suspended into 7 mg. of Tween 80, which was chosen as solvent from the results of preliminary experiments to test their tissue damage.

Quartz dust was prepared by water elutriation from grinded commercial quartz

powder of the Asahi Glass Co., which contained over 99% of free silica. Electron-microscopical estimation revealed that, about 98% of the obtained sample were under $5\,\mu$ in size. After successful sterilization, 10 mg. of the dust were suspended in 7 mg. of Tween 80 with or without a kind of bacillus fraction.

Before the experiment were started, each animal was confirmed for their negative tuberculin skin sensitivity with intracutaneous injection of 200 folds diluted old tuberculin. Hair was cut on the back skin in several sites, and 10 mg. of quartz dust suspended in 7 mg. of Tween 80 added with 0.2 mg. of one of the above mentioned fractions, were introduced subcutaneously in every sites of each two animals. Another series of groups, in which a group was consisted also from two animals, were similarly given with 0.2 mg. of one of the fractions without quartz dust. Other two animals were treated with quartz dust suspended in Tween 80, and another two were treated with Tween 80 only.
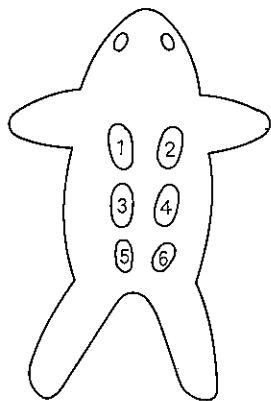
At every week after the inoculation, extent of the lesion was measured with scale before the foci was removed surgically. In all experimental animals, excision was made according to the order as seen in Fig. 1.

Through routine Zenker's fixation, paraffin embedding and H. E. and Marolly staining, the biopsy specimens were submitted to histological examination in order to observe the influences of the added tuberculous fractions upon the tissue reaction produced by quartz dust. From this stand point, the specimens from the groups inoculated solely with each tuberculous fractions or from the groups received only quartz dust were served as controls.



Fig. 1.

## EXPERIMENTAL RESULTS

Usually from a few days after inoculation, the skin at the inoculated site showed swelling and hyperemia, which allowed us to estimate roughly the extent of the lesions. Frequently, more or less evident induration became palpable in the central area of the lesions and their diameters were also measured. Due to slightly different distribution of the injected material in the subcutaneous tissue in each cases, more or less evident variations in the diameter were resulted between two animals of the same group, and also between each sites in an animal. However, it appeared that, the most extensive and persistent reaction were noticed when the wax fraction was added to the quartz dust, and the size of the lesions scarcely diminished up to the 5th week. Fraction $A_5$ made the quartz reaction almost similarly severe as seen in the addition of the wax. On the other hand, less marked influences were noticed with the addition of the fraction $A_3$ and $A_4$.

15

## HISTOLOGICAL EXAMINATIONS

*Tissue Reaction produced by Quartz Dust suspended in Tween 80.*

When quartz dust, suspended in Tween 80, was introduced into the subcutaneous tissue of the guinea pigs, moderate thick layer of familiar epithelioid-like cells was formed around the centrally situated quartz mass. A few numbers of nuclear debris were scattered around the quartz mass, however, polymorphnuclear leucocytes were practically abscent a week after the injection. Thereafter, the central aggregation of the quartz particles was gradually replaced by epithelioid-like phagocytes, and fibrosis proceeded centropetally from the outer zone. These features were quite identical with those of several foregoing descriptions, and added Tween 80 seemed to gave no essential alteration upon the proper quartz reactions.

*Tissue Reaction to Anderson's Fraction A₃ and Its Influences upon Quartz Reaction.*

A week after subcutaneous introduction of the Anderson's fraction $A_3$, suspended in Tween 80, rather slight infiltration of mononuclear cells developed around the central mass, which was gradually replaced by epithelioid cells with slight formation of intercellular collagen fiber, up to the end of the third week. Finally, edematous and hyperemic granulomatous tissue developed with coarse and rather thick bundle of collagen fiber.

Tissue reaction around the quartz dust added with fraction $A_3$, revealed no essential differences as compared with the features induced by quartz dust alone. Though slight increase of cellular response appeared to be resulted with the addition of fraction $A_3$, there was no emigration of polymorphnuclear leucocytes throught the whole course of the experiment.

*Tissue Reaction to Anderson's Fraction A₄ and Its Influences upon Quartz Reaction.*

Subcutaneously introduced fraction $A_4$ induced moderate infiltration of mononuclear cells, which converted later to epithelioid cells. Slight to moderate tendency of edema and hemorrhage was also noted. Rather loose edematous granulation tissue gradually replaced the central area of cellular infiltration up to the end of the second week, and finally fibrous capsule developed from the outer zone of the granulation.

Addition of the fraction $A_4$ to the quartz dust, resulted increase in intensity of the reaction to the quartz dust alone. A week after the injection, destructions of the infiltrated mononuclear cells were somewhat evident, and the thickness of layer of the " epithelioid-like cells " and of the fibrous capsule were obviously increased. Hemorrhage and edema in the outer fibrous layer were also assumed to be attributable to the effect of the added fraction $A_4$. However, any remarkable emigration of polymorphnuclear leucocytes was not resulted by the addition of this fraction. One of characteristic feature in this reaction was a formation of peculiar multi-

16

Fig. 2. A week after the inoculation of 50 mg. of quartz combined with 1 mg. of viable BCG. Note rather intense emigration of neutrophiles into the quartz mass. (modeaate magnification)



Fig. 3. A week after the injection of 10 mg. of quartz suspended in Tween 80. Layer of familiar epithelioid-like cells around the quartz mass. (moderate magnification)
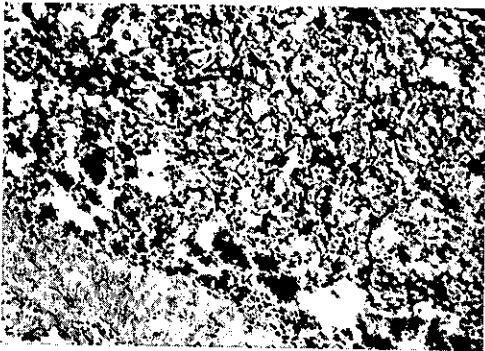


Fig. 4. A week after the injection of 10 mg. of quartz added with 0.2 mg. of Anderson's fraction A$_3$. There was no emigration of neutrophiles into the quartz mass. (moderate magnification)



Fig. 5. A week after the injection of 10 mg. of quartz added with 0.2 mg. of Anderson's fraction A$_4$. Hemorrhage in the epithelioid-like cell layer and in the fibrous layer. (moderate magnification)

nucleated giant cell with broad cytoplasm, in which numerous quartz particles were phagocytized.

*Tissue Reaction to Anderson's Fraction A$_5$ and Its Influences upon Quartz Reaction.*

After a week, centrally situated creamy mass containing fraction A$_5$ was replaced by moderate cell infiltrations which were composed of mononuclear cells intermingled with some polymorphnuclear leucocytes. Around the central area, there was rather thick layer of epithelioid cells with further outsided fibrous capsule. Leucocytic elements in the central infiltration persited up to the second week, and were almost completely absorbed until the end of the third week. Thereafter, the lesion converted to fibrous granulation tissue.

By the addition of the fraction A$_5$, tissue reaction against the quartz dust was slightly modified. Initial polymorphnuclear reaction around the quartz mass was
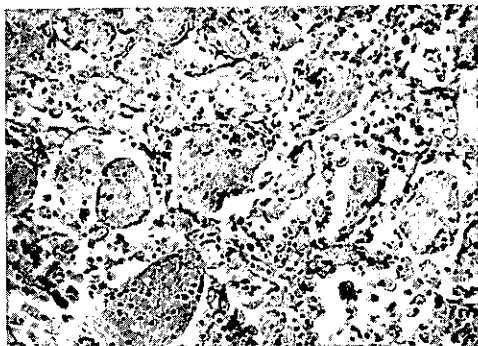
17

Fig. 6. Multinucleated giant cells in the granulation produced three weeks after the injection of quartz added with 0.2 mg. of Anderson's fraction A₄. (higher magnification)
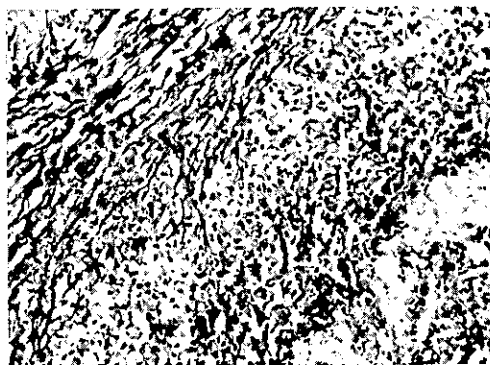


Fig. 7. A week after the injection of 10 mg. of quartz added with 0.2 mg. of Anderson's fraction $A_5$. Thick layer of epithelioid-like cells. (moderate magnification)
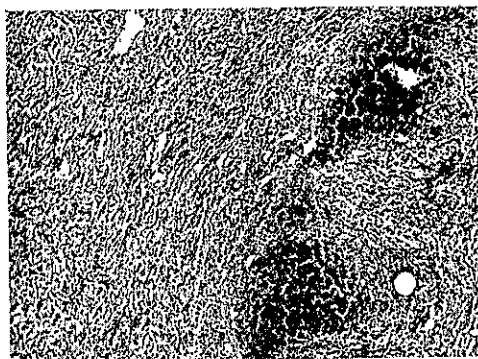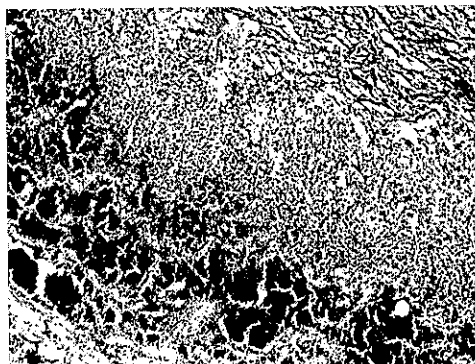


Fig. 8. A week after the injection of 0.2 mg. of Anderson's purified wax suspended in Tween 80. Minute abscess formation in the central area. (lower magnification)



Fig. 9. A week after the injection of 10 mg. of quartz added with 0.2 mg. of Anderson's purified wax. Intense emigration of neutrophiles into the quartz mass. (lower magnification)

somewhat intensified. But these leucocytes did not infiltrate into the quartz mass. From two weeks later, the tissue reaction appeared to show no essential difference from that produced by the quartz dust alone.

*Tissus Reaction to Anderson's Fraction Wax and Its Influences to Quartz Reaction.*

Tissue reaction to Anderson's purified wax was characterized by rather intense leucocytic emigration in the central area. There was accumulation of rather numerous polymorphnuclear leucocytes with slight tendency of tissue degeneration. Around such minute central abscess, there was rather intense mobilization of mononuclear cells, which converted later to epithelioid cells and then to giant cells of atypical Langhans type. After three weeks, the central abscess was absorbed and replaced with infiltrated mononuclear and epithelioid cells, and finally broad area of fibrosis was established.

18

When wax fraction was added to quartz dust, far more intense mobilization of polymorphnuclear leucocytes was evident as compared with those induced with wax fraction alone. These polymorphucleares penetrated into the mass or quartz particles and showed strong tendency of disintegration in their nuclei resulting the softening of the foci. The thick layer of epithelioid-like cells around the quartz mass was also infiltrated with some neutrophilic leucocytes. As weeks proceeded, epithelioid-like cells became more numerous and fibrosis developed from the outer zone. However, central abscess with the quartz mass persisted definitely even after four weeks. Briefly said, addition of the wax fraction to the quartz dust resulted significant mobilization of neutrophilic leucocytes into the quartz mass, and the foci persisted as an abscess unchanged at least up to the end of the fourth week. And the features of the abscess were quite similar to that described in the lesions produced by quartz dust combined with killed or viable tubercle bacilli.

## DISCUSSION

From the above discription, it is clearly revealed that, none of the studied fractions other than wax induced such intense emigration of neutrophilic leucocytes in and around the quartz mass stimultaneously injected. And the resulted persistent abscess showed remarkable similarity in every histological detail to the features of the foci decribed in the foregoing papers[1-3].

To the problem, which fraction or fractions of tubercle bacilli were responsible to convert the simple quartz reaction into such intense abscess formation under presence of tubercle bacilli, it is decidedly clear, that the responsible factor is wax fraction, so far this series of experimental studies concern. In other words, in the mechanism of such abscess formation in the experimental subcutaneous silico-tuberculosis, the biological action of wax may be one of the most important factors.

One of the authors Sakabe[3], with his collaboraters, pointed out that the tubercle bacilli, dead or viable, were capable to induce abscess formation when they introduced subcutaneously in combination with several kinds of dust other than quartz such as titanium-dioxide, which has been regarded as so-called " inert " dust. From our present results, it might be assumed quite probable that, the abscess formation in the cited papers could be also explained by the action of wax from the tubercle bacilli. If so, that is, if leucocytic infiltration in these several kinds of dust mass were similarily related to the biological action of the tuberculous wax, biological action of the dusts might be considered to have at most secondarily importance in explaining such intense neutrophiles induction.

Concerning with the action of leucocytic induction by the tuberculous wax, it should be pointed out that, the wax, when administered in combination with some tissue emulsion[6-7] or tissue extracts[6-7], was able to induce more leucocytes than those seen in the foci produced by separate administration of these components.

Furthermore, from the above described results, it is conceivable that sufficient amount of wax may posess a potency to induce some neutrophilic leucocytes. From these considerations, it is also suggested that, the severe neutrophilic emigration under discussion should be regareded as an intensified expresseion of the neutrophilic induction capacity of the wax under the influences of other several kinds of substances including dusts, for instance quartz.

Here, we have no intention going into further detailed discussion concerning the yet unclarified nature of the biological action of the tuberculous wax. We would like to refer only on the essential similarity between the tissue reaction produced by our wax and that described in the original paper[5]. Moreover, the tissue reaction around the subcutaneously introduced quartz mass was quite common in publications on several experimental silicosis in guinea pigs.

In this paper, we have described and discussed whether the tissue reaction against quartz dust was influenced with addition of some tuberculous fraction. In facts, modification of quartz reaction was not so essentially important in the case of fractions other than wax. Briefly said, if some fraction was added to the quartz dust, the main feature of the tissue reaction appeared to be determined chiefly by the quartz. And the effects of added fraction appeared to be noticed in the speed, with which the quartz mass was replaced by the mononuclear cells, in the intensity of the mononulcears mobilization and also in the alteration of the morphological appearance of these mononuclear phagocytes. For instance, when fraction $A_4$ was added to quartz dust, the epithelioid-like cells around the quartz mass frequently showed a type of multinucleated giant cell, which was not identical with that of Langhans type. Similar giant cell formation was discribed[8] by Watanabe in the lesion produced by the injection of quartz simultaneously with some of fatty acid with known chemical structure. Delayed oxidation of the tuberculous fraction or of these fatty acids under the presence of quartz particles in the cytoplasm of mononuclear cells might be possible explanation for such giant cell formation. In this respect, such phenomena could be regarded as a type of modification of tissue reaction against tuberculous fraction by the addition of quartz dust.

It has been well known that the prognosis of the silicosis was definitely influenced by the complication of tuberculous infection in human cases as well as in experimental conditions. Moreover, as seen in recent review by King et al.[9-10], it seemed highly probable, that the diffuse massive fibrosis in the coal-mine workers were also regarded as a result of superimposed tuberculous infection. In these connexion, it seemed important to know, whether there might be some causative relationship between the capacity of the tuberculous wax to alter the dust reaction and the proceeding effects of tuberculous infection against the dust lung. From the morphological observations, Shima[11] found similar abscess formation in the advanced tuberculous granulation in the lung of the guinea pigs, which

received simulataneous insufflation of quartz and viable tubercle bacilli (BCG). And the results suggest the need of further investigations.

## SUMMARY AND CONCLUSION

By addition of several fractions of tubercle bacilli, modification of the tissue reaction against quartz dust were studied in subcutaneous tissue of the guinea pigs. Among the fractions tested, addition of the Anderson's purified wax resulted intense emigration of neutrophilic leucocytes into the quarz mass, and produced long lasting abscess, which was essentially similar to that described in the foregoing experimental subcutaneous silico-tuberculosis. Other fractions, phosphatide $A_3$ and $A_4$ and ether soluble fat $A_5$ appeared to give no significant alterations to the quartz reaction in this respects.

## REFERENCES

1) Someya, S., Kusama, H., Sakabe, H. and Ohi, T.: Ann. Rep. Jap. Assoc. Tuberc. No. 1. 55-62, (1956).

2) Someya, S., Hayashi, O.. Kusama, H., Sakabe, H. and Ohi, T.: Ann. Rep. Jap. Assoc. Tuberc. No. 1. 63-69, (1956).

3) Sakabe, H., Nakagawa, M., Someya, S. and Hayashi, O.: Ann. Rep. Jap. Assoc. Tuberc. No. 1. 70-74, (1956).

4) Cummins, S. L.: Brit. J. Exp. Path. 21, 64-66, (1940).

5) Takeda, Y. and Ogata, K.: Jap. J. Tuberc. 2(3), 314-321, (1954).

6) Miyazaki, Y.: Tr. Jap. Path. Soc. 44, 1-, (1957) (Japanese).

7) Unpublished data.

8) Watanabe, J.: Tr. Jap. Path. Soc. 48, (1960) (Japanese).

9) King, E. J.: Recent Research in Infective Pneumoconiosis. Helsinki, International Congress on Occupational Health. Reports, Vol. 1, p. 283, (1957).

10) Byers, D. and King, E, J.: Lab. Invest. 8, 647-664, (1959).

11) Shima, I.: Jap. J. Indust. Med. 1, (7), 1-19, (1959) (Japanese).

## 要　　旨

## 結核菌分割の添加による石英組織反応の修飾について

山　本　秀　夫　　河　合　清　之　　坂　部　弘　之

すでに坂部およびその共同研究者によつて，弱毒結核生菌(BCG)を石英を含む種々の粉塵とともに，モルモット皮下に接種すると，その局所に強い好中球滲潤が認められ，かつこの反応は結核

菌あるいは粉塵をそれぞれ単独に注入した場合に比較して極めて高度であることが指摘された。

更にその後の検索によって，この反応を起すために要する結核菌は必ずしも生菌である必要はなく，死菌を種々の粉塵と混合して注入しても同様の膿瘍形成が認められることがわかつた。

本実験は，このような膿瘍形成が結核菌のどのような菌体成分によつて惹起されるかを知るために，Anderson の原法によつて Souton 培地に培養した人型菌青山 B 株から抽出した，類脂質 A$_3$ 及び A$_4$・エーテル可溶性脂肪 A$_5$・精製蠟等の各 0.2 mg. を 0.7 mg. の Tween 80 に懸濁して，10 mg. の石英粉塵に加えて，4 群各 2 頭のモルモットの背部皮下に注入し，週を遂つて接種局所を切除して病理組織学的に検索した。別に 6 群各 2 頭のモルモットが同様に Tween 80, 0.7 mg. の Tween 80 に懸濁した 10 mg. の石英粉塵・Tween 80 に懸濁した上記の結核菌分劃各 0.2 mg. 等の注入をうけ，同様に検索された。

得られた結果は，石英に対する本来の組織反応が，結核菌分劃の添加によつて，どのような修飾をうけるかという観点から整理されたが，事実蠟分劃以外の各分劃の添加された場合には，石英反応はその構造及び様相に本質的な変更を被るようには思われず，単核球反応の一般的な増強，A$_4$ 分劃添加の際に認められた Langhans 型とは異る粉塵を喰食した多核巨細胞の著明な形成等が，指摘を要する主な所見であつた。一方蠟分劃の添加によつて，石英粉塵塊の内部に向つて，甚た高度の好中球滲潤が起り，その結果形成された膿瘍は実験終了時即注入後 4 週を超えてもなお存続した。更にこの膿瘍の性格は，先に述べた結核菌全菌体を石英あるいは他の種々の粉塵に加えた場合に観察されたそれと，本質的に全く一致することが確められた。

以上の本実験によつて得られた成績の範囲からは，結核菌と石英粉塵の共存の下に認められる高度の好中球滲潤の発生機構を説明するには結核菌体から遊離される蠟分劃あるはその近縁物質が最も重要な役割を演じていると考えられる。また同時に石英以外の各種粉塵に対する反応も，結核菌の共存によつて同様に修飾される事実からみれば，粉塵自身の作用には粉塵には特異性を認めにくく，この意味では粉塵の生物学的作用は少くとも二次的な重要性を持つに過ぎないと考えられた。本実験の示すごとく，適当量の精製蠟にはそれ自身かなりの好中球遊出能が認められるので，この作用が石英その他の粉塵の共存によつて著しく強調された結果，そのような膿瘍形成を結果するという解釈が最も考え易い。しかし更に，粉塵のもつ一般的性格としてのこのような実験的皮下結核症の増悪作用は，人体の珪症結核あるいは Infective Pneumoconiosis の病理を考察する場合にも有意義であろうし，更に検討を要するものと考える。

# STUDIES ON THE HIGH EFFICIENCY DUST RESPIRATOR

Shigezi KOSHI

The dust respirator is widely used to prevent pneumoconiosis or other industrial poisoning caused by inhalation of harmful dust.

It may be emphasized to device a respirator to be loaded easily with a filter, with low breathing resistance, a high efficiency, and the respirator is light in weight.

Mechanical filtration depends upon the actual impingement of the particles on the fibers of filter. The breathing resistance of respirators decreases with increasing penetration rate of dust particles under the fixed effective filtering area and flow velocity. Extension of filtering area for decreasing the breathing resistance results in the increase of weight of respirator.

The effectiveness of the electrostatic mechanism for the dust collecting with filter media has been shown by the results of tests on a wool-felt filter impregnated with a phenol-formaldehyde resin, whose efficiencies with 99.99 per cent on an aerosol of 0.2 micron count mean diameter are reported[1].

Silverman et al. showed that the basic uncharged filtering efficiency can be doubled due to the mechanically induced electrical charge by wiping without any increase in resistance to air flow. But, the methods of preperation of resin used by Walton and Silverman et al. are not shown in the literature.

In this report, various phenol-formaldehyde resin were prepared and the penetration of the dust particle through the filters impregnated with these resin were tested.

Quartz of 0.28 micron of number mean particle diameter was used as test aerosol. From these tests, the filter media treated with p-ter buthyl phenol formaldehyde resin showed most effective filtering efficency among these coated filters with various resin.

## EQUIPMENT FOR PENETRATION TEST

The upstream and downstream dust concentration was measured by photoelectric penetrometer. The filtering efficiency, $E$ and penetration, $P$ were decided as follows.

$$E = 1 - \frac{C}{C_0}, \qquad\qquad P = \frac{C}{C_0}$$

where $C_0$ and $C$ refers to dust concentration upstream and downstream the filter.

Equipment for measuring the filtering efficiencey is shown in figure 1.

Dust laden air was drawn by the suction pump $P$, from the dust chamber
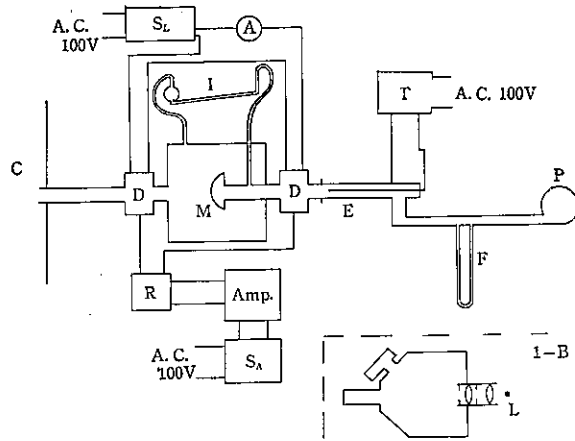
1 - A



Figure 1. Schematic diagram of equipment for penetration test.

having the capacity of about 25 cubic meters, passing through photoelectric dustiness meter $D$, a respirator or test filter mounted in the box $M$, the electrostatic precipitator $E$, and the flow meter $F$.

The cross section of dustiness meter is shown in figure 1-B. $L$ is light source and a scattered light by dust particles in air stream passing through at the right angle to the light beam was focussed on the photomultiplier, and the intensity of the scattered light was measured as a photoelectric current. Metal box $M$ connecting to the one end of the inclined manometer was deviced to be able to set and remove a dust respirator or test filter with ease. The dust particles penetrated a filter media was collected by electrostatic precipitator $E$ in order to keep clean the outlet air.

The filtering efficiency was tested with 30 liter per minute of air flow except the particular experiment. The effective filtering area of test piece was 38.5 square centimeter, so that the air passed through the test filter with velocity of 13 centimeter per second.

$S_L$, $S_A$, $R$ and $T$ are voltage stabilizers for light source and amplifier, circuit selector switch and alternative transformer of high voltage supplying to electrostatic precipitator, respectively. The current for light source was adjusted by ammeter $A$.

If the sensitivities of both dustiness meters are the same, an error of filtering efficiency or penetration may be amounted to 1 per cent, as the minimum measurable value is $\frac{1}{100}$ of full scale. In order to obtain the accurate penetration rate, the sensitivity of both dustiness meters was designed to be adjustable by the control of source intensity with optical gates. For the measurment of the low penetration such as below about 10 per cent, the sensitivity of downstream dustiness meter was

adjusted from 5 to 8 times to upstream.

When the dust cloud of heterogeneous in particle size was used as test dust, the mean particle diameter in downstream air of filter is generally smaller than in upstream. Therefore, the same penetration could not be expected in various methods for the determination of dust concentration, that is, weighing, number count or light scattering etc.. In order to compare the penetration rate determined by optical method to that by weighing method, following points must be taken into consideration.

If the total weight of dust particles is equal, the total surface area of particles increases reversely proportional to square of particle size, and the total cross sectional area increases reversely proportional to particle size. On the other hand, the intensity of scattered light by particles is complicated function of particle size, wave length of illumination, reflactive index etc.. According to the computation of light scattering in various conditions by Sinclair[2], the scattering cross sectional area $K_s$ alternatively varies from 0 to 5 with particle size below 1.1 micron and is closed to 2 for large diameter of refractive index from 1.33 to 2.0 with wave length 0.524 micron. Then, the scattering cross sectional area may be increased with decreasing particle size.

Therefore, the photoelectric method for measurment of dust concentration is more sensitive for smaller particles rather than larger particles.

Efficiencies of several dust respirators against calcium carbonate particles below 2 micron by Stokes diameter were measured by the weighing and the intensity of scattered light. These results are shown in figure 2. Efficiencies obtained by optical method showed a lower values than that by weighing method. For instance, efficiency of 70 per cent by weighing was comparable to 40 per cent by optical method.
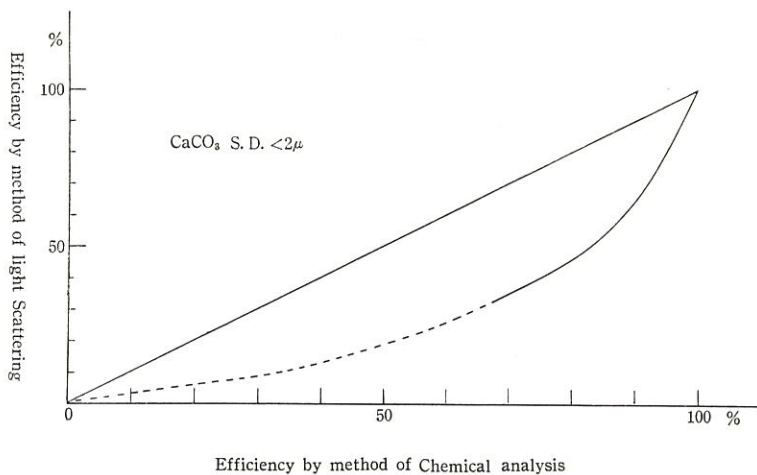


Figure 2. The comparison of efficiencies obtained by the weighing method and scattered light method.

## Test Aerosol

Fine quartz particles were used for penetration test, taking the prevention of silicosis into consideration.

Quartz powder disintegrated in ball-mill for two weeks was clouded by the disperser which modified Sinclair's " The Geyser "[5]. Then, the penetration test was carried on from one to two hours after clouding up to get the particles of similar distribution in each test.

The size distribution of test aerosol was examined for 557 particles caught by thermal precipitator with electron microscope and the results were shown in figure 3. It was confirmed from figure 3 that about 99 per cent of particles had the size smaller than 2 micron and the maximum frequency of size distribution was 0.2 micron.
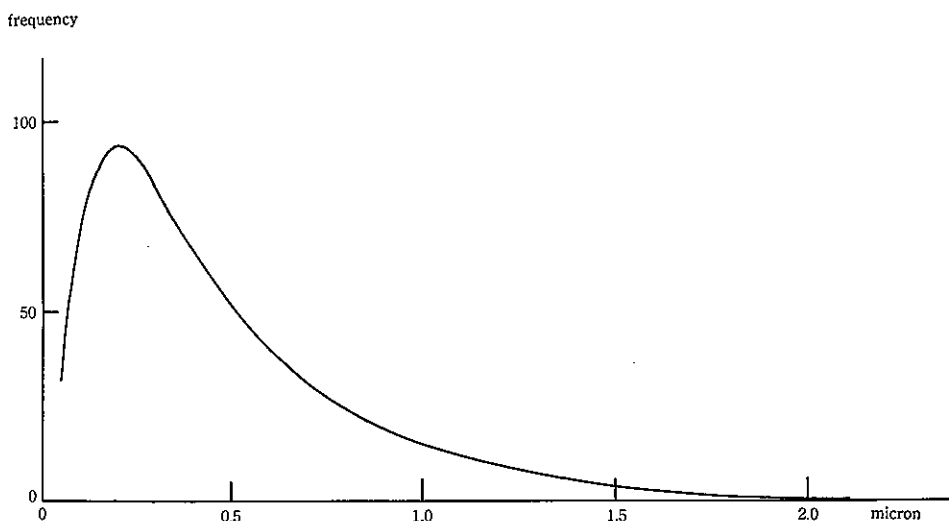


Figure 3.  Particle size distribution of test aerosol (quartz).
Size distribution was obtained on 557 particles.

## Preparation of Resins

The works on the improvement of filterling efficiency had been reported by many authors[1][4][5].

There were two methods to improve the filtering efficiency, one was the treatment of filter media with a certain substance and the other was the formation of filter media with very fine fibers such as asbestos fiber.

The former method was studied in this work.

Several phenol formalin resins were prepered with various catalyzers.

As phenol compounds, p- ter buthyl phenol, hexa tetramin tri phenol, p-cresol, m-cresol, 3.5 xylenol, *a*-naphtol and bis-phenol were used.  About 130 samples of

phenol formalin resins were obtained by various conditions of polymerization.

To screen out the effective resins from these samples, the test filters were made by following procedure. Moltplain sponge #60, 10 mm. thickness, was impregnated with methanol solution of each resin, and dried at 100°C.

Penetration test of these test filters revealed that some of them had high efficiency.

Then, the pieces of wool-felt were impregnated with these effective resins. The results of penetration test of resin wool-felt were shown in table 1. As shown

Table 1. Filtering efficiencyes of various resin wool-felt filters measured with the air velocity of 13 cm per second

| resin number | phenol compound | catalyzer | reaction temp. °C | time of reaction hr | time of after cure hr | concentration of solution for treatment % | mean efficiency for 4 test pieces | mean resistance in mm water gauge |
|---|---|---|---|---|---|---|---|---|
| B-1-3 | p-ter butyl phenol | ½N, HCl | 92 | 6 | 1.5 | 3.0 | 0.29 | 2.5 |
| B-2-3 | ,, | ½N, HCl | 92 | 4 | 2.0 | 3.0 | 0.27 | 2.5 |
| B-6-2 | ,, | 28% NH₃aq. | 92 | 0.6 | 1.0 | 3.0 | 0.47 | 2.9 |
| B-6-3 | ,, | 28% NH₃aq. | 92 | 0.6 | 1.5 | 3.0 | 0.44 | 2.5 |
| B-7-1 | ,, | 28% NH₃aq. | 92 | 1.6 | 1.0 | 3.0 | 0.33 | 2.5 |
| B-7-2 | ,, | 28% NH₃aq. | 92 | 1.6 | 2.0 | 3.0 | 0.33 | 2.5 |
| B-7-3 | ,, | 28% NH₃aq. | 92 | 1.6 | 2.5 | 3.0 | 0.69 | 2.9 |
| C-1-3 | hexa tetramin tri phenol | — | — | — | 2.0 | 3.0 | 0.34 | 2.9 |
| H-6-2 | ,, | — | — | — | 2.0 | 3.0 | 0.47 | 2.5 |
| H-7-3 | hexa tetramin tri phenol + n-buthanol | — | — | — | 2.5 | 2.0 | 0.33 | 2.5 |
| D'-6-1 | m-cresol | 28% NH₃aq. | 93 | 5.5 | 2.0 | 3.0 | 0.34 | 2.1 |
| F-0-1 | α-naphtol | — | 50 | 2.0 | 2.0 | 1.5 | 0.46 | 2.5 |
| J-6-2 | bis phenol | 28% NH₃aq. | 97 | 2.5 | 3.0 | 2.5 | 0.29 | 2.5 |
| original | — | — | — | — | — | — | 0.29 | 2.5 |

in table 1, the treatment of wool-felt with compound of α-naphtol, p-ter buthyl phenol and hexa tetramin tri phenol considerably improved the efficiency.

Compounds of p-ter buthyl phenol formed with alkaline catalyser were very effective but with acidic catalyser were not. The effectiveness of the compound of hexa tetramin tri phenol was reduced by mixing with 10 per cent n-buthanol.

To find out the suitable polymerizing condition for high effective resin, a series of p-ter buthyl phenol formaldehyd resins was prepared with various combination of amount of catalyzer, reaction temperature and time. Among these, the compound formed by following procedure showed the most high efficiency.

28 gr. of p-ter buthyl phenol was mixed with 40 ml. of 35 per cent formalin and added 4.5 ml. of 28 per cent liquid ammonia as a catalyzer, and then reacted at 92-94°C for an hour. The mixture of 40 ml. of formalin and 4.5 ml. of liquid ammonia showed an alkaline reaction.

The compound showed light brownish yellow and took a solid form at a room temperature but mollified at 70°C and liquidity increased with increasing temperature. Its molecular weight was accounted about 500-1,000 by Rast method. To investigate the infrared absorption of this compound, the sample was dissolved in carbon tetra chloride at the concentration of 2.27 weight to volume per cent and absorption were recorded.

Data are shown in figure 4. In comparison of absorption spectrum of the compound with that of p-ter buthyl phenol monomer, compound was assumed to be the syntetic product of formaldehyde and p-ter buthyl phenol. Further studies on the relation between a molecular structure and a effectiveness of resins, will be reported in other paper.
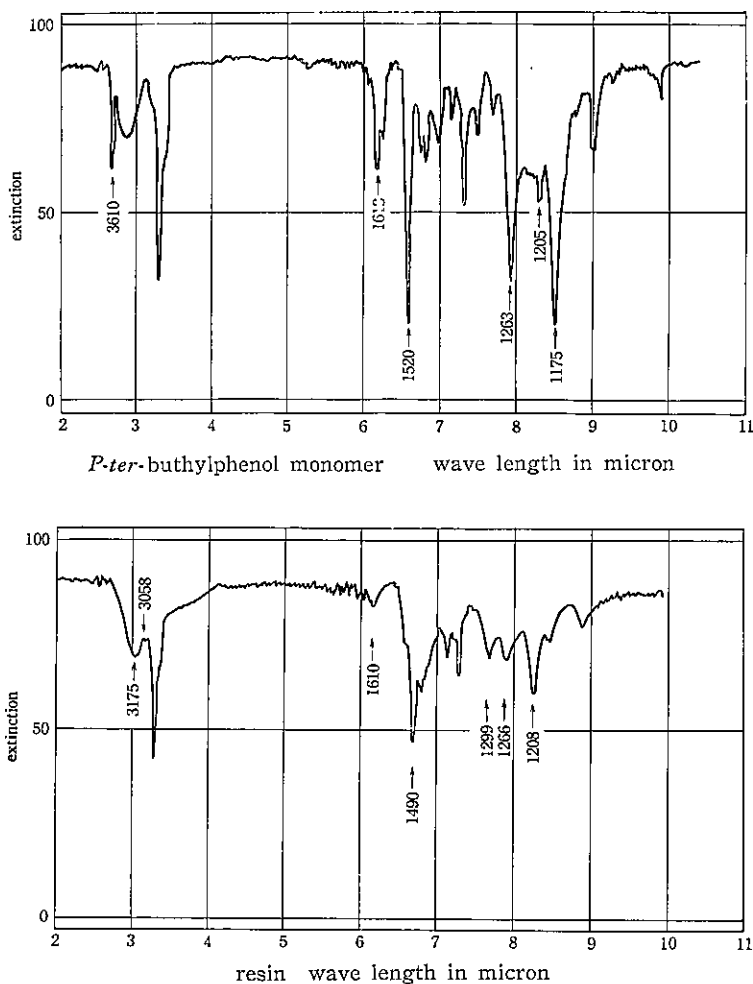


Figure 4. Infrared absorption spectrum of *p-ter*-buthylphenol monomer and resin N₂-3-3 in CCl₄ solution.

In order to test of reproducibility of resin, two resins, namely $N_2$-3-3, $N_2$-3-1, were prepared under the same condition.

Wool-felt of 2.5 mm. thickness were impregnated by each resin with concentration of 0.1, 1 and 5 per cent in benzene solution and dried at 110°C for 15 minutes. Results of penetration test on these samples were shown in figure 5-A. The
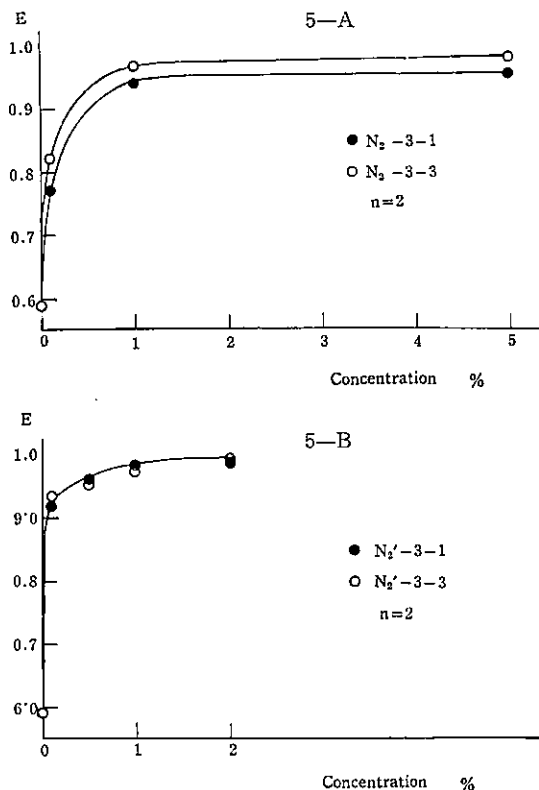


Figure 5.  Filtering efficiency of resin wool-felt
treated with various concentrations.

efficiency of the filter impregnated with $N_2$-3-3 or $N_2$-3-1 reached to nearly maximum at the concentration over about 1 per cent. However, the filter treated by $N_2$-3-3 was more effective than that by the other in any concentration.

When both resin was heated at 120°C, the color of resin changed to a fresh yellow making blister gradually. These treated resins were named $N_2'$-3-3 and $N_2'$-3-1 respectively.

The solution of these resins in benzene showed a maximum absorption at 425 milli-micron of wavelength as shown in figure 6.

Results of penetration test of filters impregnated with $N_2'$-3-3 and $N_2'$-3-1 were shown in figure 5-B. The relation between filtering efficiency and concentration of solution was the same on the both resin. And filtering efficiencies of these filters
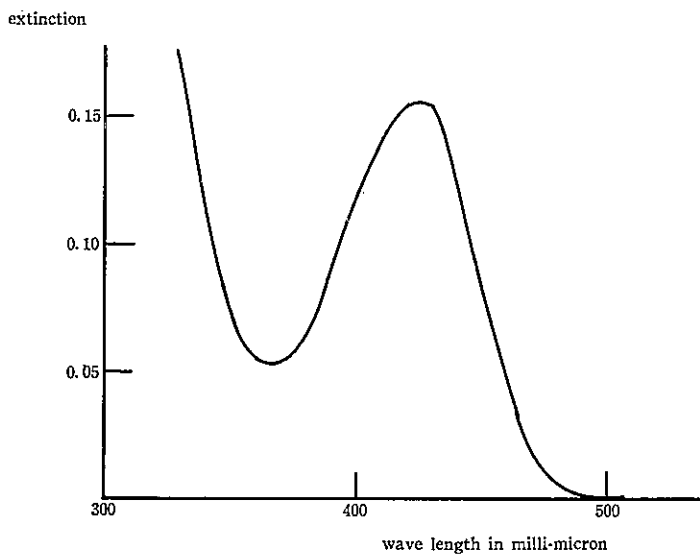
Figure 6. Absorption curve of resin (N-3-3) 0.1% solution in benzene.

increased considerably compared with that treated by $N_2$-3-3 or $N_2$-3-1. The difference of flow resistance between impregnated and untreated original filter was practically not significant.

From the results of four penetration tests during one week with same filters impregnated with 1 per cent solution of $N_2'$-3-1, it was found that the efficiency decreased appreciably, but the filters treated with 2 per cent solution did not. Decreased efficiency of the former was recovered by drying 40 minutes at 110°C. Therefore, it may be considered that an environmental high humidity reduces the efficiency of filter impregnated with low concentration.

## EFFECTS OF SOLVENT

The resin, $N_2'$-3-3 or $N_2'$-3-1, is soluble to various organic solvents. It is convenient for the treatment of filter to use a solvent which has high solubility, high vapour pressure and no toxicity. But, the solvent may affect the effectiveness of resin filter. Then, the effect of various solvents were examined.

Considering the molecular structure, benzene, toluen, aceton, methanol, and hexan were chosen as solvents. The wool-felt with thickness of 1 mm. were impregnated by 1 per cent resin solution of each solvent except last two solvents. As the solubility of resin to methanol and hexan was not exceed 1 per cent, 0.8 and 0.9 per cent solutions were used for these solvents. Results of penetration test were seen in table 2.

The resin wool-felt filter with benzene solution showed the highest efficiency and there were some differences among each solvent. It is difficult to explain these results by physical characteristics of solvents.

30

Table 2.  The efficiencies of resin wool-felts used various solvents in treatment

| solvent | dipol moment of solvent | vapour pressure of solvent | mean efficiency of two filters |
|---------|------------------------|---------------------------|-------------------------------|
| benzene | 0 | 75.16 | 0.338 |
| hexan | 0 | 121.3 | 0.263 |
| toluol | 0.52 | 23.5 | 0.240 |
| methanol | 1.73 | 96.0 | 0.275 |
| aceton | 2.79 | 179.6 | 0.248 |
| original | — | — | 0.137 |

## RELATION BETWEEN PENETRATION RATE AND FLOW VELOCITY

The efficiency of filter varies with flow velocity passing through the filter. The pattern of this variation closely depends on the mechanism of filtering action. Among the mechanisms of filtering actions, the deposition by Stokes law, the inertia effect, the diffusion effect and the electrostatic attractive force are most important.

The efficiency of any filter may be decided by the combination of these actions. The penetration pattern with flow velocity and particle size depends on the most dominant filtering action.  Mechanisms of filtering action were studied theoretically and experimentally by many authors.

The relations between filtering efficiency and particle size or flow velocity are illustrated in table 3 from the results obtained by former workers[6) 7) 8)].

Table 3.  Mechanisms of filtering action under the different flow velocity and particle size

| mechanisms of filtering action | advantageous for flow velocity | | advantageous for particle size | |
|--------------------------------|-------------------------------|-------|-------------------------------|---------|
| | higher | lower | larger | smaller |
| deposition by Stokes law | | ◯ | ◯ | |
| inertia effect | ◯ | | ◯ | |
| diffusion effect | | ◯ | | ◯ |
| electrostatic attractive force | | ◯ | ? | ? |

The filtering action by Stokes law deposition is more effective for larger particles and for lower flow velocity and that by diffusion effect is decreased with increasing the particle size or the flow velocity.

And that by inertia effect is increased with increasing particle size and flow velocity.  Then, for the collection of particles by the electrostatic atractive force, the low flow velociy is advantageous, but concerning particle size, the relation between particle size and charge density on the particle is not clear.

The flow velocity characteristic curves of various filter media, which was observed with the flow velocity from 6.7 cm. per second to 21.7 cm. per second, were shown in figure 7.  The efficiency of impregnated resin wool-felt was decreased with increasing flow velocity, whereas increased for untreated other filters.  From
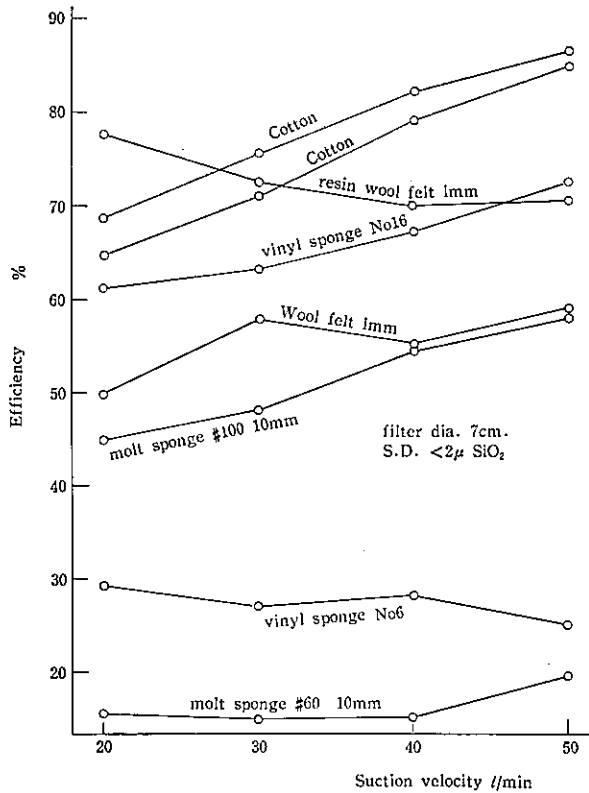
Figure 7. Flow velocity characteristic curves for each
filter media of effective area of 38.5 cm².

this result, it may be considered that the inertia effect is dominant for the filtering by untreated filters and electrostatic attractive force was added to the inertia effect for filtering by the resin wool-felt.

Formerly, the author suggested the following empirical relation between filtering efficiency and flow resistance for a filter whose inertia effect is the most dominant action[9]. If the particle size distribution and flow velocity are fixed,

$$E = 1 - \exp.(-KR^{\frac{1}{2}})$$

where $E$ is filtering efficiency, $R$ is flow resistance in mm. water gauge and $K$ is numerical constant decided by each filtering medium.

The effectiveness of filter increases with the value of $K$. Value of $K$ for various test pieces accounted from the experimental results were plotted against flow velocity in figure 8. The resin wool-felt showed especially large $K$ value at low flow velocity, nevertheless there were no marked difference for other pieces over all flow velocity. This is important in the application of filter for dust respirator. Both penetration and resistance of resin wool-felt can be decreased by extension of effective area. Accordingly, it is easy to design a dust respirator with high efficiency and low resistance by broadening the filtering area of resin wool-felt.
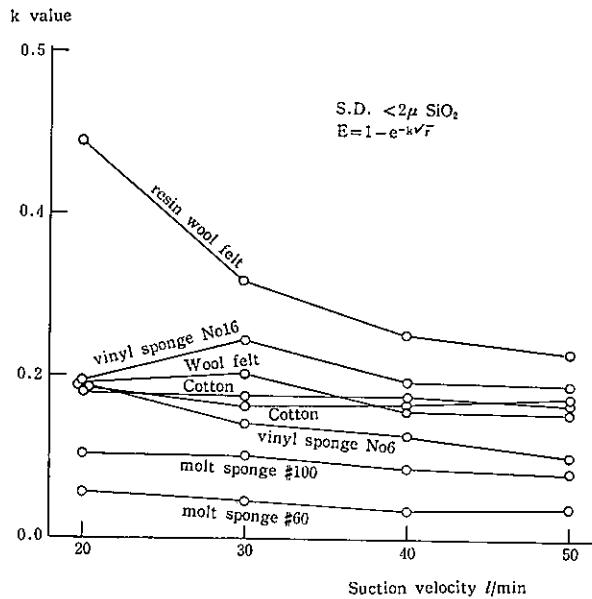
Figure 8. Change of $K$ values with flow velocity for various filter media of effective area of 38.5 cm².

## EFFICIENCIES WITH PARTICLE SIZES

The variation of efficiency of respirators with particle size was examined on a few dust respirators and newly designed respirator described in next chapter. The efficiencies of respirators for test are shown in table 4. For the test of filtering

Table 4. The filtering efficiency and inspiration of three test respirators

| respirator | with SiO₂ particle under S. D. 2 micron | | with CaCO₃ particle under S. D. 5 micron | |
|---|---|---|---|---|
| | efficiency | resistance mm H₂O | efficiency | resistance mm H₂O |
| A | 0.949 | 2.62 | 0.991 | 3.1 |
| B | 0.752 | 2.45 | 0.965 | 3.1 |
| C | 0.662 | 11.90 | 0.949 | 14.0 |

efficiency, weighing and photoelectric method were used. The method of weighing was the same with the approval test of dust respirator in Japan, that is, calcium carbonate particle below 5 micron diameter was used as test aerosol and dust particles in upstream and downstream of respirator were collected by electrostatic precipitator, and then each dust concentrations were estimated by chemical titration.

The respirator A and B were newly designed respirators and both had the same structure and the same filtering area. The difference between A and B was only that the wool-felt for filter was treated with resin in A respirator and not in B.

To study the relation between the filtering efficiency and particle size, the particles passed through the respirator were collected on the sheet mesh for electron

33·

microscope inserted to high volume electrostatic precipitator. The size distribution of penetrated quartz particle was observed on about 500 particles by electron microscope at the magnification of 5,000×. In advance, it was confirmed that the size distribution obtained by this method is the same to that by thermal precipitator.

The flow velocity passing through the filtering media was 3.4 cm. per second for respirator A and B, 7.9 cm. per second for C. These velocity are comparable to volume velocity of 30 liter per minute. The relation between particle size and efficiency accounted from size distribution and particle number in upstream and downstrem air was shown in figure 9. Respirator A showed higher efficiency than B or C especially at small size range.
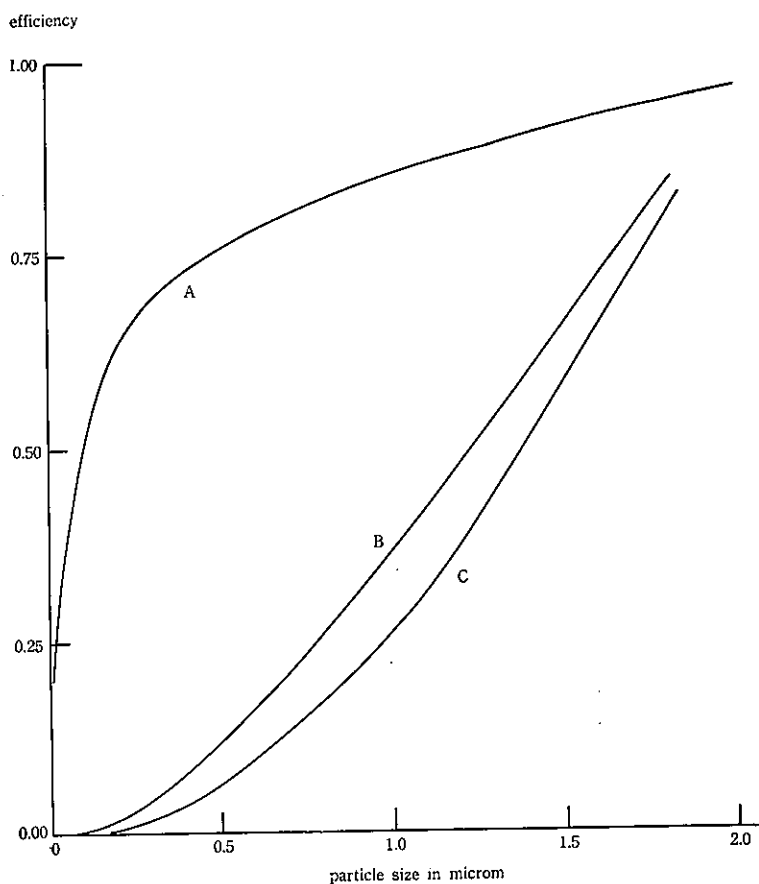
Figure 9. The filtering efficiencies with particle size
for three kinds of test respirator.

## DESIGN OF NEW DUST RESPIRATOR

New dust respirator with resin wool-felt was designed as illustrated in photograph 1. The principal part of face piece was made by Hyzex and vinyl rubber was used for the part coming with skin surface.

34
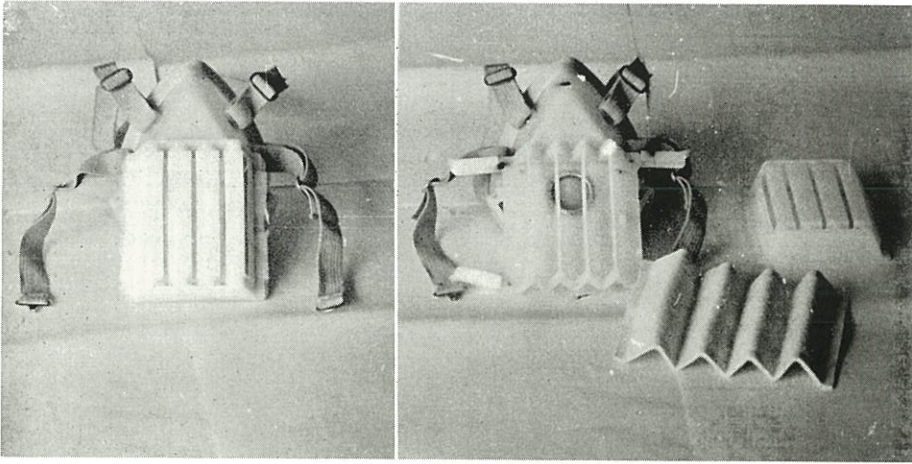
Photograph 1. Newly designed dust respirator

It is easy to take and out the resin wool-felt filter impregnated with 2 per cent resin solution, size of $10 \times 20$ cm. and thickness of 1.5 mm.. It weights approximately 145 gr., and is designed to have a inspiratory resistance of 3.0 mm. water gauge at 30 liter per minute of air flow and to arrest 98.5 per cent of a fine quartz particle and 99.3 per cent of calcium carbonate cloud.

## DURABILITY TEST IN METAL MINE

For the durability test, filters impregnated with 1 per cent solution were applied. Initial efficiencies of 135 respirators used for the durability test were shown in table 5.

Table 5. Initial filtering efficiency of 135
respirators applied to durability test

| filtering efficiency | number of respirator |
|---|---|
| over—0.99 | 8 |
| 0.98—0.99 | 38 |
| 0.97—0.98 | 57 |
| 0.96—0.97 | 24 |
| 0.95—0.96 | 8 |

The durability of these respirators were tested at a pit face, the other underground work place and dressing plant in 8 metal mines.

The efficiency and resistance of each respirator were measured before application and after the use for one week, one month and three monthes. The results of durability test were shown in table 6.

The difference of durability of dust respirator among these working places may be explained by the working time, dust concentration and environmental humidity.

Table 6.  Results of durability test at 8 metal mines

| test duration | | a pit face | the other underground work place | dressing plant |
|---|---|---|---|---|
| one week | number of respirator | 18 | 21 | 10 |
| | mean applied time (hours) | 29.0 | 29.5 | 31.1 |
| | mean efficiency after use | 0.896 | 0.904 | 0.913 |
| | mean resistance in mm $H_2O$ | 2.90 | 2.83 | 2.82 |
| one month | number of respirator | 15 | 12 | 10 |
| | mean applied time (hours) | 118.3 | 144 | 160.0 |
| | mean efficiency after use | 0.870 | 0.894 | 0.907 |
| | mean resistance in mm $H_2O$ | 2.96 | 2.84 | 2.87 |
| three months | number of respirator | 10 | 11 | 5 |
| | mean applied time (hours) | 305.0 | 349.0 | 46.0 |
| | mean efficiency after use | 0.812 | 0.866 | 0.866 |
| | mean resistance in mm $H_2O$ | 3.10 | 2.81 | 2.69 |

The durability of the resin wool-felt filter was not determined from these experiment, as the effects of environmental and other conditions were complicated. However, the filters were colored gradually by adherence of dust particles. The filtering capacity of the filter can be roughly estimated by the change of color on the surface of filter. Both surfaces of the filter were illustrated in photograph 2. As shown in photograph 2-A, the unused filter has a light yellow. The filter which was used for 34 hours (one week) at dressing plant was shown in photograph 2-B. The inlet side was colored by adherence of dust but the opposite side was not. The efficiency of this filter was 94 per cent.

In photograph 2-C, a spot of dust was found not only on the inlet side but also clearly on the opposite side. This filter was used for 138 hours (one month) at the other underground work place and showed the efficiency of 90 per cent.

The efficiency dropped by application still longer time and the same intensity of color of dust spot was seen on both sides as shown in photograph 2-D. This filter was applied for 218 hours (three monthes) at a pit face and showed efficiency of 68 per cent.

If the filter is exchanged before the spot is found on the opposite side, the amount of dust inhalation may be reduced below 10 per cent of environmental dust concentration for fine quartz particles, and below 3 per cent for ordinary industrial dust.
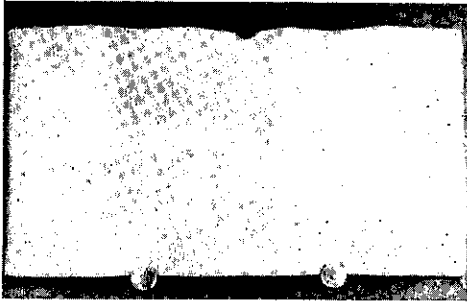
## SUMMARY

In order to design a respirator with high efficiency and low breathing resistance, many phenol formaldehyde resins were prepered and the method of treatment of filter by resin was studied. The penetration rates of dust through filters were
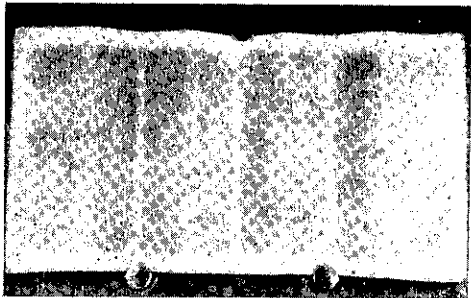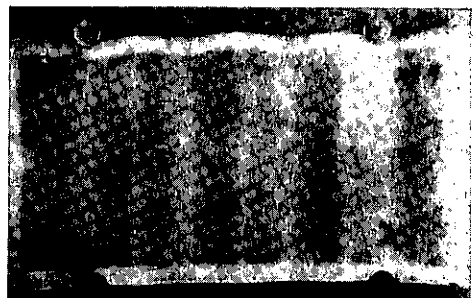
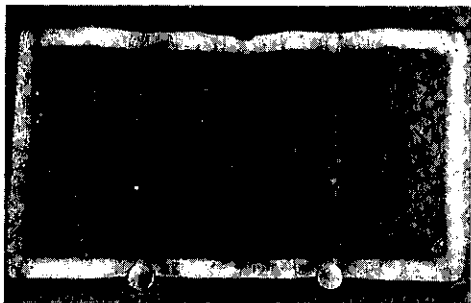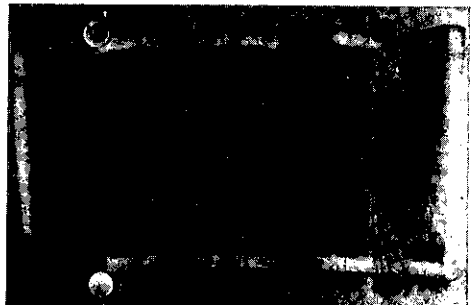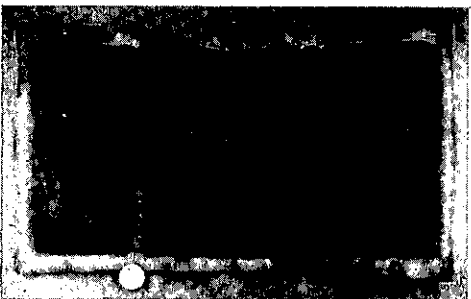air inlet side                                    opposite side



2-A: Original resin wool-felt, efficiency of 98.5 per cent



2-B: Applied at a dressing plant for 24 hours (one week), efficiency of 94 per cent



2-C: Applied at other underground for 138 hours (one month), efficiency of 90 per cent



2-D: Applied at a pit face for 218 hours (three months), efficiency of only 68 per cent

Photograph 2.

tested by photoelectrically.

The resin wool-felt impregnated by one of the compound polymerized from p-ter butyl phenol showed a high efficiency without increasing the resistance of original wool-felt. Some characteristics of this resin wool-felt filter such as effects of flow velocity, humidity and solvents, and penetration rates with the change of particle size were examined.

Newly designed dust respirator with resin wool-felt showed the filtering efficiency of 99.3 per cent for calcium carbonate particles and of 98.5 per cent for fine quartz particles with breathing resistance below 4 mm. water gauge at 30 liter per minute.

Results of durability test for three monthes with 135 respirators at 8 metal mines were reviwed.

## REFERENCES

1) Walton, W. H.: Chem. Defense Exp. Station, Porton, England, Dec., (1942).
2) Sinclair, D. and La Mer, V. K.: Chem. Rev. 44, 245, (1949).
3) Sinclair, D.: Handbook on aerosol, U. S. A. E. C. Washington, DC., 77, (1950).
4) Green, H. L. and Lane, W. R.: Particulate clouds, 329 (1957).
5) Rossano, A. T. and Silverman, L.: Heating and ventilating's reference section, 102 May (1954).
6) Rodebush, W. H.: Handbook on aerosol, U. S. A. E. C. Washington, DC., 117 (1950).
7) Green, H. L. and Lane, W. R.: Particulate clouds, 167–205 (1957).
8) Pereles, E. G.: Safety in Mines Res. Est. Res. Rept., No. 144 (1958).
9) Koshi, S. and Sakabe, H.: J. of Science of Labour, 27, 449 (1951).

## 要　旨

### 高性能防じんマスクに関する研究

#### 輿　重　治

一般に防じんマスクは沪じん効率が高いものでは通気抵抗が大きいか，あるいは重量が重い欠点がある。この研究では通気抵抗が 4 mm $H_2O$ 前後で，かつ沪じん効率が 95% 以上であつて，重量 150 gr 以下の防じんマスクを作ることを目的とした。このためには従来の沪層では不可能であるのでフェルトその他の沪材に特殊な加工を施すことによつて沪層自身の効率を抵抗の上昇なしに向上させる研究を行ない，この結果にもとづいて所期の防じんマスクを設計することが出

来たので報告する。

効率測定は 2μ 以下の石英（分布の最大値は 0.2μ）を使用し，光学的方法によつて行なつた。この方法は従来の方法に比べて低い沪じん効率を示す。

沪層の裏面処理の材料としてフエノール系のフオルマリン樹脂約 130 種類のうちから有効な樹脂をさがし出すことができた。

この樹脂の 2% ベンゾール溶液によつて処理されたフエルトは処理されないフエルトに対し 2 倍の効率を示す。

この樹脂は *p-ter* buthylphenol のフオルマリン重合体であるが，酸性触媒によるものは全く効果はなく，アンモニアまたは苛性ソーダを触媒として使つたときにのみ有効である。

処理に用いる溶媒としては，多くの有機溶媒が考えられるが，沪層の有効性はベンゾールを溶媒としたときが最も高い。この原因については更に研究を進める必要がある。

処理した沪層の最も大きな特徴は，一般に用いられている従来の沪層では通気速度が大きくなると通気抵抗とともに効率も上昇するが，この沪層では通気速度の上昇とともに効率が低下することである。このことは非常に重要なことである。すなわち従来の沪層では通気抵抗を少くするために沪道面積を大きくすると効率は低下する，これに反し処理を受けた沪層は沪層面積の増大とともに効率が上昇するので通気抵抗を少くすること，効率を上昇させることが同時に可能になる。

主としてこの流速特性から，この処理沪層ではある程度静電引力の粉じんを捕集する効果が利用されていると考えることができる。

次にもう一つの特徴はこの沪層が非常に小さい粒子までも捕集することができる点である。石英粒子で実験した結果では 0.2μ の粒子に対しても 60% 以上の効率をもつている。

以上のような特性をもつた沪層が出来たのでこれを利用した防じんマスクを試作した。

面休はハイゼマクスを用い接顔部にはゴム状のビニールを用いた。全重量は 145 gr で通気抵抗は初抵抗約 4 mmH$_2$O であつて，効率は 2μ 以下の石英に対して 98%，国家検定と同様に 5μ 以下の炭酸カルシウムを用いたときは 99% 以上である。

マスクの耐久性を調べるために 135 箇のマスクを坑内で使用し，1 週間，1 ヵ月，3 ヵ月目にそれぞれ効率抵抗およびマスクの破損を調べた。

135 箇のうち 3 ヵ月の使用で破損したものは全体の 5% 以下であつた。効率の低下は作業時間，環境中の粉じん濃度，湿度等に関係するので一概に期間を決めることはむづかしいが，粉じんの付着による沪層の汚れが裏面にまではつきりと認められるようになると効率は 90% 以下になる。このような状態になる使用日数は選鉱場では 2〜3 ヵ月切羽では約 1 ヵ月，その他の坑内作業では 1〜2 ヵ月位であつた。
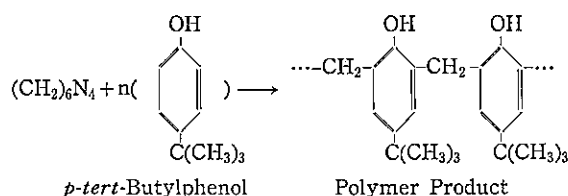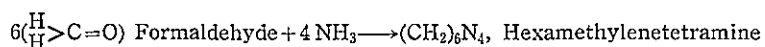
裏面にはつきりした汚染が認められる以前に新しい沪層を交替して使用するようにすれば，このマスクによつて一般の作業場粉じんに対し常に 95% 以上の効率を保持し得るものと考えられる。

# AN INVESTIGATION OF MOLECULAR STRUCTURE OF THE POLYMER SYNTHESIZED FROM *p-tert*-BUTYL-PHENOL AND FORMALINE WITH AMMONIA BY MEANS OF AN INFRARED SPECTROSCOPY*

Reisuke SODA

It was reported by S. Koshi[1] that the efficiency of a dust respirator was increased and the charging power of a fiber was appreciably strengthened when the fiber of a mask filter was treated with the product synthesized from *p-tert*-butylphenol and formaline with ammonia. This report intended to interpret these phenomena on the standpoint of the theory of a molecular structure by means of an infrared absorption spectroscopy and to aid the investigation for a more effective and useful mask.

The reaction of the polymerization is the same one as that of the alkaline catalytic phenol resin, therefore the mechanism of this reaction can be described as follows.

$$6(\substack{H\\H}{>}C{=}O) \text{ Formaldehyde} + 4\,NH_3 \longrightarrow (CH_2)_6N_4, \text{ Hexamethylenetetramine}$$



*p-tert*-Butylphenol          Polymer Product

The result of the measurement suggests that the molecular weight of the polymer is about 1,000. This seems to be the mean molecular weight, and the degree of the polymerization is considered to be not so large.

This paper includes the measurement of infrared absorption spectra of these substances in several states and the discussion of the molecular structure which each substance can take in several states.

## METHOD

The samples were given from S. Koshi. *p-tert*-Butylphenol were recrystallized from chloroform and the polymer N-1, 2, 3 and 6 were recrystallized from benzene. (Sometimes *p-tert*-butylphenol was distilled under vacuum.)

---

* Presented at the 13th Annual Meeting of the Chemical Society of Japan held in Tokyo, April, 1960.

The solvents used—benzene, carbon tetrachloride, carbon disulfide, toluene and actone—were c. p. grade or spectral grade and were not purified furthermore. The thickness of the rocksalt window cell which was used for the measurement of the solution spectrum was about 0.1 mm. The concentration of the solution was the order below 4% by the weight per volume. The measurement of the solid spectrum was carried out with a nujol mulling method, a hexachlorobutadiene mulling method and the method by which the thin layer of the sample was formed from its solution by the evaporation of the solvent on the rocksalt crystal plate. Since the orientation of the solid sample on the rocksalt plate was scarcely observed in the last process, most of all the measurements of the solid spectra were carried out by the last method.

The infrared absorption spectra were measured with the Perkin Elmer Model 137 Infracord Spectrophotometer. More detailed spectra were obtained by the Perkin Elmer Model 321 Spectrophotometer and the Shimazu Seisakusho Type IR Spectrophotometer at the Government Chemical Industrial Research Institute, Tokyo. The Spectra in the region of C-H stretching vibration were measured with the Perkin Elmer Model 112 G Grating Spectrophotometer at the Department of Chemistry, Faculty of Science, University of Tokyo.

## RESULTS

*1 The Spectra of the Solids.*

Aspects of the spectra of the solids were resembled to those of the high degree of the polymerization of other phenol resins[2]. In the high polymer of the phenol resins, the chain bridges are made at both of "ortho" and "para" positions to an OH group of a benzene nuclei as follows.
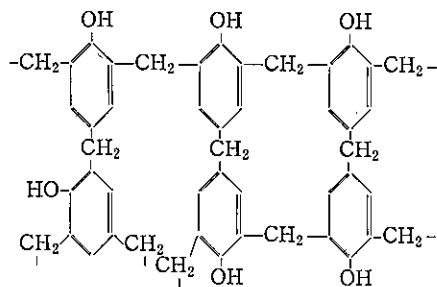


Then the resemblances may be interpreted from the fact that the "para" position of *p-tert*-butylphenol is occupied by the tertiary butyl group and may not be considered as the evidence proving that the polymer has essentially a high molecular weight.

As illustrated in Fig. 1 and 2, comparing the spectra of the polymers N-1, 2, 3 and 6, and *p-tert*-butylphenol and hexamethylenetetramine which was produced as
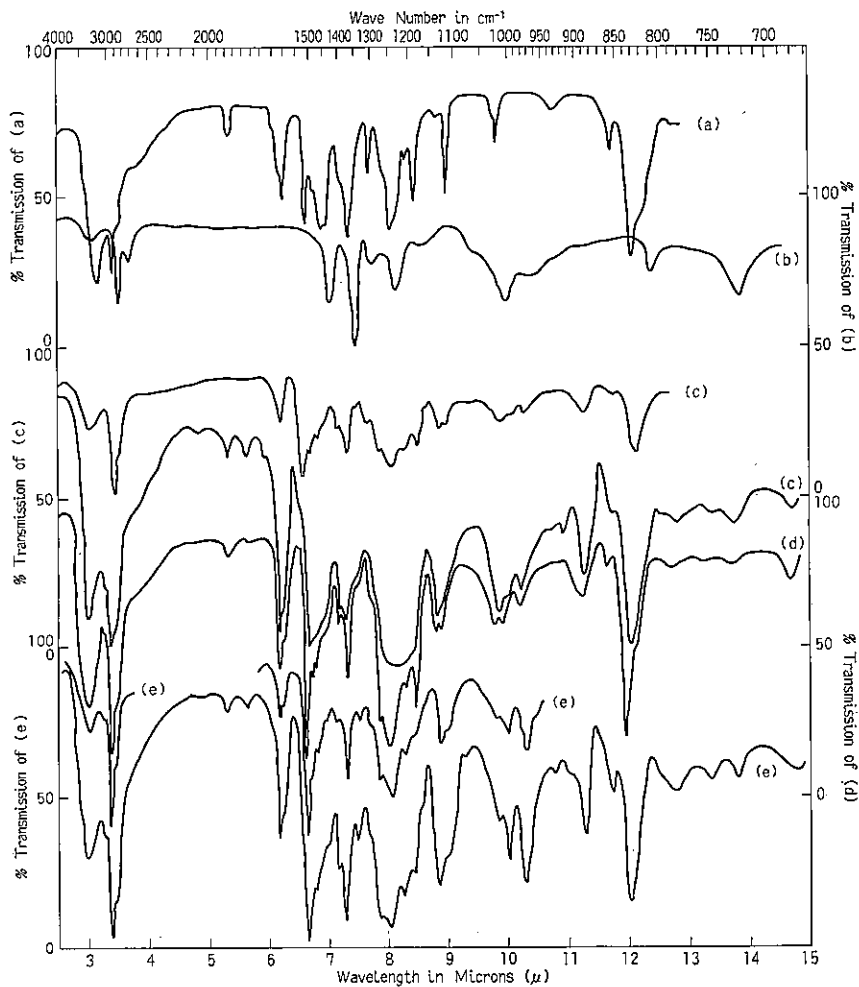
Fig. 1.   Spectra of solids (thin films between two rocksalt crystal as like as sandwitch)
(a)   *p-tert*-Butylphenol recrystallized from CHCl₃ (but no absorption bands due to CHCl₃ are observed).
(b)   Hexamethylenetetramine (c. p. grade) in nujol (mulling method).
(c)   Polymer N-1-3, thin film is made with same method as (a), thicker film and thinner film.
(d)   Polymer B-91, viscous liquid is pressed between crystal plates.
(e)   Polymer N-3-1, thin film is made with same method as (a), thicker film and thinner film.

the intermediate product of the reaction, it was recognized that some components of the impurities in the polymers, N-1, 2 and 3, are these reactants.   It was assumed that the absorption bands drawn with the arrows in the spectra were attributable to the vivration modes of these substances.   The spectrum of the sample N-6 showed that this sample was a typical and highly pure substance.   From the efficiency of the mask and the process of the synthesis, this conclusion was also supported.
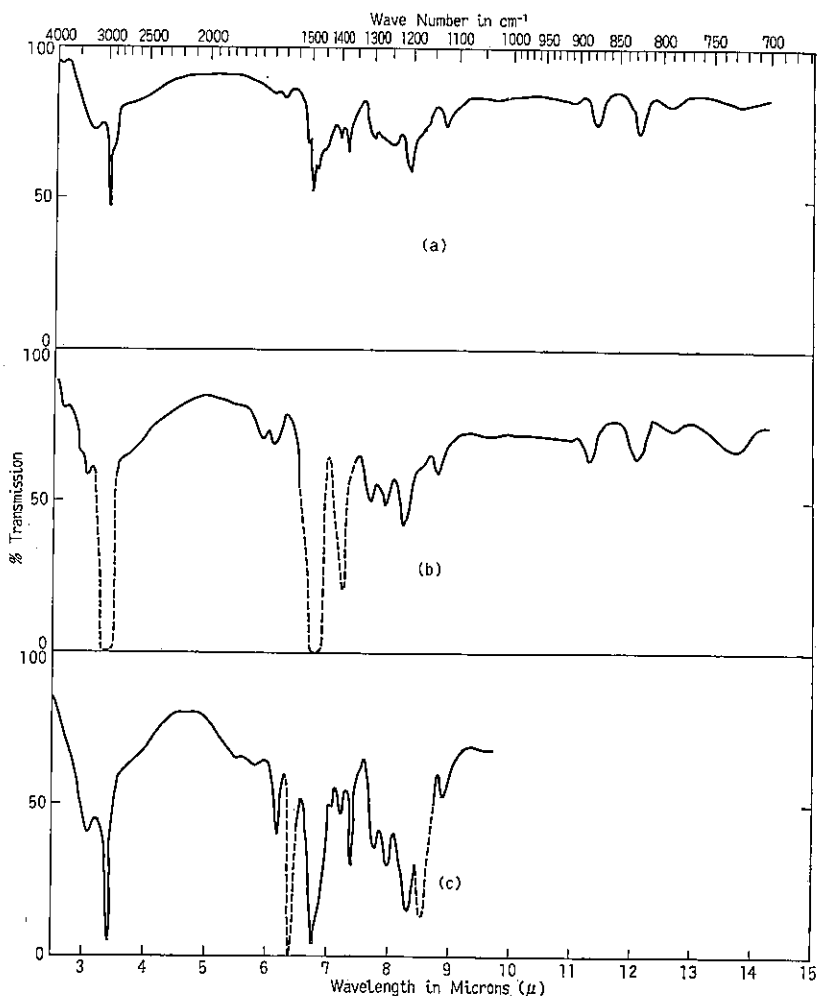
Fig. 2.  Spectra of solids of polymers N-6 in several mediums

(a)  Thin film is formed by evaporation of solvent benzene from dilute solution on rocksalt crystal plate. (no absorption band due to benzene is observed).
(b)  Nujol mulling method (paste between two crystal plates).
(c)  Hexachlorobutadiene mulling method (paste between two crystal plates).
       Interruption of mulling medium is indicated with broken line in spectral curve.

Therefore, for the measurements of the spectra of the solutions, the sample N-6 was used.

## 2   *The Spectra of the Solutions.*

The infrared absorption spectra of the solutions of the samples in the region of 2 to 15 microns were illustrated in Fig. 3, 4, 5 and 6. In the region of about 3 microns, the spectrum of a solid state of *p-tert*-butylphenol showed the very broad absorption band at the center of about 3,200 cm.$^{-1}$ but spectrum of its solution showed the sharp 3,600 cm.$^{-1}$ band accompanied with the broad band near 3,450 cm.$^{-1}$. In the

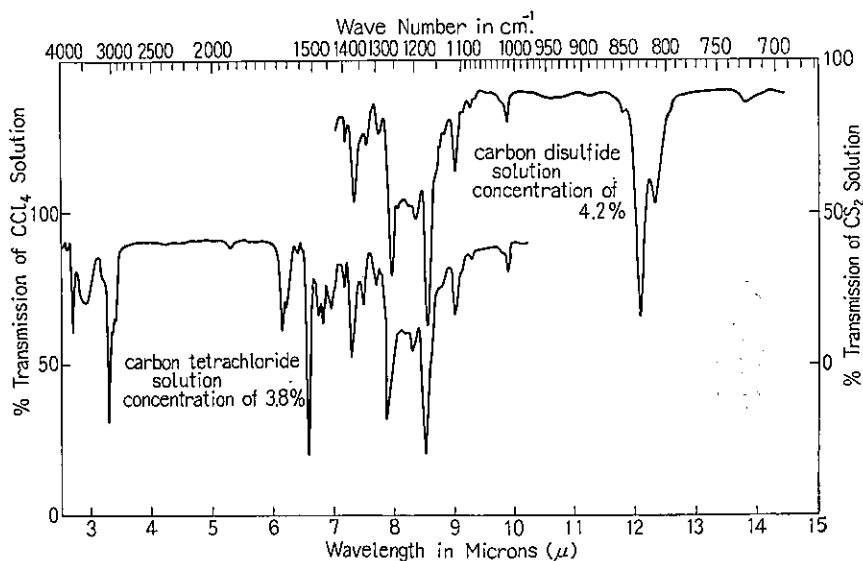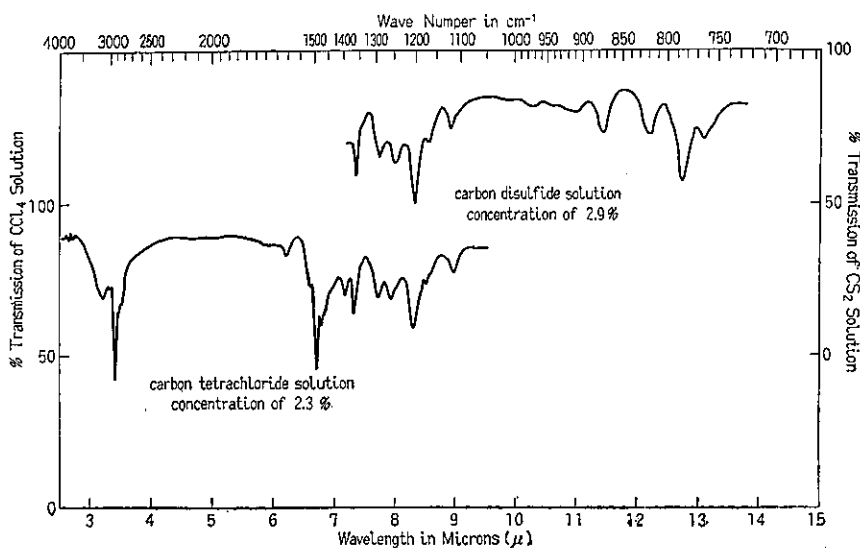Fig. 3(a). Spectra *p-tert*-butylphenol in carbon tetrachloride and in carbon disulfide



Fig. 3(b). Spectra of polymer N-6 in carbon tetrachloride and in carbon disulfide

solution, a relative intensity of these two bands changed with the concentration. The spectrum of the benzene solution had an aspect that the 3,600 cm.$^{-1}$ band became more intense comparing with the broad 3,450 cm.$^{-1}$ band. The spectrum of the polymer N-6 showed no appreciable difference between the solution and the solid. Only the spectrum of the benzene solution showed a very weak but sharp band at 3,600 cm.$^{-1}$ beside the strong broad band at 3,200 to 3,300 cm.$^{-1}$ The spectrum of the acetone solution showed a relatively stronger and sharp band at 3,500 cm.$^{-1}$ comparing with the benzene solution, but the absorption of acetone interrupts this
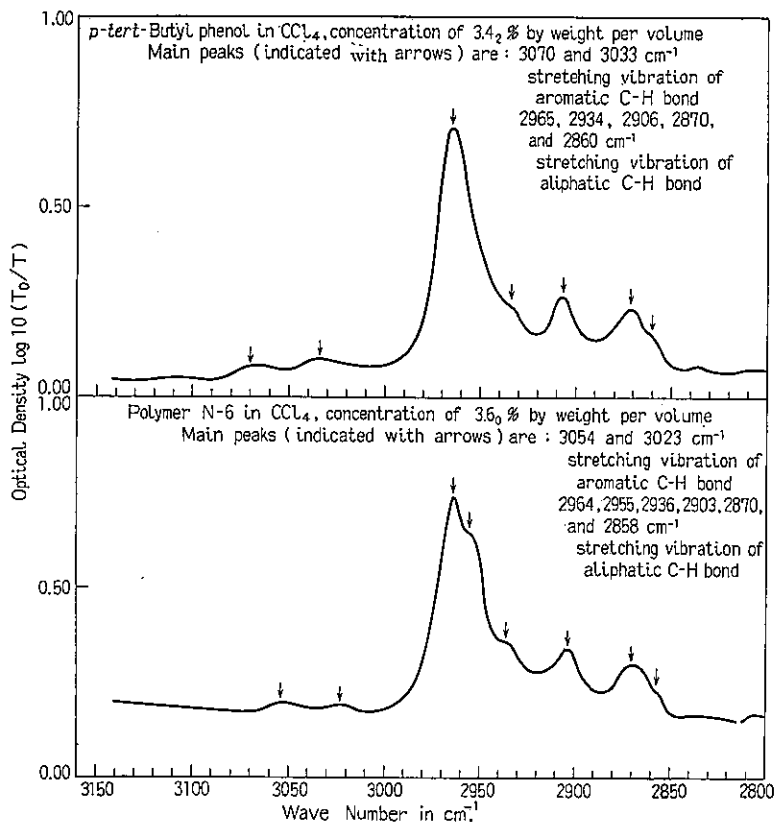
Fig. 4. Spectra in the region of 2,800 to 3,100 cm.⁻¹, measured by means of Perkin Elmer Model 112 G Grating Spectrophotometer. Upper spectrum is of *p-tert*-butylphenol and lower of polymer N-6
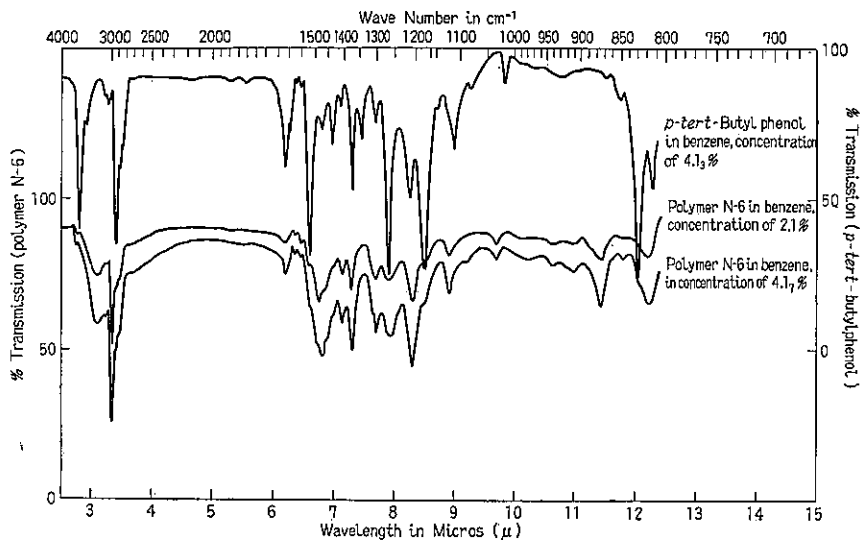


Fig. 5. Spectra of polymer N-6 and *p-tert*-butylphenol in benzene
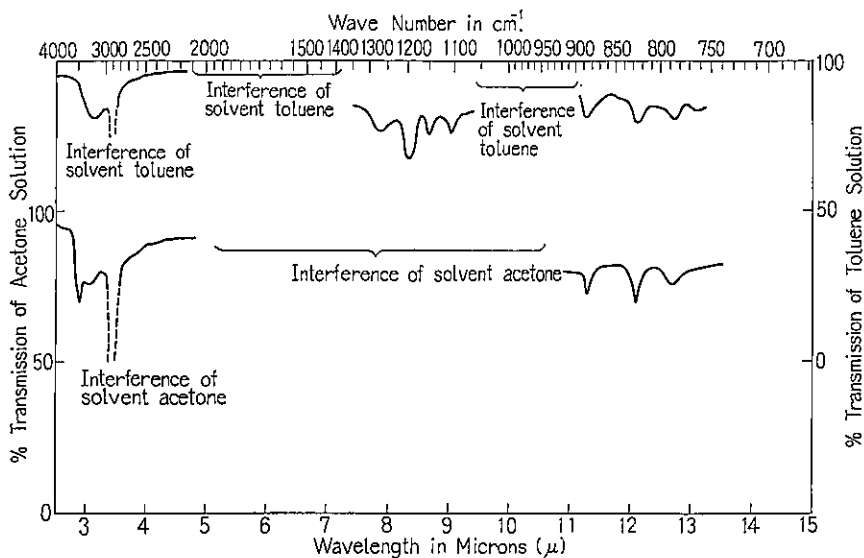
45

Wave Number in cm⁻¹



Fig. 6.  Spectra of polymer N-6 in toluene and in acetone.
Upper spectrum is in toluene and lower in acetone

band, so the result is uncertain.  A relative intensity of these bands in the benzene solution showed no difference when the concentration of the solution is varied.

In the other regions of the spectra of *p-tert*-butylphenol, appreciable differences were observed between the solid state and the solution in the band groups of 1,520 cm.⁻¹, 1,460 to 1,480 cm.⁻¹, 1,430 cm.⁻¹, and of 1,270 to 1,170 cm.⁻¹  The band group 1,620 cm.⁻¹ showed a slight difference similarly, but the differences of the other bands were considered to be not reliable from the resolution and the accuracy of the spectrophotometer.  The spectrum of the polymer N-6 showed no such an appreciable difference.

DISCUSSION

1  *Assignments of the Absorption Bands.*

In order to build up a molecular structure of this polymer from the data of the spectra obtained, it is necessary to assign the bands, i. e. to clear to which type of the vibration of each bond is the band attributed.  Considering from the knowledge of the chemical configuration of the compound and many results of the references[2~9], it is able to make tentative assignments as written in Table 1 and 2.

The band due to the O-H stretching vibration gives rise to near 3,600 cm.⁻¹ generally when the O-H bond is free and to the range 3,400 to 3,200 cm.⁻¹ or below when the O-H bond is bound by an intramolecular or intermolecular hydrogen bond. The band of the stretching vibration of the aromatic C-H bond gives rise to near 3,030 cm.⁻¹ or upper and those of the aliphatic C-H bond, in the range 2,960 to

46

Table 1. Band position and assignment of infrared spectrum of *p-tert*-butylphenol

| Solutions | | | | Solid | Assignments |
|---|---|---|---|---|---|
| $C_6H_6$ | $CCl_4$ | $CCl_4$* | $CS_2$ | | |
| 3,580 | 3,610 | | | | Stretching of free O–H |
| 3,450 | 3,410 | | | 3,220 | Stretching of bonded O–H |
| 3,030 | 3,070 | 3,070 | | 3,030 | |
| | | | | 3,033 | Stretching of aromatic C–H |
| 2,970 | 2,990 | 2,965 | | | |
| | | 2,934 | | | ⎫ Antisymmetric stretching of C–H of –$CH_3$ ⎭ |
| 2,930 | 2,940 | 2,906 | | 2,940 | Symmetric stretching of C–H of –$CH_3$ |
| | | 2,870 | | | |
| 2,900 | 2,920 | 2,860 | | 2,860 | ⎫ Symmetric stretching of C–H of –$CH_3$ ⎭ |
| | | | | 1,890 | Overtone or combination tone |
| | | | | 1,640 | Overtone or combination tone |
| 1,618 | 1,618 | | | 1,616 | |
| 1,600 | 1,603 | | | 1,603 | Benzene ring (para substituted) |
| 1,563 | 1,565 | | | | |
| 1,555 | 1,550 | | | | |
| 1,517 | 1,520 | | | 1,513 | Benzene ring (para substituted) |
| | 1,486 | | | 1,477 | |
| 1,464 | 1,467 | | | 1,460 | |
| 1,435 | 1,432 | | | 1,439 | Antisymmetric deformation of $CH_2$ of –$C(CH_3)_3$ |
| 1,403 | 1,397 | | 1,393 | 1,391 | |
| 1,368 | 1,368 | | 1,364 | 1,362 | Symmetric deformation of $CH_2$ of –$C(CH_3)_3$ |
| 1,337 | 1,333 | | 1,329 | | |
| 1,299 | 1,299 | | 1,294 | 1,302 | Deformation of >CO–H |
| 1,266 | 1,263 | | 1,258 | 1,266 | Rocking of C–$CH_3$ of –$C(CH_3)_3$ |
| (1,220) | (1,220) | | 1,217 | 1,244 | |
| 1,209 | 1,205 | | 1,202 | 1,205 | Rocking of C–$CH_3$ of –$C(CH_3)_3$ |
| 1,176 | 1,175 | | 1,170 | 1,185 | Stretching of >C–OH |
| 1,140 | 1,140 | | 1,136 | 1,139 | |
| 1,110 | 1,110 | | 1,110 | 1,127 | In plane bending of ring C–H |
| 1,083 | 1,081 | | 1,081 | | |
| | 1,023 | | 1,022 | 1,024 | In plane bending of ring C–H |
| 1,012 | 1,011 | | 1,012 | 1,018 | In plane bending of ring C–H |
| 928 | | | 930 | 933 | Skeletal of –$C(CH_3)_3$ |
| 850 | | | 848.9 | 855 | |
| 830 | | | 827.1 | 830 | Out of plane bending of ring C–H (para substituted) |
| 813 | | | 811.0 | 818 | Skeletal of –$C(CH_3)_3$ |
| | | | 806.5 | | |
| | | | 720.5 | 735 | |
| | | | | 718 | |
| | | | | 680 | |

* measured with Perkin Elmer Model 112 G Grating Spectrophotometer.

Table 2. Band position and assignment of infrared spectrum of polymer N-6

| Solutions | | | | Solid | Assignments |
|---|---|---|---|---|---|
| $C_6H_6$ | $CCl_4$ | $CCl_4$* | $CS_2$ | | |
| 3,600 | | | | | Stretching of (perhaps) free O–H |
| 3,220 | 3,180 | | | 3,130 | Stretching of bonded O–H |
| 3,060 | 3,060 | 3,054 | | | Stretching of aromatic C–H |
| | | 3,024 | | | |
| 2,960 | 2,960 | 2,964 | | | Antisymmetric stretching of C–H of –CH₃ |
| | | 2,955 | | | Antisymmetric stretching of C–H of –CH₂ |
| | | 2,936 | | | Antisymmetric stretching of C–H of –CH₃ |
| 2,930 | 2,920 | 2,903 | | 2,890 | }Symmetric stretching of C–H of –CH₃ and of –CH₂– |
| 2,890 | 2,870 | 2,870 | | 2,850 | |
| | | 2,858 | | | |
| 1,613 | 1,610 | | | 1,610 | Benzene ring |
| (1,570) | | | | | |
| (1,550) | | | | | |
| 1,515 | 1,515 | | | 1,510 | Benzene ring |
| 1,481 | 1,490 | | | 1,484 | Deformation of CH₂ of –CH₂– |
| 1,471 | 1,468 | | | 1,462 | Antisymmetric deformation of CH₂ of –C(CH₃)₃ |
| 1,458 | 1,458 | | | 1,440 | |
| (1,429) | | | | | |
| 1,397 | 1,403 | | 1,389 | 1,390 | Symmetric deformation of CH₂ of –C(CH₃)₃ |
| 1,368 | 1,370 | | 1,361 | 1,362 | |
| 1,297 | 1,299 | 1,289 | 1,289 | 1,299 | Deformation of >CO–H |
| 1,263 | 1,266 | | 1,250 | 1,262 | Rocking of C–CH₃ of –C(CH₃)₃ |
| | | | | 1,243 | |
| 1,206 | 1,208 | | 1,203 | 1,206 | Rocking of C–CH₃ of –C(CH₃)₃ |
| 1,179 | 1,179 | | 1,170 | 1,176 | Stretching of >C–OH |
| | | | | 1,166 | |
| 1,122 | 1,124 | | 1,120 | 1,124 | In plane bending of ring C–H |
| 940 | | | 939 | | Skeletal of –C(CH₃)₃ |
| 909 | | | 910 | 909 | |
| 876 | | | 873.4 | 880 | Out of plane bending of ring C–H (free CH) |
| (849) | | | 840 | 833 | |
| 828 | | | 825 | 820 | Out of plane bending of ring C–H (two adjacent CH) |
| 819 | | | 819 | | Skeletal of –C(CH₃)₃ |
| | | | 784.3 | | |
| | | | 782.5 | (781) | Skeletal of –CH₂– |
| | | | 774 | | |
| | | | 763.4 | | Skeletal of –CH₂– |
| | | | | (725) | |

* measured with Perkin Elmer Model 112 G Grating Spectrophotometer.

2,860 cm.$^{-1}$. These assignments are applicable to the present data. Thus the assignments of the stretching vibrations of O-H and C-H are made as written in the Tables.

The band due to the O-H deformation vibration gives rise to near 1,450 or 1,300 cm.$^{-1}$ and the coupling with the C-O stretching vibration or with the other neighbour bond vibrations occurs. *p-tert*-Butylphenol forms an intermolecular hydrogen bond strongly in the state of the solid and establishes the equilibrium between the free state and the hydrogen bonded state in the solutions, thus the O-H deformation vibration frequency also might differ between the solid and the solution state. Therefore the bands near 1,450 cm.$^{-1}$ or 1,300 cm.$^{-1}$ are attributed to the phenol O-H deformation vibration and 1,180 cm.$^{-1}$ to the C-OH stretching vibration and these vibrations couple with each other. The spectrum of the polymer N-6 showed no differences between solid and solution. From an above mentioned viewpoint, the O-H deformation vibration and the C-OH stretching vibration (or these coupled vibrations) are assigned as written in Table 2. The band near 1,520 cm.$^{-1}$ can not be assigned to the O-H deformation vibration generally, from the theoretical and experimental reason. It is allowed from the experimental data of the many references that the bands in the 1,620 to 1,520 cm.$^{-1}$ are assigned to the benzene ring skeletal C=C stretching vibrations.

The bands due to the C-H deformation vibrations of the tertiary butyl group give rise to near 1,450, 1,390 and 1,360 cm.$^{-1}$, the C-CH$_3$ deformation (rocking) vibrations near 1,260 and 1,200 cm.$^{-1}$, and the -C(CH$_3$)$_3$ skeletal vibrations near 930 cm.$^{-1}$ and 820 cm.$^{-1}$. In the case of the polymer N-6, other than the bands due to the tertiary butyl group, the band due to the CH$_2$de formation vibration gives rise to 1,460 cm.$^{-1}$ and the -CH$_2$- skeletal vibration below 780 cm.$^{-1}$. The band near 1,120 cm.$^{-1}$ is assigned to the ring C-H bending vibration in plane for the polymer, and 1,110cm$^{-1}$ and 1,030 cm.$^{-1}$ bands, to those for *p-tert*-butylphenol. The spectrum of *p-tert*-butylphenol showed strong band neor 830 cm.$^{-1}$. This is a typical band of the " para " substituted benzene which is assigned to the out of plane deformation vibration of the aromatic C-H bond. This band appears when the two adjacent C-H bonds in one benzene ring exist. The band near 820 cm.$^{-1}$ of the polymer is also assigned to the out of plane vibration of the aromatic C-H of the two adjacent C-H bonds. And the band 870 cm.$^{-1}$ is assigned to the out of plane C-H vibration of only one free C-H bond in the ring, for example, in the case of 1, 2, 3, 5-*tetra*-substituted benzene.

## 2 *The Effect of the Solvent and the Molecular Structure.*

It is well recognized from the spectral data that *p-tert*-butylphenol in the benzene and the carbon tetrachloride solution holds the equilibrium of an association, and the relative number of the molecule in the equilibrium varies according to the difference of the interaction with the solvent. That is, in the region of 3 micron,

the sharp absorption band near 3,600 cm.$^{-1}$ which is attributed to the free O-H stretching vibration is more intense in the benzene solution than in the carbon tetrachloride solution comparing with the broad band in the range 3,400 to 3,200 cm.$^{-1}$ which is attributed to the hydrogen bonded O-H stretching vibration. This fact interprets that the number of the free molecule of *p-tert*-butylphenol which exists in the solution is much more in benzene than in carbon tetrachloride. This phenomenon can be explained as the existence of the state in which the association is more loose or the hydrogen bond is less intense in benzene than in carbon tetrachloride. Both phenomena are observed also in the other solutions generally, and suggest that the interaction of the benzene molecules with the solute molecule are stronger than those of carbon tetrachloride.

In the solid state of *p-tert*-butylphenol no free O-H vibration could be observed and the very broad band attributed to the hydrogen bonded O-H stretching vibration was observed in the range 3,100 to 3,200 cm.$^{-1}$. These results support furthermore the above mentioned inferences. In the solution the molecule gets the more freedom of the motion than in the solid, then the intermolecular hydrogen bond is weakened and the free O-H group exists appreciably in the solution, particularly, of the low concentration. These phenomena also appear in the region of the O-H deformation vibration. In Table 1 and Fig. 3, the bands 1,520 cm.$^{-1}$, 1,450 cm.$^{-1}$ and 1,250 to 1,300 cm.$^{-1}$ are attributed to the deformation vibration of the O-H bond. The shift (to the lower wave number according to the change of the phase from the solid to the solution) was observed slightly in the band 1,300 cm.$^{-1}$ and not in the band 1,450 cm.$^{-1}$. Then from a general conception of an infrared spectroscopy, the band 1,300 cm.$^{-1}$ is assigned mainly to the deformation vibration of the O-H bond. This fact also support the behavior of the O-H group in the solution solid as already stated. The variations of the other bands are very small compared with the above mentioned bands. These are only small change in the intensity. These are interpreted as the effect of the change of the environment of each molecule and as the disturbance caused by the position of the band of the solvent upon that of solute. The change of the environment causes a distortion of the molecular structure or a potential curve concerned with the each vibration mode and the change of the electronic state. These processes cause the change of the band intensity more or less. Therefore it is accepted to say that the bands except 1,300 cm.$^{-1}$ and 1,450 cm.$^{-1}$ (and 1,180 cm.$^{-1}$, perhaps) are almost not concerned with the O-H deformation vibration.

In the case of the polymer N-6, there was seen almost no difference in the band shape (the band position and the band relative intensity) with the change of the phase (from the solid to the solution) and the kinds of the solvents. As shown with the spectra, in the carbon tetrachloride and the toluene solution, the band due to the O-H stretching vibration in the solution had the almost similar shape as

50

those in the solid state, and there was not observed any sharp band in the higher wave number side of the observed broad band when the concentration of solute in solution was made lower and lower. Therefore, the polymer N-6 does not form any intermolecular hydrogen bond but the intramolecular hydrogen bond. The intramolecular hydrogen bond is stronger than the intermolecular hydrogen bond and then the band due to former is observed in the lower wave number than the latter band. This is the case of the spectrum of the polymer N-6 in which there is ween an appreciably lower wave number O-H stretching vibration band than those of *p-tert-* butylphenol. The intramolecular hydrogen bond is not loosen appreciably by the change of the environment of the molecule and then the concentration variation does not affect the band of the O-H stretching vibration of the polymer in the solution. But if the solvent has a more intense bonding property, the intramolecular hydrogen bond becomes loose appreciably by the change of the environment of the molecule and is displaced by the intermolecular hydrogen bond with the solvent. This is the case of the acetone solution. A keto group of acetone forms generally the hydrogen bond with the O-H group of the other compounds. Perhaps the phenol O-H group of the polymer forms the intermolecular hydrogen bond with the $C=O$ group of the solvent acetone. This band gives rise to near $3,500$ cm.$^{-1}$. In the benzene solution besides the broad band near $3,200$ cm.$^{-1}$ assigned to the hydrogen bonded O-H stretching vibration, a sharp but very weak $3,600$ cm.$^{-1}$ band was observed. The intensity of the latter band relative to the broad band did not vary with the change of the concentration. This fact can be explained as follows. In the benzene solution, the O-H groups of the polymer molecule combine with each other by the intramolecular hydrogen bond, but the interaction between the $\pi$ electron system of the benzene ring and the O-H groups, looses the strengths of the intramolecular hydrogen bonds and then some part of the O-H groups exists as the shape similar to the free O-H group or forms a weak intermolecular hydrogen bond with the $\pi$ electron system of the benzene ring. Under these circumstances, the number of the O-H groups directed to the benzene ring is nearly constant even if the concentration of the polymer is varied in the range of the low concentration in which there exist many numbers of the benzene molecules enough to neglect the change of the number of the benzene molecule compared with the change of the numbers of the solute molecules. These conclusions are illustrated schematically in Fig. 7.

3  *A Structure of the Polymer N-6.*

From the spectra of the carbon disulfide solution and the solid, some informations can be obtained respect to the chemical configuration of the polymer. Since the method of the synthesis is similar as general phenol resin, it is considered that the benzene rings are combined with the methylene bridge each other and the two
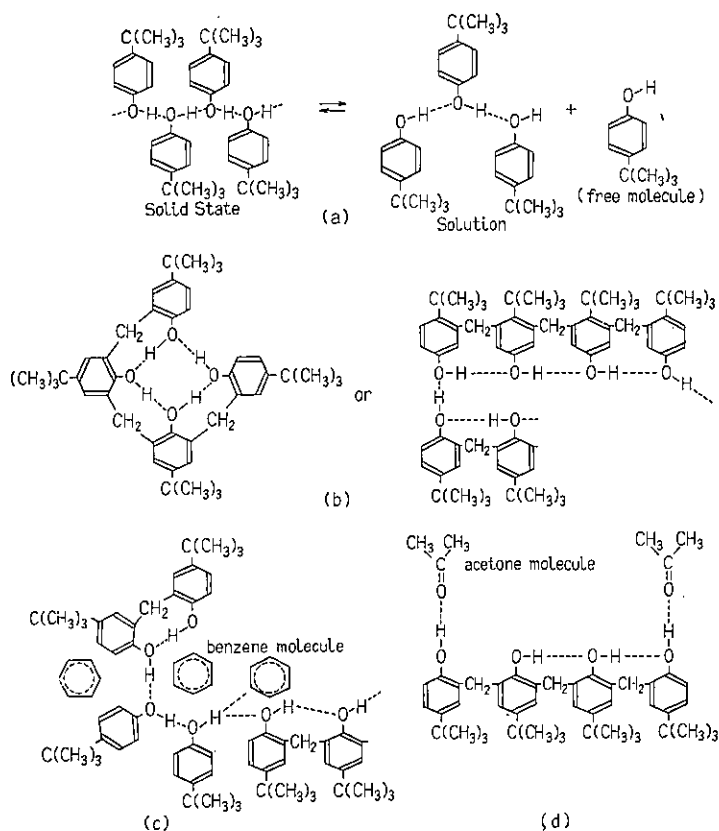
Fig. 7. Schematic diagrams of molecular structures of
*p-tert*-butylphenol and polymer in several states
(a) Example of *p-tert*-butylphenol in solid state and solution.
(b) Example of polymer in solid state and in inert solvent.
(c) Example of polymer in benzene solution.
(d) Examyle of polymer in acetone solution.

methylene groups attached to the two "ortho" positions against the phenol O-H position of the benzene ring. The "para" position is occupied by the tertiary butyl group, then the linear chain polymer is produced. The band assigned to the C-H out of plane vibration of the benzene ring gave rise to near 830 cm.$^{-1}$ in the case of *p-tert-* butylphenol. This band is very strong and assigned to the C-H out of plane vibration of the "para" substituted benzene ring, or in other words, to it of only two adjacent hydrogen atoms attached to one benzene ring. In the case of polymer there were two medium intense bands at 820 and 870 cm.$^{-1}$. The former band is assigned to the C-H out of plane vibration of only two adjacent hydrogen atoms attached to the benzene ring, and the latter to that of one free hydrogen atom, in the adjacent position of which no hydrogen atom exists. Considering also the result that the molecular weight of this polymer is relatively small (1,000), it is reasonable to infer that about four molecules of *p-tert*-butylphenol polymerize into

52

one molecule of the polymer, then this molecule of the polymer has the structure in which the benzene rings exist at the both sides as illustrated in Fig. 7. The bands due to the keto group C=O and the acid group $-C\langle^O_O$ or the ester group $-C\langle^O_{O-R}$ give rise to 1,660 to 1,700 cm.$^{-1}$ or upper and strong generally. The spectra of the polymer showed no such bands. Therefore it can be allowed to express the structure of the polymer as illustrated in Fig. 7. Other groups $-NH_2$, $=NH$, etc. are also eliminated in the possibilities of the existences from the similar reason as mentioned above.

## CONCLUSION

Some assignments of the absorption bands include a few ambiguity and are tentative. But in the consideration of the bands due to the stretching vibration of the O-H group and the C-H out of plane vibration and the other few assignments, following conclusions can be obtained.

(1) Comparing the spectra of the polymer N-1, 2, 3 and 6, it can be concluded that the difference of the condition of the synthesis and perhaps of the effectiveness of the mask, can be explained as the difference of the structure of the polymer and the impurities, (the substances which does not yet react) in the products.

(2) The spectra of the solutions imply evidently the possibilities as follows:

In the benzene solution the structure of the polymer takes a specific form comparing with the other solution acetone, toluene, carbon tetrachloride, etc. and at the process of the adsorption or the combination (the linkage) on the fiber of the mask filter this molecular structure in the benzene solution plays a specific role, then the effectiveness of the mask depends partly upon this mechanism. There can be considered with some possibilities that in the good mask filter, the O-H groups of the polymer orient to the direction of the fiber of the filter and the tertiary butyl groups to the atmosphere. There are perhaps a specific orientation of the molecules of the polymer upon the fiber.

(3) The polymer is the relatively small molecule (the lower molecular weight than those of common polymer), and has the structure in which the benzene rings occupy at the both sides of one polymer molecule.

## REFERENCES

1) Koshi, S.: This Bulletin, No. 3, 23–39, (1960).

2) PB 11438, (Infrared Spectra of Plastics and Resins), United States Department of Commerce, Office Technical Service, pp. 20.

3) Edited by West, W.: "Chemical Application of Spectroscopy", Interscience Pub. Ltd., London (1956), Chapter III. pp. 187 to 245 (by A. B. F. Duncan) and Chapter IV. pp. 247 to 580 (by R. Norman Jones and Camille Sandorfy).

4) Bellamy, L. J.: "The Infrared Spectra of Complex Molecules", Metheu & Co., Ltd., London, J. Wiley & Sons Inc., New York. (1954).

5) Tsutsumi, S. and Iwai, E.: "Kagaku no Ryoiki" (Region of Chemistry) Zokan 21, Infrared Absorption Spectrum No. 1, 101 (1956).

6) Nakanishi, K.: ibid., 111.

7) Nakamoto, K.: ibid., 23, 2, 79 (1956).

8) Oi, N.: ibid., 29, 4, 41 (1958).

9) Kakiuchi, Y.: ibid., 38, 8, 1 (1959).

## 要　旨

### アンモニアを用いて *p-tert*-Butyl Phenol とフオルマリンから 合成した重合物の分子構造の赤外線分光学による研究

#### 左　右　田　礼　典

表題の重合物で防塵マスク繊維を処理する時その除塵効率が増すことまた繊維の帯電が著しく強くなる事実を分子構造論の立場から解明し，マスクの研究発展の一助とする目的で赤外吸収スペクトルを測定し，得られた結果をもとに二三の考察を試みた。

スペクトル測定には Infracord 分光器を主として用い，場合により分解能および精度の高い分光器を二三使用した。溶媒はベンゼン，トルエン，アセトン，四塩化炭素および二硫化炭素を使用，厚さ 0.1 mm のセルを用いた。溶液の濃度は重量/容積で 4% 以下のものである。固体のスペクトルは流動パラフインやヘキサクロルブダジエンの mull 法と岩塩板上に溶液から溶媒を飛ばして薄膜をつくつて測定した。試料は興重冶から提供されたものである。

固体のスペクトルを比較するとマスクに余り良好な結果を与えない試料には *p-tert*-butyl phenol および hexamethylene tetramine が不純物として明かに含まれているという結果を得た。またその他の吸収帯の様子から N-6 試料が最も純粋であり構造も典型的なものと考えられた。溶液の試料はすべて N-6 を用いた。

溶液のスペクトルについては *p-tert*-butyl phenol が分子間水素結合を作つた会合体と自由な単分子との間に平衡のあることが O–H 伸縮振動と帰属される 3,600 cm$^{-1}$ の吸収帯と 3,200 cm$^{-1}$ 位の吸収帯（前者は単分子，後者は会合体によるもの）の挙動から結論された。固体では全部分

子間水素結合で固定された構造が考えられる。一方 polymer の場合には固体と溶液とでこのような明瞭な差が見られないことから強い分子内水素結合で O-H 基 が結ばれていると結論された。ベンゼン溶液の場合にはやや事情が異り 3,600 cm⁻¹ に弱い鋭い吸収帯の存在とそれが濃度によつて相対強度が変化しないことから僅かに分子内水素結合がゆるみベンゼンの π 電子との相互作用により自由な形に近い O-H 基が存在していると結論された。アセトンのように水素結合で水素受容体となる溶媒ではアセトン分子との間に分子間水素結合が出来上つている可能性がやはり 3 ミクロン付近の吸収帯から推定された。

　800 cm⁻¹ 付近の吸収帯の測定から重合物の構造として両端がベンゼン環 でそれらをメチレン基の橋と p-tert-butylphenol との直鎖的連結がつないでいる形が推定された。 またケト基その他の構造がなくいわゆる比較的低分子のフェノール樹脂と類似の構造が考えられる。

---

# ACUTE CADMIUM SOAP POISOING IN INDUSTRY

Hiroyuki SAKABE and Koichi USHIO*

## 1. SIGNS AND SYMPTOMS

In December, 1958, a worker who engaged in the manufactuing of metal soaps came to our hospital complaining anaemia, giddiness, breathlessness, nausea and fatigue. Physical and laboraory examination of this patient could not find out any abnormalities except slight anaemia with 3.07 million red corpuscles, in spite of the subjective symptoms. As he stated that the other workers in the same working place had the same complaints, we have examined the plant where the patient worked.

The plant was manufacturing metal soaps and alkyl-tin compounds which were mainly used as stabilizing agents of polyvinylchloride. Metal soaps manufactured in this plant were Cd stearate, Cd laurate, Pb stearate, Ba stearate, and Ca stearate, and these were produced and handled in the separate building apart from the main building producting alkyl-tin compounds. These soaps were not manufactured simultaneously, but successively, and manufacturing of one sort of these soaps usually took from 3 to 7 days.

Our patient worked in the room, where these metal soaps were dried, powdered, sieved and packed. Processes after drying were very dusty. No special precautions for dust suppression were taken, and the workers did not wear a dustrespirator. Seven persons were working in this room, and two of them in the hospital when we have investigated. One of these two patients was ours and the other was under treatment with diagnosis of toxic gastric ulcer in another hospital.

All workers complained the gastric disturbances during manufacturing Cd stearate or laurate, but there were no complaints among workers with manufacturing and handling other metal soaps. Therefore, it was assumed that the exposure to cadmium soap dust only produced the gastric disturbances.

Sensitive workers complained epigastric distress and loss of appetite from three to four hours after exposure to Cd soaps dusts, and in some cases, severe anorexia, nausea, vomiting, gastric pain and unconsciousness were seen, but in workers who were not so sensitive these symptoms took place two or three days after the starting of cadmium soap manufacturing.

These gastric disturbances continued during the exposure to cadmium soap dusts, and disappeared after the finishing of manufacturing of cadmium soaps,

---

* Workmen's Accident Compensation Hospital in Kanto District.

namely during the production of metal soaps other than cadmium soaps. Laboratory studies of the workers could not reveal any abnormalities on the blood, urine, gastric juice, liver function, and electrocardiograph. And also, no abnormal findings were found in X-ray examination of the chest.

Typical example of the case report:

C. A. forty-eight, female, engaged in packing of metal soaps for two years. She felt the disorder after two or three days of exposure to cadmium soap dust. At first, she felt lying heavy on the stomach and tasteless smoking. Her appetite fell off, and then suffered from nausea and sometimes vomiting. These gastric symptoms did not improve as far as she was exposed to cadmium soap dust, but in three or four days after the release from the exposure to cadmium soap dust these symptoms disappeared. She never felt such a gastric disorder with the exposure to other metal soap dust.

## 2. ENVIRONMENTAL DUST CONCENTRATION

Suspended cadmium stearate dusts in the working place were collected by electric precipitator. Collected dusts were washed out with 0.1% surface detergent solution from the collecting tube of electric precipitator. 100 cc of this dust suspension was evaporated to 50 cc, and then heated strongly with 50 cc of conc. HCl. The amount of $CaCl_2$ was measured by polarograph. As shown in Fig. 1. cadmium stearate dust concentration in the working place is considerably high.
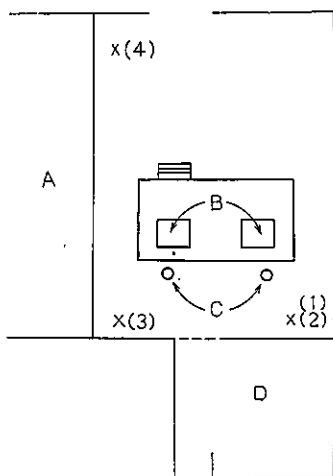


Fig. 1. Environmental Cadmium Dust Concentration

|  |  | Cd (mg/m) | Cd stearate (mg/m) |
|---|---|---|---|
| ( 1 ) | crusher not in motion | 16.5 | 85.2 |
| ( 2 ) | crusher in motion | 18.5 | 95.2 |
| ( 3 ) | sieve in motion | 97.6 | 504.0 |
| ( 4 ) | crusher and sieve not in motion | 18.0 | 92.9 |

Note: A: Drying room, B: Crusher, C: Sieve, D: Packing room.

### 3. Filtering Efficiency of Dust Respirator against Cadmium Stearate Dust

Since the mean size of cadmium stearate dusts was $5\mu$ in diameter, we expected the effective removal of dusts by using dust respirator. Filltering efficiency of dust respirators against cadmium stearate dust was measured by the approved method of the Japanese Industrial Standard for Dust Respirator. Tested results are shown in table 1. Table shows the filtering efficiency and resistance of seven kinds of dust respirators against three kinds of test dusts.

Table 1. Efficiency and Resistance of Dust Respirators against
Cadmium Stearate and Other Dusts

| | cadmium stearate dust | | quartz dust | | calcium carbonate dust | |
|---|---|---|---|---|---|---|
| | eff. | resist. | eff. | resist. | eff. | resist. |
| | % | mmH$_2$O | % | mmH$_2$O | % | mmH$_2$O |
| treated felt | 97.3 | 2.62 | 94.9 | 2.62 | 98.4 | 2.62 |
| nontreated felt | 93.2 | 2.45 | 75.2 | 2.45 | 76.0 | 2.62 |
| commercial dust respirators | | | | | | |
| A (H 2) | 89.4 | 11.20 | 66.2 | 11.90 | 70.6 | 11.19 |
| B (H 2) | 95.2 | 7.69 | 84.5 | 7.34 | 87.9 | 6.47 |
| C (H 2. 3) | 84.7 | 1.05 | 40.3 | 1.92 | 53.8 | 1.92 |
| D (W. H. L. 4) | 81.9 | 3.72 | 19.5 | 4.20 | 41.0 | 4.02 |
| E (H. L. 4) | 83.7 | 5.60 | 29.9 | 5.94 | 42.0 | 5.41 |

Notes: 1. Mean sizes of test dusts are as follows:
  cadmium stearate dust, $5\mu$,
  quartz dust, $0.3\mu$,
  calcium carbonate dust, $1\mu$.
2. Resistance is the mm in H$_2$O measured at the flow rate of 301/min.
3. Treated felt is the felt treated with p-tertially butyl phenol resine.

Treated felt showed very low resistance with remarkable high filtering efficiency against various dusts, and the detailed studies of this material will be reported in the other part of this Bulletin. It seems to be interesting that all tested dust respirator had a very high efficiency against cadmium stearate dust, despite that some of them showed a very low efficiency against silica dusts. This would be explained by the particle size of the test dust. From these data it would be expected that dust respirator is very useful for the personal protection against the poisoning in this case.

### 4. Discussion

Occupational hazards with reference to cadmium were reported in smelting of ores and manufacturing of alloys, in spraying of cadmium pigment, in electroplating, etc. In these cases, intoxication was produced by the inhalation of cadmium oxide fume or metallic cadmium dust. The predominant symptoms of industrial cadmium

poisoning are dryness of throat, cough, headache, vomiting, and a sense of constriction of the chest.

Recently, Friberg[1] summarized the chronic cadmium poisoning, and he paid attention to the pulmonary emphysema, anosmia, small ulceration of the nasal mucosa, proteinuria, renal damage, and nephrolithiasis. Our cases did not show any clear symptoms of respiratory system and proteinuria, but remarkable gastric disturbances. In regard to an impediment in stomach evoked by soluble cadmium Frant and Kleeman[2] reported the violent, acute gastritis in cadmium 'food poisoning'.

Since cadmium stearate is assumed to be soluble in the gastric acid as shown in the second report, it may be expected that dissolved cadmium ion has a harmful effect on the gastric function. As cadmium stearate dust has relatively large size of $1\,\mu$ to $10\,\mu$ in diameter, inhaled particles would deposit on the upper respiratory tract, and be expectorated by ciliar motion. Alber and Arnett[3] showed that most of the radioactive iron oxide dusts of $3.4$-$4.3\,\mu$ in diameter were cleared from the lung in 2 or 4 hours after the inhalation. In our case, it may be assumed reasonably that the greater part of inhaled cadmium soap dusts deposit on the upper respiratory tract and then the dust are expectorated into the stomach where they are hydrolyzed with acidic gastric juice.

It may be explained by the short exposure time that we could not find out any other symptoms than digestic disturbances. To protect the workers against this poisoning, plant installed the suitable dust exhaust system, and dust respirators were supplied to workers according to our advice.

## 5. SUMMARY AND CONCLUSIONS

We have experienced the acute cadmium soap poisoning in industry. Main symptoms were the digestive disturbances, and appeared after a few hours or days of exposure. Symptoms were improved promptly after the stop of exposure to cadmium soap dust. Environmental dust concentration was measured and dust filtering efficiency against cadmium soap dust was investigated. Some discussions were made on deposition at the respiratory tract, expectoration into the stomach, and dissociation in the stomach.

## REFERENCES

1) Friberg, L.: Arch. Indust. Health, **20**, 401, (1959).

2) Frant, S. & Kleeman, I.: J. A. M. A. **112**, (2), 86, (1941).

3) Alber, R. E. & Arnett, L. C.: Arch. Indust. Health, **12**, 99, (1955).

# 要　旨

## カドミウム石けんによる急性中毒について

### 坂 部 弘 之　　牛 尾 耕 一　（関東労災病院）

　昭和33年12月12日某工場の金属石けんの製造に従事していた一労働者が，下血と貧血を訴え，胃潰瘍の疑で関東労災病院に入院した。この患者の自覚症状はめまい，息切，嘔気，全身倦怠感であつたが，他覚的には軽度の貧血の他に著変はなかつた。患者の訴えでは同じ職場に働く同僚にも胃の障害があるというので，患者の作業していた職場，即ちその工場の金属石けんを製造する工程を調査した。この工場で製造する金属石けんは，ステアリン酸カドミウム，ラウリン酸カドミウム，ステアリン酸バリウム，ステアリン酸鉛，ステアリン酸カルシウム等である。これらは主にポリ塩化ビニールの安定剤として使用されるものである。製造はステアリン酸からナトリウム石けんを作り，更に夫々の金属石けんを作製し乾燥し，粉砕し，篩分けし，袋詰めにする一連の工程からなる。このうち粉塵の飛散する乾燥以後の工程において，特にステアリン酸カドミウム及びラウリン酸カドミウムの製造に従事する際，労働者に胃症状の発現が見られる。即ち早い人ではカドミウム石けんの粉じんにバクロし始めてその日の午後，一般には二，三日後に食欲不振を主とする胃症状が現われる。軽症の時は作業が3〜7日で終るので我慢しているうちにカドミウムの取扱いが終り，他の金属石けん製造中に，症状も軽快するが，重症に経過する時は，食欲は完全に消失し，嘔気嘔吐があり，胃に鈍痛を覚え，更に進行すると失神する場合がある。作業場のステアリン酸カドミウムの濃度は大体 85〜95 mg/m³ カドミウムとして大体 16〜18 mg/m³ で篩作業においてはカドミウムとして 97 mg/m³ にも及ぶ。カドミウム石けんの粒子は 1〜10 μ 程度の比較的大きいものであるため呼吸と共に吸入されたものが上気道に沈着し，後胃に行き，胃の塩酸によりカドミウムイオンに解離されて其の影響を及ぼすものではないかと考えた。カドミウム石けん粒子の大きいことは発じん防止対策の実施についても考慮を要するが，防じんマスクの低抵抗のものか比較的高い沪塵効率を示した。

# EXPERIMENTAL STUDIES ON CADMIUM
# STEARATE POISONING
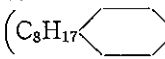
## I. DISSOCIATION CURVE AND TOXICITY

Hiroshi YOSHIKAWA, Noboru HARA, and Kiyoyuki KAWAI

Cadimium stearate is used as stabilizer of polyvinyl chloride. As reported in the previous paper in this Bulletin,[1] the inhalation of cadimium stearate dust during the manufacture of metal soaps, especially, in the processes of crushing, sieving and packing produced the gastric disturbance.

It is not clear whether the cadmium stearate has the same toxic effect as cadimium oxide or cadimium metal.[2,3,4] The present paper deals with the results of the experiments which have been undertaken on toxicity of cadmium stearate.

### METHODS

1) Dissociation: The dissociation of cadmium stearate at various pH was observed by the use of three kinds of buffer solution, namely, acetate buffer solution, veronal buffer solution, and citrate buffer solution. Various pH solution from pH 1.04 to pH 11.72 of each buffer solution were prepared and 100 mg. of cadmium stearate was added to 50 ml. of each pH solutions with mixing. Then a detergent $\left(C_8H_{17} \left\langle \quad \right\rangle O(CH_2CH_2O)_{18}H\right.$; $\theta$-p-octyl-phenyl-octa decyl-ethyleneglycol. This material had no injury by subcutaneous injection in mouse.$\left.\right)$ at 0.1% of total volumes was added in order to obtain the homogeneous suspension of cadmium stearate in water. These preparative solution was left with mechanical shaking for one hour at 39°C. After the incubation, the suspension was filtered with filter paper (Toyo Roshi No. 5. Filter Paper). The cadmium content in the filtrate was determined by a polarographic procedure.[5]

2) Toxicity: The toxicity presented by means of $LD_{50}$ following intraperitoneal injection of cadmium stearate and cadmium chloride in 5% glucose solution (Detergent was added at 0.1% of the solution) is presented in Table 1. Cadmium choloride was used in order to compare the toxicity of relatively insoluble cadmium stearate with soluble cadmium salt.

One hundred and ten healthy mice (the same strain of mouse) weighted 15 to 20 grams were used for this experiment. The mortality rate was recorded seven days after intraperitoneal injection. The $LD_{50}$ was calculated by the method of van den Vaerden.[6]

3) Oral toxicity in rats: To study the continued cadmium stearate feeding, four healthy growing male rats (Wistar-King strain) weighing about 100 grams at the onset of experiment were used. These rats were placed on diet to which cadmium stearate has been added with thorough mixing to give the desired concentrations, and the concentration of cadmium stearate were gradually increased from 0.1% to 1.0%. All animals were weighed and daily food intakes were determined in all of four rats for a period of 90 days. Cadmium excreted in urine was analyzed by the Dithizone method[7] three times during the period of cadmium stearate treatment.

## RESULTS

### 1. Dissociation Curves.

The dissociation of cadmium stearate in various pH solutions is presented in Figure 1. As shown in this figure, inflexion points of dissociation curves are shown between pH 4.5 and 5.5 on each of three buffer solutions. The dissociation of cadmium stearate was scarcely seen with neutral and alkaline solution. On the con-
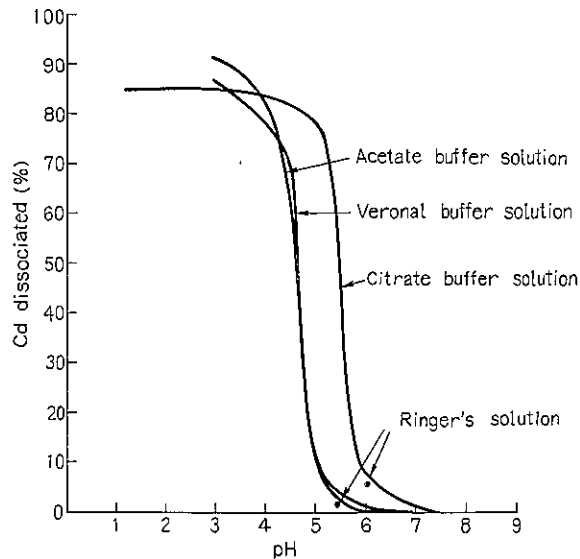


Fig. 1. Dissociation Curve of Cadmium Stearate
in Various Buffer Solutions.

trary, the dissociation was remarkable with acid solution, and about 85% of cadmium stearate dissociated at the pH less than 4.0. It is reasonable to assume that the cadmium stearate was dissociated remarkably with the gastric acid in the stomach, as pH of the gastric juice is about 1.5. The same inflexion point (pH 4.5) of dissociation curves is observed in acetate buffer and veronal buffer solutions, but it

is pH 5.5 in citrate buffer solution.

2. $LD_{50}$

The mortality results following intraperitoneal injection of cadmium stearate and chloride are presented in Table 1. In mice injected with a cadmium chloride, the difference in mortality rates is not observed between the animals treated for 24 hours and 7 days. But there is the difference in the mortality rates during the period of observation in mice injected with a cadmium stearate, and so the mortality rates of the mice treated for 24 hours, 3 days, and 7 days are listed.

Table 1. Mortality after Intraperitoneal Injection of Cadmium Stearate and Chloride

(A) Cadmium Chloride

| Cadmium Dose, mg/kg | Rats, No. | Surviving Mice | | Mortality Rate |
| --- | --- | --- | --- | --- |
| | | No. after One Day | No. after 7 Days | No. after 7 Days (=after 1 Day) |
| 2.25 | 10 | 10 | 10 | 0/10 |
| 3.38 | 10 | 9 | 9 | 1/10 |
| 5.06 | 10 | 2 | 2 | 8/10 |
| 7.59 | 10 | 1 | 1 | 9/10 |
| 11.39 | 10 | 0 | 0 | 10/10 |

$LD_{50}$=4.48 mg Cd per kilogram of body weight.

(B) Cadmium Stearate

| Cadmium Dose, mg/kg | Rats, No. | Surviving Mice | | | Mortality Rate | | |
| --- | --- | --- | --- | --- | --- | --- | --- |
| | | No. after One Day | No. after 3 Days | No. after 7 Days | No. after One Day | No. after 3 Days | No. after 7 Days |
| 5.06 | 10 | 10 | 10 | 10 | 0/10 | 0/10 | 0/10 |
| 7.59 | 10 | 9 | 9 | 6 | 1/10 | 1/10 | 4/10 |
| 11.39 | 10 | 8 | 5 | 4 | 2/10 | 5/10 | 6/10 |
| 17.09 | 10 | 6 | 1 | 0 | 4/10 | 9/10 | 10/10 |
| 25.63 | 10 | 4 | 0 | 0 | 6/10 | 10/10 | 10/10 |
| 38.44 | 10 | 0 | 0 | 0 | 10/10 | 10/10 | 10/10 |

$LD_{50}$=18.57 mg Cd per kilogram (1 day observed)
$LD_{50}$=11.38 mg Cd per kilogram (3 days observed)
$LD_{50}$= 9.31 mg Cd per kilogram (7 days observed)

In the case of observation for 7 days, $LD_{50}$ were 4.48 mg. of cadmium per kilogram of body weight for cadmium chloride and 9.31 mg. of cadmium per kilogram of body weight for cadmium stearate. The toxicity expressed by $LD_{50}$ of cadmium chloride was approximately twice as much compared with cadmium stearate.

The intraperitoneal $LD_{50}$ of cadmium stearate was 18.57 mg. of cadmium per kilogram with observation for 24 hours and 11.38 mg. of cadmium per kilogram for 3 days, and with the prolongation of the periods of observation, $LD_{50}$ was

gradually decreased. This may be explained by the fact that cadmium stearate reveals its toxicity progressively in animal body with the progress of its dissociation.

3. Cadmium Stearate fed to Rats.

The diet contained cadmium stearate were continuously given to rats for 90 days. Since rats refused to take the diet which contained 1% of cadmium stearate, the concentration of cadmium stearate was progressively increased from 0.1% to 1.0%. Growth and food consumption data of rats are presented in Figure 2. Animals in experimental group were remarkably stunted in growth in contrast to those in control group. A stunt of growth was observed in animals which fed the
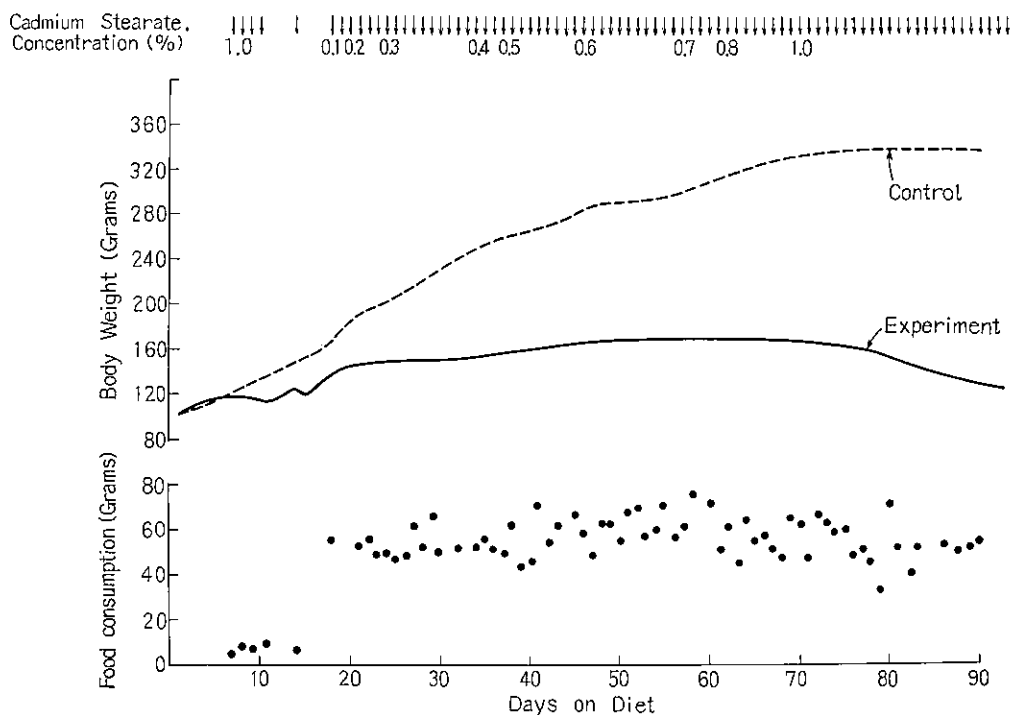


Fig. 2. The Effects of Ingested Cadmium Stearate on the Decreased Growth Rates and Food Consumption in Rats

diet contained low concentration of cadmium stearate, and the body weight remained stable in spite of the increase of cadmium stearate in the food. But, body weight tended to decrease after 80 days.

As shown in Figure 2, the amount of food consumption remains at constant level during the whole observation period. The nontreated healthy rats took the increased amount of food with the increase in body weight. The treated

animals show a decrease in body weight at the end of experiment, but their food consumption is constant.

The excretion of cadmium in urine is shown in Table 2. Renal elimination of cadmium does not show any constant trend, and relatively large individual difference are noted.

Table 2. The Urinary Excretion of Cadmium after Ingestion of Cadmium Stearate
($\mu$g of cadmium per day)

| Rat No. | after 48 days | after 60 days | after 85 days |
|---------|---------------|---------------|---------------|
| 2 | 25.2 | (−) | 12.5 |
| 6 | 94.0 | 20.0 | 91.0 |
| 9 | 15.8 | 29.5 | 7.0 |
| 11 | 29.8 | 22.0 | (−) |

After about three months, all four animals were sacrificed and complete autopsy were made. Moderate catarrh with occasional formation of shallow erosions were observed in the stomachs (Fig. 3) and in the small bowels (Fig. 4). Moderate to severe degeneration of the germinal cells in the testicles (Fig. 5) were also a characteristic feature. The liver and kidneys (Fig. 6) showed degenerative changes of their epithelial parenchyma. These changes in visceral organs were somewhat slighter as compared to those observed in the animals subjected to more acute and servere intoxications produced by intraperitoneal or subcutaneous injections. Detailed histopathological descriptions will be given in the following report in preparation.

## DISCUSSION

It is of the importance to establish a physicochemical character to evaluate the toxicity of materials. This physicochemical character of toxic agent is of fundamental importance to elucidate injurious systemic effects. Ahlmark et al[8] suggested that the disparate clinical findings evoked by prolonged exposure to cadmium among American and European workers might be attributable to certain physicochemical properties of the dusts, especially the difference in solubility of cadmium in water. Cadmium stearate is insoluble and hydrophobic in water.

As reported in the previous paper in this bulletin,[1] the clinical findings caused by exposure to cadmium stearate dust were different from those caused by cadmium oxide or cadmium metal. Therefore, we have studied the physicochemical character of cadmium stearate comparing with the cadmium chloride.

The dissociation of cadmium stearate occured only in the acid solution *in vitro*. Namely, it is easily supposed that the cadmium stearate is dissociated remarkably

with the gastric juice, and the dissociated cadmium has toxic effect. Cadmium stearate administered to rats remarkably hindered growth, and histological observations revealed definite damage in some of the visceral organs. In studies[9,10,11] on the toxicity of orally administered cadmium chloride, rats receiving 50 ppm for cadmium in food[10] and water[11] were reported to be stunted in growth and those receiving 0.025% of cadmium in food[9] were also stunted. In our case, the rats were stunted in growth by the diet added at the rate of 0.2% for cadmium stearate, and this concentration of cadmium stearate corresponds to about 0.03% of cadmium diet.

The toxicity of cadmium stearate and chloride was evaluated by means of $LD_{50}$ following intraperitoneal injection in mice. Cadmium stearate showed a weak toxicity as compared with cadmium chloride. However, the toxicity of cadmium stearate revealed progressively in the body.

From these results, it must be considered whether cadmium stearate dissociates or not in the tissue or cavity in where it is difficult to expect such a strong acidity as gastric juice. Pathological findings of peritoneal cavity of rat evoked by the peritoneal injection of cadmium stearate and chloride showed the signs of peritonitis. But the degree of change varied, and cadmium stearate showed a more severe fibrinous inflammation in comparison with that of cadmium chloride. The acidification of tissue caused by the inflammation might be contributive to the dissociation of cadmium stearate. Furthermore, as seen in the dissociation curve, the pH at inflexion point by the citrate buffer solution was more higher than those of the other two, and cadmium stearate was dissolved in only a few percent at pH 6.2. Therefore, citric acid may concern in the dissociation mechanism of cadmium stearate *in vivo*.

## SUMMARY

1. Cadmium stearate was remarkably dissociated with acid veronal or acetate buffer solution, but not with neutral and alkaline solution. The inflexion point of dissociation curves was at pH 4.5 in both solutions. In the citrate buffer, the inflexion point was at pH 5.5, and small quantity of cadmium stearate was dissolved in neutral solution.

2. The acute intraperitoneal $LD_{50}$ of cadmium stearate and chloride for mice was 9.31 mg. and 4.48 mg. of cadmium per kilogram of body weight, respectively. The toxicity of cadmium stearate revealed slowly in mice.

3. Cadmium stearate was fed to rats for a period of 90 days. All test animals exhibited growth suppression during the experimental periods. Definite morphological changes were observed histologically in the stomach, the intestine, the testicles as well as in some other visceral organs. Food consumption was constant throughout the experiment.
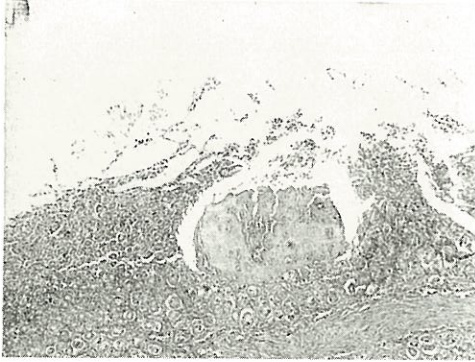
Fig. 3.　Stomach: Moderate catarrh in the mucosa of the stomach with a foci of necrosis tended to erosio formation.
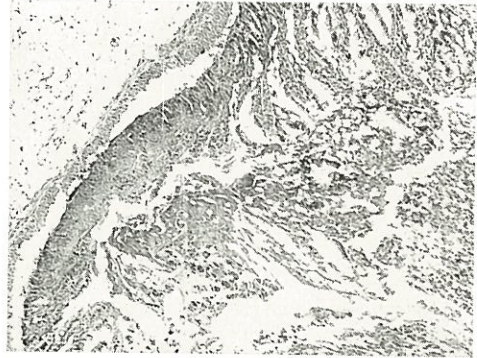


Fig. 4.　Intestine: Rather marked enteritis with a necrotic lesion resambling to that of the stomach.
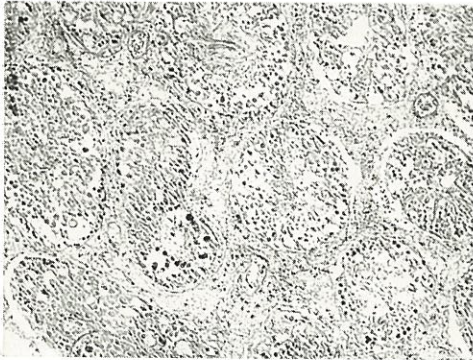


Fig. 5.　Testicle: Moderate degeneration of the germinal parenchyma of the testicles. In the severely affected cases, far more advanced a complete necrosis of coagulation type were noted.
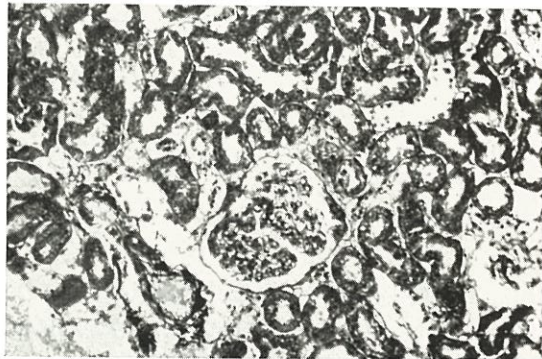


Fig. 6.　Kidney: Note swollen glomerulus and cloudy swelling of the tubular epithelium. Almost complete degeneration and desquamation of the epithelium were also noted.

REFERENCES

1) H. Sakabe and K. Ushio: Bulletin of the National Institute of Industrial Health, No. 3, 56-60, (1960).
2) Lars Friberg: Acta med. scand., Supple., **240**, 1-124, (1950).
3) J. A. Bonnell: Brit. J. Indust. Med., **12**, 181-197, (1955).
4) Ronald, E. Lane, and A. C. P. Campbell: Brit. J. Indust. Med., **11**, 118-122, (1954).
5) M. Ishibashi and T. Fujinaga: Method of Polarographic Analysis, Maruzen, pp. 198, (1956).
6) N. Kajii: Japan. J. Public Health, **6**, (6), 290-294, (1959).
7) J. C. Smith, J. E. Kench, and R. E. Lane: Biochem. J., **61**, (4), 698-701, (1955).
8) A. Ahlmark, L. Friberg, and Harriet Hardy: Indust. Med. & Surg., **25**, (11), 514-516, (1956).
9) R. H. Wilson, Floyd De Eds, and Alvin J. Con: J. Pharmacol. & Exper. Therap., **71**, 222-235, (1941).
10) J. T. Ginn and J. F. Volker: Proc. Soc. Exp. Biol. & Med., **57**, 189-191, (1944).
11) L. E. Decker, R. U. Byerrum, C. F. Decker, C. A. Hoppert, and R. F. Langham: Arch. Indust. Health, **18**, (3), 228-231, (1958).

要　旨

ステアリン酸カドミウムの実験的研究

第1報　解離曲線と毒性について

吉　川　　博　　　原　　登　　　河　合　清　之

金属石鹸の製造工場に於いて，ステアリン酸カドミウム並にラウリン酸カドミウムの粉砕・篩・袋詰作業に従事し，これらカドミウム石鹸の粉塵に曝露された時に，胃障害，即ち著明な食慾不振と味覚異常を示すことを前報に報告した。従来の報告によれば，金属カドミウム並に酸化カドミウム粉塵の吸入による障害は，呼吸器に見られる。かくの如く，カドミウム石鹸と金属カドミウムによる障害の間に著明な差異がある。

著者等は，ステアリン酸カドミウムによる障害を実験的に研究した。即ち，本物質による毒性が，ステアリン酸カドミウム自身によるのか，生体内で解離して生じたカドミウムによるのかについて考慮し，本報告では，ステアリン酸の解離，LD$_{50}$，並びに経口投与による毒性に関して実験した結果について述べた。

即ち，ステアリン酸カドミウムは in vitro では，酸性溶液中で著明に解離し，中性並びにアルカリ性溶液中では殆んど解離せず，生体内では胃液で著しく解離し，このカドミウムが毒性を示すものと想像される。食餌中にステアリン酸カドミウムを混入して，ラッテに摂取させると，

発育は著明に阻止される。従来の塩化カドミウム摂取の実験の結果も同様であり，経口的投与ではカドミウム中毒と同一の態度を示すものと思われる。

　毒性は，マウスの腹腔内注入による $LD_{50}$ から検討したが，$LD_{50}$ は 9.31 mg Cd/kg で，塩化カドミウムの $LD_{50}$（＝4.48 mg Cd/kg）に比し，毒性は弱かつた。併し，ステアリン酸カドミウムの毒性は，生体内で徐々に現われるという結果を得た。

　胃液の様な強い酸度の期待しにくい組織に注入しても，明らかに毒性を示した。この場合の毒性が，ステアリン酸カドミウム自身によるか，解離したカドミウムによるかに関しては，更に検討を加え実験中である。併し，腹腔内注入による腹腔の病理所見では，強い線維性炎症像を呈し炎症による組織の酸性化が，ステアリン酸カドミウムの解離を助長し，又，クエン酸緩衝液では中性液でも数パーセントの解離がみられ，生体内でクエン酸が，ステアリン酸カドミウムの解離を助長していることも想像される。

# THE APPLICATION OF ACOUSTIC FILTER
# TO THE EAR PROTECTOR

Toshisuke MIWA

The ear protectors have been used for prevention of high intensity noise in the factories. Their characteristics are indicated in the Table I. Among these devices an ear plug had been used most popularly, for its conveniency and low cost. It

Table 1

| Kind of Ear Protectors | Advantage | Disadvantage |
|---|---|---|
| Ear-plug | ( i ) Possible to use the other head cover at the same time.<br>( ii ) Convenient to bring.<br>(iii) Cheap. | ( i ) Discomfort.<br>( ii ) Painful to use and inflamable.<br>(iii) Individual difference for attachment. |
| Semi-insert | ( i ) No indivisual difference for attachment.<br>( ii ) Not discomfort.<br>(iii) Smaller in size than the earmuff. | ( i ) Inconvenient because of the head band. |
| Ear-muff | ( i ) No indivisual difference of attachment.<br>( ii ) Not discomfort. | ( i ) Impossibl to get the effective attenuation below 1,000 c/s.<br>( ii ) Expensive. |
| Helmet | ( i ) Capable to prevent from bone conduction for high level sound. | ( i ) Expensive.<br>( ii ) Necessary to have many types.<br>(iii) The same effect as the ear muff. |

has a hole to equalize the ambient pressure between inside and outside of the plug in the outer canal of the ear. Moreover, it acts as a low pass acoustic filter. That is, the hole corresponds equivalently to the electric inductance, and the low frequency sound can pass through it, but the high frequency sound cannot do. However, this acoustic filter is so small that the desirable attenuation cannot be expected.

The author has studied the acoustic filter for several years to prevent the exhaust noise of automobile engines. The principle of the filters can be applied to the ear protector. For this purpose, the miniature acoustic filter, the effective frequency range of which is from 500 c/s to 4000 c/s, has been examined.

The semi-insert type filter was examined by the acoustic system and by human ears. It was attached to the ear with a head band and the attenuation was mesured by threshold method.

# THE APPLICATION OF ACOUSTIC FILTER TO THE EAR PROTECTOR

## PRINCIPLE OF ACOUSTIC FILTER AND MEASUREMENT
## OF THEIR ATTENUATION CHARACTERISTICS

The wave equation of sound in an infinite long tube can be expressed as follows, neglecting viscosity of air and heat conduction, (Fig. 1),

$$\partial^2\phi/\partial x^2 = -k^2\phi$$

where $\phi$ is velocity potential, $\omega = 2\pi f$, $c$: sound velocity and $\omega/c = k$.

The solution of this equation is

$$\phi = a\exp(jkx) + b\exp(-jkx)$$



Fig. 1.

$a$ and $b$ are arbitrary constants.

For periodic wave,

$$p = \rho\dot\phi = \rho j\omega(a\exp(jkx) + b\exp(-jkp))$$

$$V = -S\,\partial\phi/\partial x = -Sjk(a\exp(jkx) - b\exp(-jkx))$$

Where $p$ is sound pressure, $V$ is volume velocity and $S$ is the cross section of the tube.

From above four equations the following equation can be derived, relating the points $x_1$ and $x_2$, $(x_2 - x_1 = l)$

$$\begin{pmatrix} P_1 \\ V_1 \end{pmatrix} = \begin{pmatrix} A & B \\ C & D \end{pmatrix}\begin{pmatrix} P_2 \\ V_2 \end{pmatrix} = \begin{pmatrix} \cos kl & j(\rho c/S)\sin kl \\ j(S/\rho c)\sin kl & \cos kl \end{pmatrix}\begin{pmatrix} P_2 \\ V_2 \end{pmatrix}. \tag{1}$$

We generally call this matrix acoustic four terminal matrix, (Fig. 2).

When two matrices 1 and 2 are connected in cascade as seen in Fig. 3, the resulting matrix will be,

$$\begin{pmatrix} A & B \\ C & D \end{pmatrix} = \begin{pmatrix} A_1 & B_1 \\ C_1 & D_1 \end{pmatrix}\begin{pmatrix} A_2 & B_2 \\ C_2 & D_2 \end{pmatrix}$$
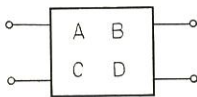


Fig. 2. Four terminal constant of distributed constant circut
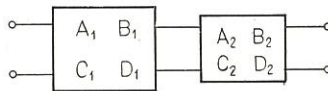
Fig. 3. Cascade connection of two classes of four terminal constants
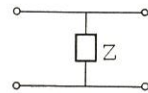
Fig. 4. Parallel connection of impedance, $z$

If impedance $Z$ is connected in parallell as in Fig. 4, the four terminal matrix of this element is,

$$\begin{pmatrix} A & B \\ C & D \end{pmatrix} = \begin{pmatrix} 1 & 0 \\ 1/Z & 1 \end{pmatrix}$$

Among several types of acoustic filters, the cavity type with internal tubes showed excellent characteristics,[1] then the series connection of these type filters has been

71

examined.

The equivalent circuit is shown in Fig. 5 and its four terminal matrix will be calculated as follows,

$$
\begin{pmatrix} A & B \\ C & D \end{pmatrix} = \begin{pmatrix} \cos kl_1 & j\dfrac{\rho c}{S}\sin kl_1 \\ j\dfrac{S}{\rho c}\sin kl_1 & \cos kl_1 \end{pmatrix} \begin{pmatrix} 1 & 0 \\ \dfrac{1}{z_1} & 1 \end{pmatrix} \begin{pmatrix} \cos kl_2 & \dfrac{\rho c}{S_2}\sin kl_2 \\ j\dfrac{S_2}{\rho c}\sin kl_2 & \cos kl_2 \end{pmatrix} \begin{pmatrix} 1 & 0 \\ \dfrac{1}{z_2} & 1 \end{pmatrix} \begin{pmatrix} \cos kl_3 & j\dfrac{\rho c}{S}\sin kl_3 \\ j\dfrac{S}{\rho c}\sin kl_3 & \cos kl_3 \end{pmatrix}
$$

$$\cdots\cdots\cdots\cdots\cdots(2)$$



Fig. 5.  Cavity type with internal tubes and Equivalent circuit of this system

Four terminal constants of this system

$$A = \{\cos^2 kl_1 - \sin^2 kl_1\}\cos kl_2 + j2\frac{\rho c}{S}\frac{1}{Z}\sin kl_1 \cos kl_1 \cos kl_2 - j\frac{S}{S_2}\left(\frac{\rho c}{S}-\frac{1}{Z}\right)\sin^2 kl_1 \sin kl_2$$

$$- \left\{\frac{S_2}{S}+\frac{S}{S_2}+\frac{S}{S_2}\left(\frac{\rho c}{S}-\frac{1}{Z}\right)^2\right\}\sin kl_1 \cos kl_1 \sin kl_2 + j\frac{S}{S_2}\left(\frac{\rho c}{S}-\frac{1}{Z}\right)\cos^2 kl_1 \sin kl_2$$

$$B\ /\ j\frac{\rho c}{S} = 2\sin kl_1 \cos kl_1 \cos kl_2 + j2\left(\frac{\rho c}{S}-\frac{1}{Z}\right)\sin^2 kl_1 \cos kl_2 + \frac{S}{S_2}\cos^2 kl_1 \sin kl_2$$

$$- \left\{\frac{S_2}{S}+\frac{S}{S_2}\left(\frac{\rho c}{S}-\frac{1}{Z}\right)^2\right\}\sin^2 kl_1 \sin kl_2 + j2\frac{S}{S_2}\left(\frac{\rho c}{S}-\frac{1}{Z}\right)\sin kl_1 \cos kl_1 \sin kl_2$$

$$c\ /\ j\frac{S}{\rho c} = 2\sin kl_1 \cos kl_1 \cos kl_2 + \left\{\frac{S_2}{S}+\frac{S}{S_2}\left(\frac{\rho c}{S}-\frac{1}{Z}\right)^2\right\}\cos^2 kl_1 \sin kl_2$$

$$- j2\left(\frac{\rho c}{S}-\frac{1}{Z}\right)\cos^2 kl_1 \cos kl_2 + j2\frac{S}{S_2}\left(\frac{\rho c}{S}-\frac{1}{Z}\right)\sin kl_1 \cos kl_1 \sin kl_2 - \frac{S}{S_2}\sin^2 kl_1 \sin kl_2$$

where, $\quad \dfrac{1}{Z}=\dfrac{1}{z_1}=\dfrac{1}{z_2}=j\dfrac{S_3}{\rho c}\tan kl_4, \quad l_4=l_5, \quad S_3=S_2-S, \quad l_1=l_3, \quad l_4=l_5.$

The attenuation of this acoustic filter was measured by the acoustic system which is shown in Fig. 6 and the equivalent crciuit is illustrated in Fig. 7 (a) and (b). The sound from the speaker is fed into the system through high impedance acoustic tube which is filled with wires.[2)]  The both ends of the conducting tube is packed with glass wool to avoid the reflection.  The filter is inserted between two conduct-

ing tubes. First, the attenuator is adjusted to the proper value of the vacuum tube voltmeter, then the filter is remove and the conducting tubes are connected together. Then the attenuator is adjusted to the same value of the previous case. From the difference of the attenuator reading, the attenuation of the acoustic system can be measured.
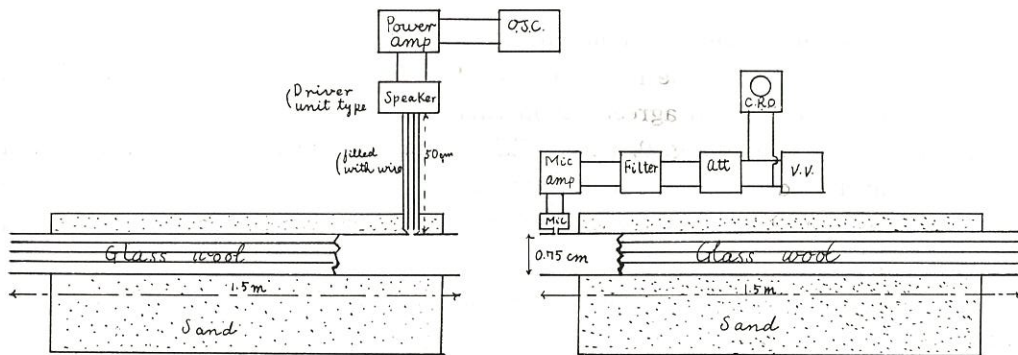


Fig. 6.  The measurement system of the attenuation value

$$(\text{Attenuation value}) = 10 \log_{10} \frac{1}{4} \left| A + \frac{S}{\rho c} B + \frac{\rho c}{S} C + D \right|^2$$

$\rho$: The density of air,    $c$: sound velocity
$S$: the cross-section of this measurment system
$A. B. C. D.$  the four terminal constans of the acoustic filter



Fig. 7.

(a)  The system without the filter

(b)  The system with acoustic filter
    $S$: the cross section of this conducting tube
    $\rho$:  the density of air
    $c$:  sound velocity in air
    $A. B. C. D.$: the four terminal constants of the acoustic filter

From the figure 7(a)

$$\begin{pmatrix} P_1 \\ V_1 \end{pmatrix} = \begin{pmatrix} 1 & 0 \\ S/\rho c & 1 \end{pmatrix} \begin{pmatrix} 1 & 0 \\ S/\rho c & 1 \end{pmatrix} \begin{pmatrix} P_2 \\ 0 \end{pmatrix} \tag{3}$$

From (b)

$$\begin{pmatrix} P_1' \\ V_1 \end{pmatrix} = \begin{pmatrix} 1 & 0 \\ S/\rho c & 1 \end{pmatrix} \begin{pmatrix} A & B \\ C & D \end{pmatrix} \begin{pmatrix} 1 & 0 \\ S/\rho c & 1 \end{pmatrix} \begin{pmatrix} P_2' \\ 0 \end{pmatrix} \tag{4}$$

As the sound source is high impedance one, $V_1$ in (3) and (4) is the same value.

73

Then,

$$P_2/P_2' = (1/2)[A + D + (S/\rho c)B + (\rho c/S)C]$$

The attenuation of this system is expressed in terms of the four terminal constants as follows,

$$\text{Att.} = 10 \log(P_2/P_2')^2 = 10 \log_{10}(1/4) A + D + (S/\rho c)B + (\rho c/S)C^2$$

For checking the measuring system, the cavity type acoustic filter was inserted between conducting tubes, the result is indicated in Fig. 8. Both theoretical and observed values are in good agreement in this case. The result of the cavity with internal tube is shown in Fig. 9, a little difference between theoretical and observed value is seemed to depend upon imperfection of one dimensional assumption. The star marks in Fig. 9 are the results of the same filter with glass wool, 0.5 gr, packed in it.

The attenuation of the cascade connection of cavities with internal tubes is also shown in Fig. 10.
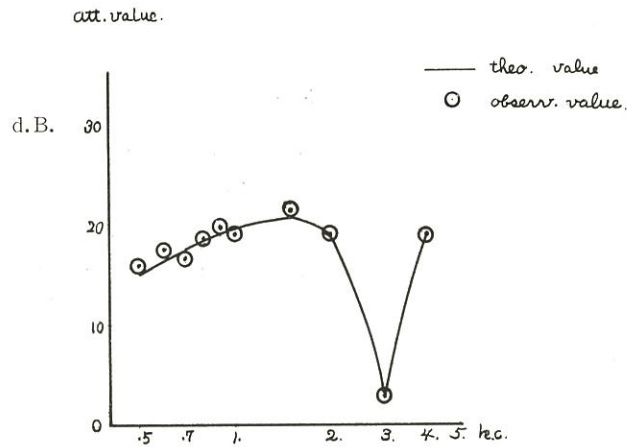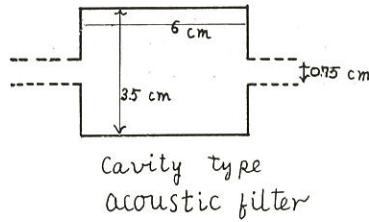
Fig. 8. The cavity type acoustic filter and its attennation
value measured in the accoustic system
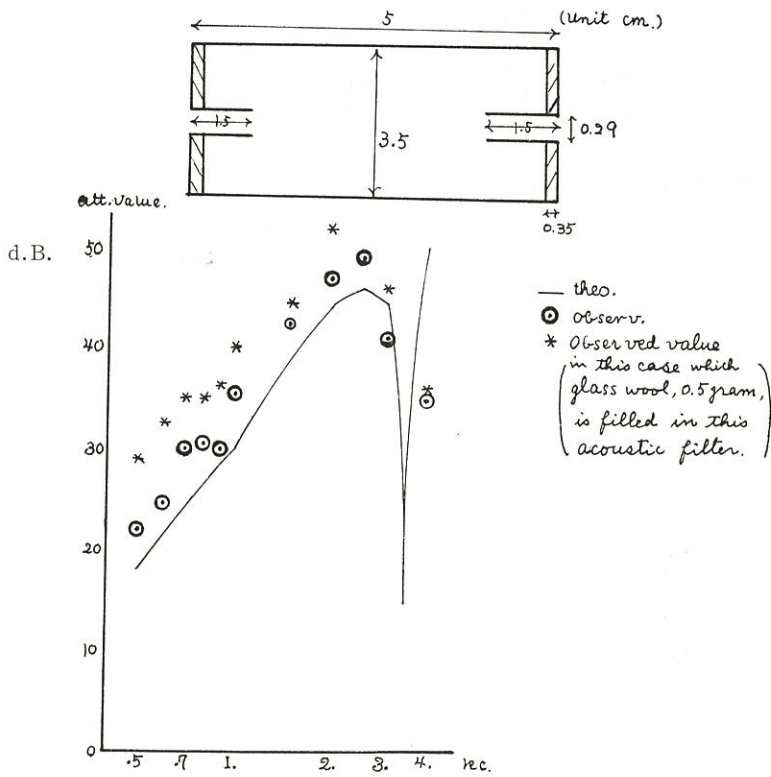
Fig. 9.   The cavity with internal tubes acoustic filter and its
attenuation value measured in the acoustic system.
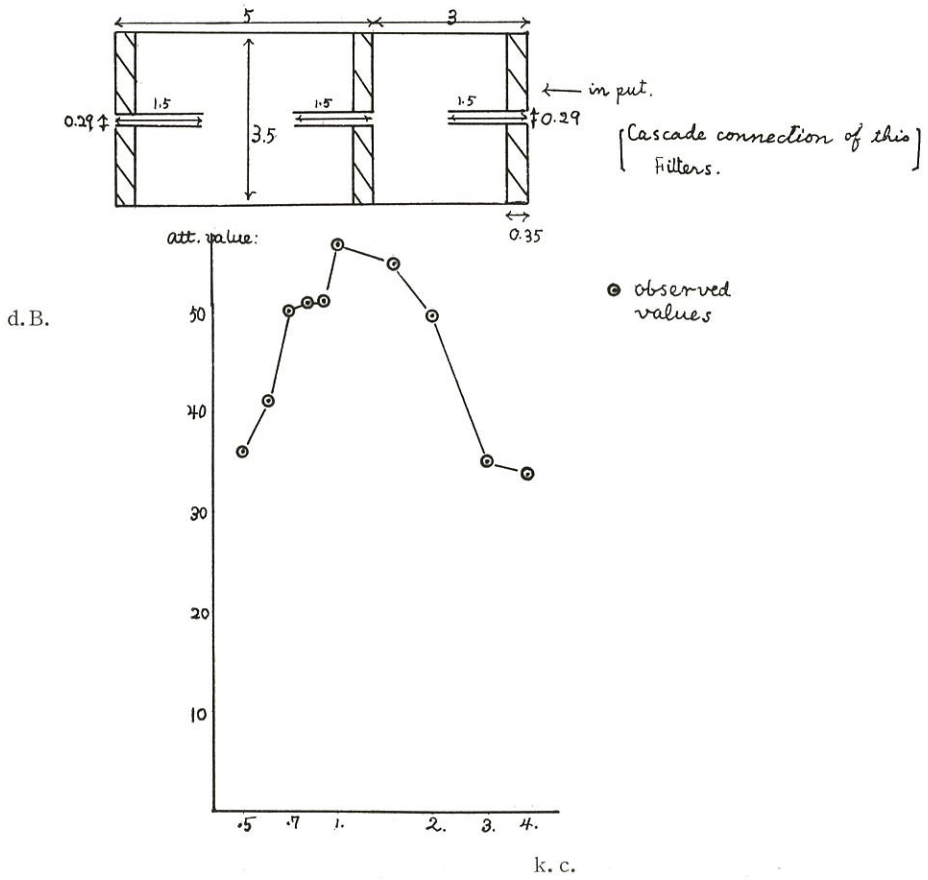
Fig. 10. The cascade connection of cavities with internal tubes and its attenuation value measured in the acoustic system

## THE ATTENUATION MEASURED BY THE THRESHOLD METHOD

The small acoustic filter of vinyle cylinder which had skrew inside was made to be able to insert several pieces of separation, and was filled with glass wool, 0.5 gr, to prevent resonance in the cavity. It was attached to human ear with soft polyethylene ear attachment and is illustrated by schema in Fig. 11. The set of filters was held on the ears by a head band with the pressure 800 gr in total. The attenuation of this ear protector was measured by the threshold method in free sound field. Six person having normal ears were selected as subjects. The head was supported by a prop to a chair and the distance from the ears to the speaker
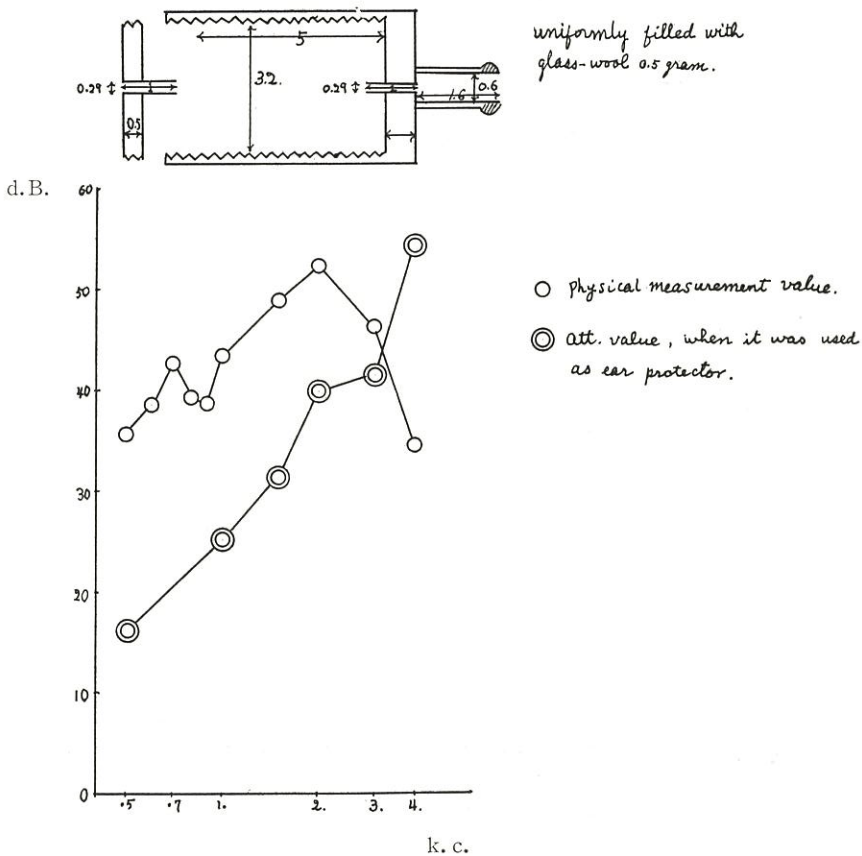


Fig. 11. Acoustic filter produced as an experiment and its attenuation values measured in the acoustic system and by the threshold method

was 1.5 meters. The threshold was measured with and without the ear protector.[3] The results measured by the physical system and human ears are shown in Fig. 11.

Owing to the bone conduction[4] and impedance difference[5] in both cases the results do not always agree well.

## APPLICATION TO PRACTICAL USES

An ear protector must be designed comfortable in practical use. Therefore the semi-insert was attached to the out-put of the filter. The protector was attached to the ears with a head band made of piano wir. The pressure of head band affects the results greatly because the sound would penetrate into the ears directly if it is less than 5.5 gr/cm². The vinyl cylinder ear protector without separation plate or glass wool was examined. The pressure of the head band was chosen as 5.5 gr/cm², 55 gr/cm² and 66 gr/cm².

The results of 7 persons are shown in Fig. 12. The result of maximum pressure shows good attenuation, but it could not be applied in practice, because any one can not bear for suffering from pain.
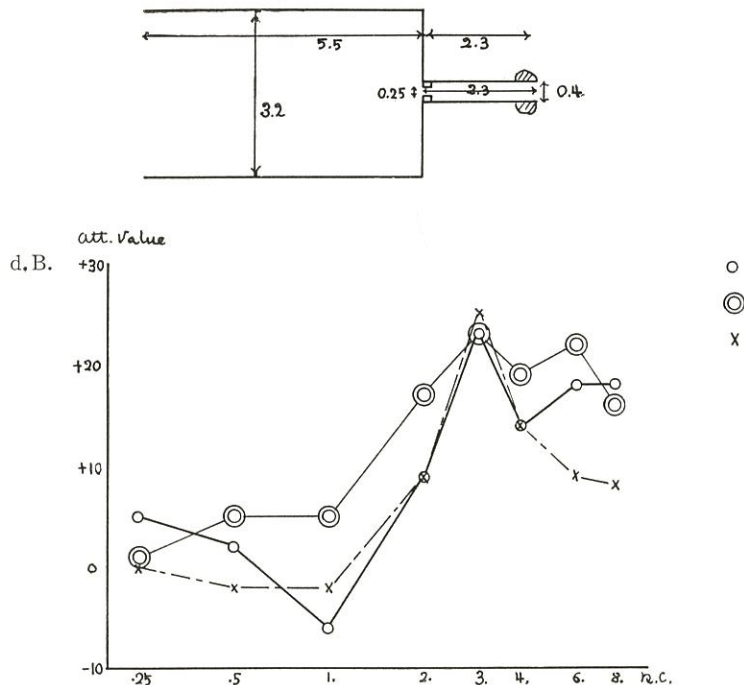




Fig. 12. The acoustic filter used as an examination of the attaching pressure and it's attenuation values measured by the threshold method

From the results in Fig. 12 the head band pressure was chosen as about 30 gr/cm² thererafter.

As the test sample, the ear protector having above mentioned characteristics was constracted (Fig. 13).

The attenuation of this test sample was compared with three of the ordinary sorts of ear protectors, that is, "semi insert" (as I could not get any semi-insert, the modified ear plug having no hole but with head band was measured), "ear muff" (made in U.S.A. the pressure of the head band was 3.9 gr/cm) and "ear plug" (with no hole).

The attenuation of these four types of ear protectors were measured by means of the orthogonal disposition table $L_{64}$ ($4^{21}$) in the experimental design method.[6] The result was shown in Fig. 13 and each point had $\sigma=5.03$ by the analysis of variance and fiducial limit$=\pm3.5$ db in the reliability 95 percent. There was no difference between the semi insert and the test sample at frequencies 0.5 kc, 2 kc and 8 kc, but this test sample showed the best attnuation effect at 4 kc. It is better than the ear muff and the ear plug about 10 db in all frequency range.
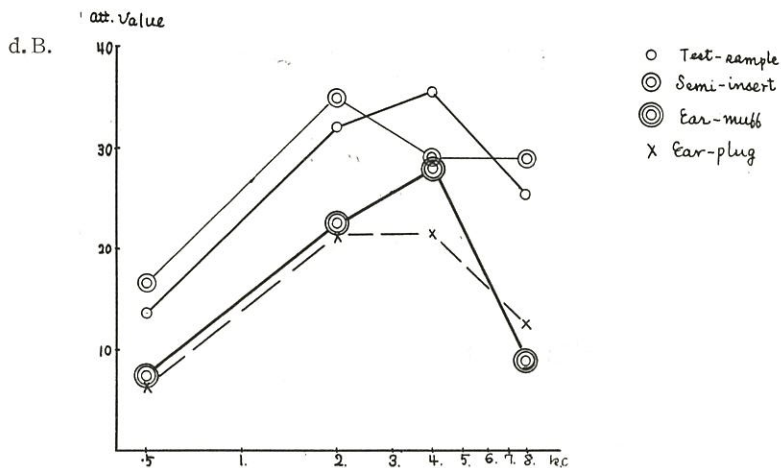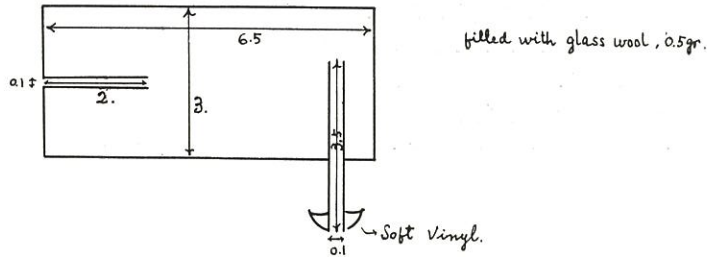




Fig. 13. Test sample of the accoustic filter finally produced and comparison of the attenuation value with four types of ear protectors by the threshold method

## Conclusion

The acoustic low pass filter was applied to the ear protector of semi-insert type and it was compared with the ear protectors in common use. The results showed that the test sample is the most effective of all. The problem for the practical use for labourers is now being studied.

## Acknowlegement

79

### REFERENCE

1) T. Miwa and J. Igarashi: Fundamentals of the acoustical silencers.
   (II) Determination of four terminal constant of acoustic elements.
   Aeronautical Research Inst. Univ. Tokyo Report No. 344.
2) Beranek: Acoustic measurement, John Wily Inc. 1950.
3) Zwislocki: J. A. S. A. **27**, 1154, (1955).
   Hershkowitz: J. A. S. A. **29**, 889, (1957).
   Shaw and Thiessen: J. A. S. A. **30**, 24, (1958).
4) Zwislocki: J. A. S. A. **29**, 795, (1957).
5) Morton: Acustica **8**, 33, (1958).
6) Genichi Taguchi: Experimental design method, Maruzen, 2nd ed. (1958).

## 要　　旨

## 音響沪波器の耳防具えの応用

### 三　輪　俊　輔

　騒音職場での耳防具に対する必要性は益々増大しているが，耳防具の共通の欠点である不快感，余り効果がないこと，高価であること等の為に労働者が使用したがらないのが現状である。私は消音器の研究を進めて来たが，之を耳に応用したならば，極めて有効な，しかも上述の欠点を補う様な耳防具を作り得ると考え本実験に着手した。

　此の目的に適つた小型音響沪波器を作り，その特性を音響系で測定したところ，500〜4000 c/s で有効であつた。之をセミインザート型にして耳に装着し，閾値法でその減衰効果を求めた結果，在来の耳栓や，イヤーマフ等より平均10 db 減衰が増加し，しかも余り不快感を起さない耳防具を作る事が出来たので報告する。

　自動車用消音器では理論的にも，実験的にもキャビティ中に管を挿入した型をカスケードにつないだものが，もつとも減衰効果がよい。耳に装着する為に非常に小型にし音響系（Fig. 6）で減衰量を実測した結果 Fig. 9 を得た。即ち 1000 c/s〜4000 c/s で可成の減衰効果が期待出来る。之をカスケードにつなげば Fig. 10 の如く更に減衰効果はよくなるが，実用上なるべく作り易い構造のものがよいので，以下は此の単一ユニットのみを使つた。

　次に試験的に Fig. 11 図型のものに 0.5 gr のグラスウールをつめて共鳴をのぞいた。之をベッドバンドで頭部に固定し，着用時と非着用時の閾値の移動量を無響室の自由音場で測定して減衰量と定義した。此の結果は Fig. 11 に示す様に有効である事が解つた。

　次に実用化に就て考えた。ベッドバンドはピアノ線2本を用い，圧着力が減衰効果及び不快さに重大な効果をもたらすので圧着力 5.5 gr/cm²，55 gr/cm²，66 gr/cm² にして減衰量を求めると Fig. 12 を得る。これでは 66 gr/cm² が最も有効であるが疼痛を感ずる。又 5.5 gr/cm²〜55 gr/cm² では余り変化はないと見てよい。此の結果よりして圧着力は約 35 gr/cm² を選んだ。

　以上の諸測定値に基いて作つたテストサンプルと在来のイヤーマフ，耳栓（孔のないもの）及びセミインザート（入手出来ないので自作，孔のないもの）の3種と比較して Fig. 13 に示す結果を得た。即ちイヤマフ，耳栓より平均 10 db 高い減衰量を各周波数で得た。

――――――――――――

# 某 製 鋼 工 場 の 騒 音 分 析

三 輪 俊 輔

## NOISE ANALYSIS IN AN IRON AND STEEL FACTORY

Toshisuke MIWA

　私は前報で某自動車修理工場の騒音測定の結果について報告したが，今回は某製鋼工場の騒音を測定し，略々100ホン以上の場所につき，その分析を行つたので茲に報告する。

　先ず選択した作業場の騒音を携帯録音器で録音し，之を東通工CP1型再生器で再生して，ブリューエル・ハイ・スピード・レベルレコーダに各オクターブバンド値を自記させて周波分析を行つた。

　又，時間分布はテープの再生電圧でレベルセレクターを駆動して求めた。本測定に使用したマイク，テープレコーダー等音響機器の較正は航研無響室を借用して行つた。

　測定職種は次の通りである。

　大ハンマー作業……直径2米程度の歯車を6人程度の作業者がハンマーをもつて成形する。

　試験材剪断……金属板を切断器で切る。

　鉱滓綿……熔鉱炉のカスを圧縮空気でふきとばして綿状物を作る。

　鉱石クラッシャー……鉱石をくだく。

　圧延作業……鋼塊を厚板にする。

　厚板分割……厚板を分割する。

　グラインダー作業……金属板の薄板，又は厚板のキズをグラインダーでけずる。

　送風器室……熔鉱炉に送風する。

　動力室……電動モーター，駆動。

　空気圧縮室

　以上の騒音職場について測定を行つた。

## 1. Octave band 分析値 (図1～図8)

　各録音は最小2分，パルス音は5分間録音し，再生は各 band について10秒，パルス音については1分間とした。その間のバラツキの上下を直線で示し，折線でその平均値を示した。

　この折線によれば

　山形曲線は，空気圧縮室の吸入口附近 .大ハンマー作業，厚板分割，圧延，材料剪断，グラインダー，鉱石クラッシャーで見られ，

　Low pass 型は動力室，空気圧縮室，送風機室，

　High pass 型は鉱滓綿で見られた。

　此の場合，感覚的には山形曲線を示す職場では，一般的にうるささが感ぜられるが，Low Pass 型の職場では胸を圧する感じを受け，High pass 型ではいらだたしさを受ける。

　この様なはつきりした特徴は騒音曲線を人間の感覚上から如何に分類すべきかと云う今後の研

某製鋼工場の騒音分析
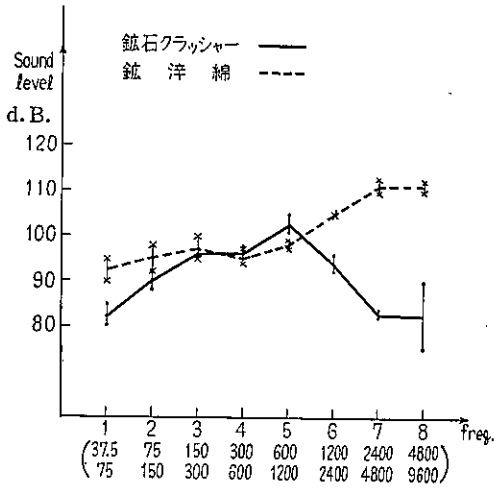


(図 1)
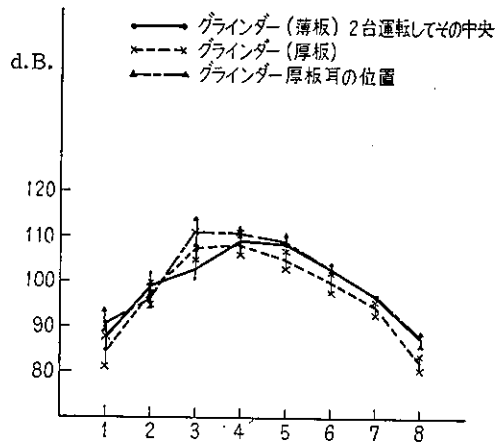


(図 2)
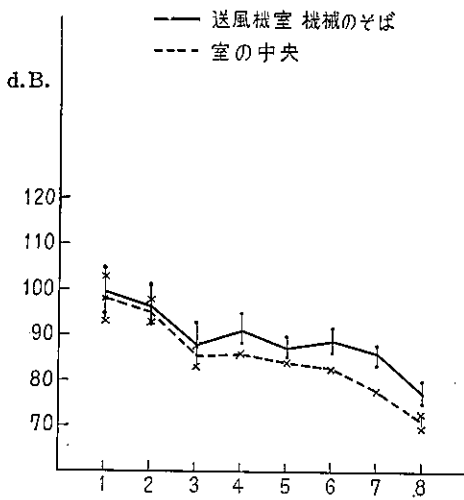


(図 3)
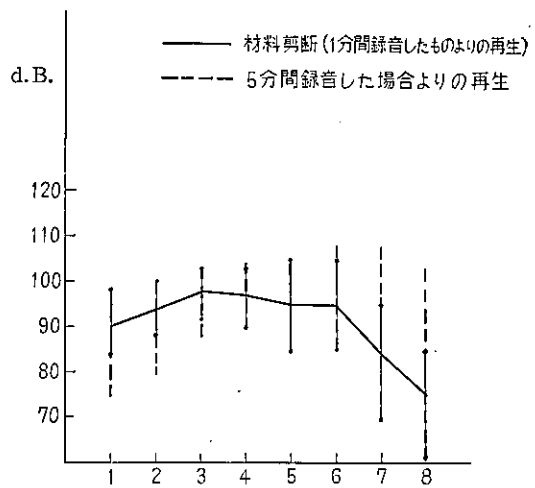


(図 4)
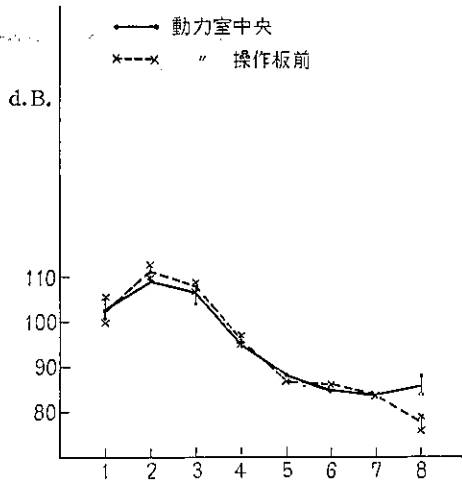
（図　5）
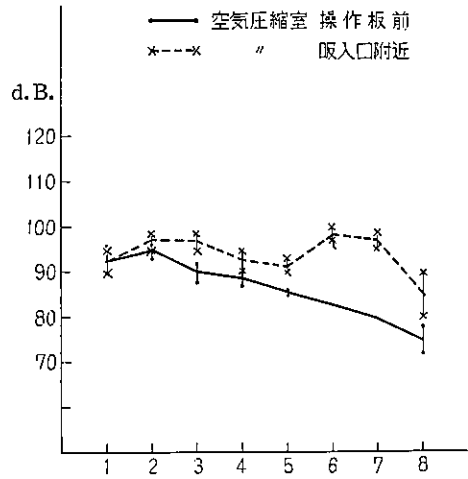
（図　6）
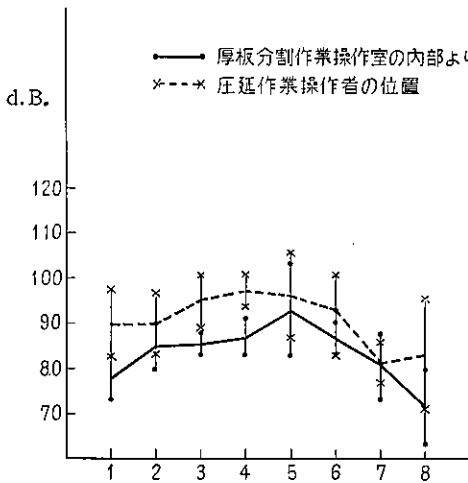
（図　7）
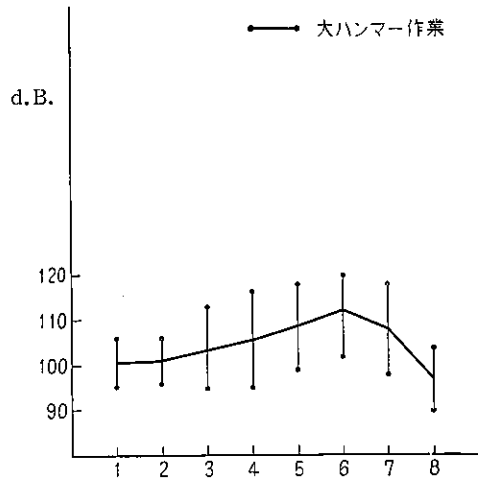
（図　8）

究課題を提起している。

## 2. Time study （図9〜図12）

　　当研究所報第1報で述べた様に，レベルセレクターによつて時間的分布を求めた。各 data は逆累積曲線で示した。大ハンマー作業及び厚板分割作業を除いては，直立した曲線が多いのが，此の調査の特色である。大ハンマー作業（パルス音）に130 db 以上の音が10% も含まれている事は，本作業が acoustic trauma にも関係している事を示している。

某製鋼工場の騒音分析



（図　9）



（図　10）



（図　11）



（図　12）

# 労働省労働衛生研究所研究報告

## 第 三 号

### 昭 和 3 5 年

## 内 容 目 次

# Bulletin

## of

## The National Institute of Industrial Health

## CONTENTS